CRITICAL ROLE OF ORGANIC MATTER IN THE NATURAL ATTENUATION OF ACID MINE DRAINAGE

A thesis submitted to the University of Manchester for the degree of Doctor of Philosophy in the Faculty of Engineering and Physical Sciences

2014

By

Martha Elena Jiménez-Castañeda

School of Earth, Atmospheric and Environmental Sciences

Contents

Word count: 39000

List of Tables

List of Figures

Abstract

The study of acid rock and mine (ARD and AMD) environments mainly focused on the mineralogical and microbiological conditions and responses of such systems. Most of the research that involved some organic viewpoint was related to the amelioration of the environmental conditions, sometimes with contradictory results. How organic matter (OM) participates and which organic fractions are involved in ARD and AMD processes remain unclear.

In this work we have applied organic geochemistry tools combined with mineralogical ad molecular microbiology techniques to study of ARD and AMD environments. The main objectives were to identify and characterise the natural sources of OM occurring both at ARD and AMD sites, and to determine whether the OM sources identified are involved in the generation or amelioration of AMD/ARD.

This study shows that multiple OM sources occur naturally in acid drainage environments, included plant derived material and mature, petroleum-derived hydrocarbons, originating from the source rocks, apparently have not directly influence on the processes. This suggests that the generation of ARD and AMD is a completely chemoautotrophic process.

Particle size of the iron phases present at ARD sites seems to be involved in the iron bioavailability. The presence of goethite in ARD/AMD systems may have a relationship with the presence of OM.

Stimulation of ARD sediments using plant derived OM, abundantly present in and around ARD and AMD ponds systems does not result in the neutralisation of ARD or AMD. This suggests that plant material is not used by Fe(III)-reducing bacteria. However, it fuels fermentation processes and it is likely that fermentation products such as acetate, detected in microcosms and *in situ*, could limit Fe(III)-reduction.

In contrast, the stimulation of ARD sediments using manure (particularly sheep manure) raises the pH up to near neutral conditions. Although it remains unclear which OM fraction from the manure is actively involved in the neutralisation of ARD; these results suggest that manure may make an interesting and non-expensive electron donor in AMD/ARD treatments.

DECLARATION

No portion of the work referred to in this thesis has been submitted in support of an application for another degree or qualification of this or any other university or other institute of learning.

COPYRIGHT STATEMENT

i. The author of this thesis (including any appendices and/or schedules to this thesis) owns certain copyright or related rights in it (the "Copyright") and s/he has given The University of Manchester certain rights to use such Copyright, including for administrative purposes.

ii. Copies of this thesis, either in full or in extracts and whether in hard or electronic copy, may be made only in accordance with the Copyright, Designs and Patents Act 1988 (as amended) and regulations issued under it or, where appropriate, in accordance with licensing agreements which the University has from time to time. This page must form part of any such copies made.

iii. The ownership of certain Copyright, patents, designs, trade marks and other intellectual property (the "Intellectual Property") and any reproductions of copyright works in the thesis, for example graphs and tables ("Reproductions"), which may be described in this thesis, may not be owned by the author and may be owned by third parties. Such Intellectual Property and Reproductions cannot and must not be made available for use without the prior written permission of the owner(s) of the relevant Intellectual Property and/or Reproductions.

iv. Further information on the conditions under which disclosure, publication and commercialisation of this thesis, the Copyright and any Intellectual Property and/or Reproductions described in it may take place is available in the University IP Policy (see http://documents.manchester.ac.uk/DocuInfo.aspx?DocID=487), in any relevant Thesis restriction declarations deposited in the University Library, The University Library's regulations (see http://www.manchester.ac.uk/library/aboutus/regulations) and in The University's policy on Presentation of Theses.

ACKNOWLEDGMENTS

I would like to thank my academic supervisors, Dr. Bart E. van Dongen, Prof. David J. Vaughan and Prof. Jonathan R. Lloyd for their help, guidance and continuous supervision during the course of my PhD studies.

I gratefully acknowledge receipt of a PhD scholarship, funded by The Mexican National Council for Science and Technology (CONACyT) and a complementary scholarship for Postgraduate Studies Abroad funded by the Secretariat of Public Education of Mexico (SEP).

I am indebted to P. Wincott†, A. Bewsher, P. Lythgoe, C. Davies, C. Boothman and J. Waters, for their advice and technical assistance with various laboratory procedures.

Thanks to my friends and colleagues of the Organic Geochemistry and the Geomicrobiolology groups of the University of Manchester for their continuous support.

I am extremely grateful to my parents, for their love and continuous encouragement.

CHAPTER 1

Introduction

1.1 Overview

1.1.1 Impact of acid mine drainage

Fresh water is undoubtedly linked to the development of human civilization. Water quality is a key factor for human health and consequently 77% of countries have recognised the human right to water but millions of people are still exposed to biological and chemical contaminants due to poor or inadequate management of agricultural, urban and industrial wastewater (WHO 2012).

Amongst the major environmental hazards that endanger water quality, the acid drainage is one of the most widespread forms of contamination. Two types of acidic waters may occur in the environment; the so-called Acid Rock Drainage (ARD) that is generated by the natural oxidation of pyrite, and the Acid Mine Drainage (AMD) that is a man-induced process associated with active and abandoned mine working. AMD/ARD are characterised by waters with high concentrations of iron and sulfur and a great diversity of other dissolved metals (Akcil and Koldas 2006). The acidity ranges typically from pH 2 to pH 3, although more extreme conditions have been reported at Richmond mine, USA (Nordstrom et al. 1999). Due to these characteristics, the discharge of ARD/AMD in the environment causes severe ecological problems (Figure 1.1).

For example in 1998 an accident in the Aznalcóllar tailing pond (Spain) released 4 million m^3 of AMD and 2 million m^3 of toxic mud, eliminating the aquatic communities of the Agrio and Guadiamar rivers over a length of 60 km. The discharge contained approximately 16000 t of Zn and Pb; 10000 t of As; 4000 t of Cu; 1000 t of Sb; 120 t of Co; 100 Tl and Bi, 50 t of Cd and Ag; 30 t of Hg and 20 t of Se and other metals. This lowered the pH of the marshes from pH 8.5 to pH <4.5. This accident caused the

destruction of crops, agricultural lands and affected also the Doñana Park, the largest reserve of birds in Europe (Pain et al. 1998, Grimalt et al. 1999, Solà et al. 2004).

Reported cases in China indicated that AMD from the Dabaoshan mine has contaminated drinking and irrigation waters, affecting agricultural soils, aquatic life (Lin et al. 2007) and caused health problems for people living downstream (Chen et al. 2007, Zhou et al. 2007). Other AMD case has been reported in the Potosí region (Colombia), where people are exposed to lead levels sixteen times higher than the acceptable limit when consuming fish from the Pilcomayo River (Rosenberg et al. 2001, Smolders et al. 2003). In Philippines, approximately 1.6 million m^3 of toxic tailings were released into the Boac-Makalupnit River in March, 1996, endangering the inhabitants of the towns of Hinapulan, Binunga and Mainit (David 2003). Another example is the Witwatersrand watershed (South Africa) that is believed to be receiving a daily discharge of 350,000 m^3 of AMD since 2002 (Naicker et al. 2003, Tutu et al. 2008).

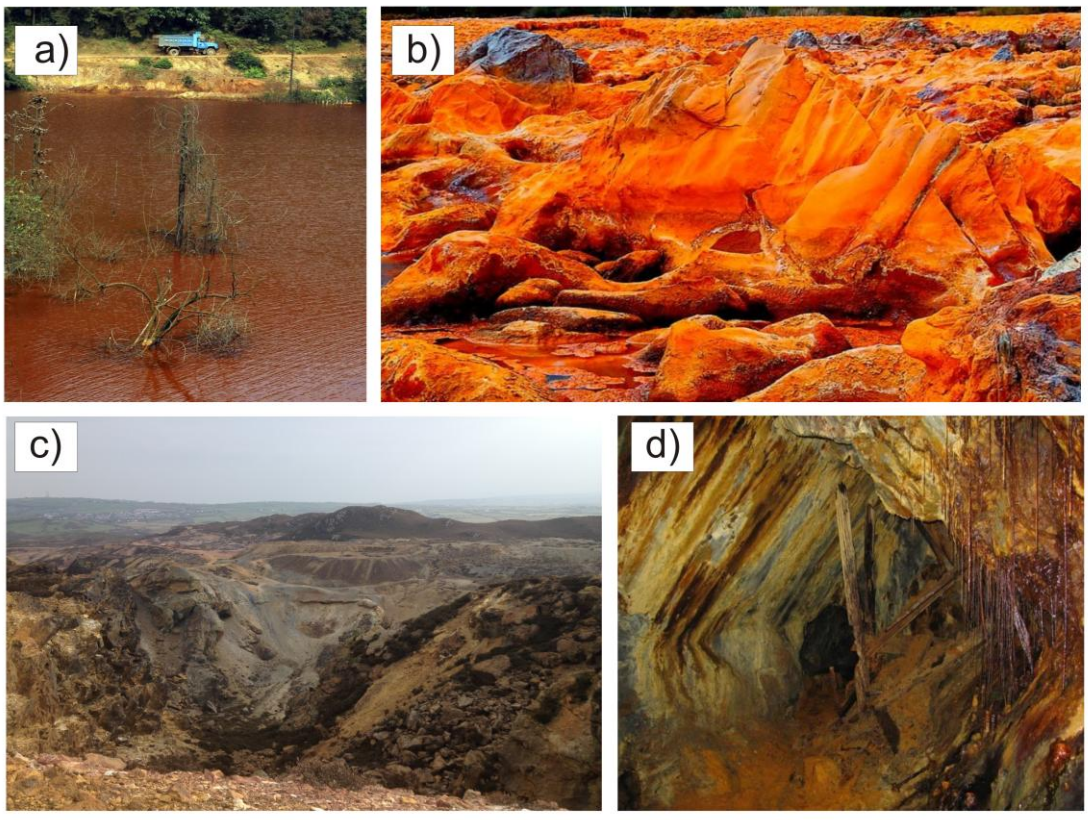

Figure 1.1. AMD sites. a) Dabaoshan mine, China; b) Rio Tinto, Spain; c) Parys Mountain, UK; d) Wheal Jane, UK. All images are in the public domain.

Also across the UK there are many examples of AMD discharges from abandoned coal and metal mines (Gordon 1994, Younger 1997, Banks and Banks 2001, Younger 2001). Two well known cases are the Wheal Jane mine accident that delivered 50,000 m^3 (Banks et al. 1997) of a very toxic and dramatic AMD plume to the River Carnon and the Fal River in the Fal estuary in 1992 (Bowen et al. 1998, Neal et al. 2005, Whitehead and Prior 2005) and the drainage works carried out at Parys Mountain in 2003, that released 7.5 t of copper, 3.1 t of manganese and 14.8 t of zinc to the Irish Sea (Coupland and Johnson 2004). All these cases show clearly that AMD is a worldwide problem.

1.1.2 Methods for AMD treatment

Because the effects of AMD may persist in the environment for centuries (e.g. Davis Jr et al. (2000), Coupland and Johnson (2004)), several strategies have been implemented for treating the problem. Basically there exist two broad groups of treatments. The first group are the passive treatments, which are affordable technologies (Table 1.1) and require little or no maintenance and/or some chemical or biological additions that enable living organisms the removal of contaminants while increase the pH of the system. Some of the most commonly applied passive treatments are the compost bioreactors, which generate alkalinity using organic wastes and sulfate reducing bacteria (Gibert et al. 2005, Cole et al. 2011, Choudhary and Sheoran 2012) and the wetlands, which reduce the metal concentrations and neutralise the acidity of AMD streams (Mitsch and Wise 1998, Mays and Edwards 2001, Hallberg and Johnson 2005).

The second group are the active treatments. Those are very efficient technologies but in contrast to passive treatments are dependent on continuous attention, can be dangerous and also very expensive (Table 1.1). The active methods consist on mechanised procedures with the addition of diverse chemicals, such as lime, to raise the pH and to promote the precipitation of metals as hydroxides and carbonates (Tünay and Kabdaşli 1994, Matlock et al. 2002, Herrera et al. 2007, Harvey et al. 2011). For instance, the High Density Sludge (HDS) process is an improvement of the lime neutralisation method that promotes the nucleation re-circulating the sludge into the treatment plant (Coulton et al. 2003). Other examples are the cation-anion exchange (Schoeman and Steyn 2001) and membrane flotation (Sudilovskiy et al. 2008) processes.

Table 1.1. Minimum and maximum capital and operating costs by AMD treatment type data collected in diverse countries for March 2013.

Cost (£M)	Basic neutralisation		Passive treatment		High Density Sludge (HDS)		Membrane separation		Other	
	Min	Max	Min	Max	Min	Max.	Min	Max	Min	Max
Capital	0.07	22.8	0.03	0.81	0.54	12.97	0.98	20.31	0.08	3.01
Operating	0.01	3.86	0.02	0.77	0.02	4.64	0.41	0.41	0.14	2.71

Data from Zinck and Griffith (2013).

1.1.3 Origin of acidic waters

Iron plays a key role in many biotic and abiotic processes. It forms the sulfide minerals that drive AMD generation, in particular pyrite (FeS_2) which is the most important and the most ubiquitous of all sulfides (Craig et al. 1998). The crystal structure of pyrite is cubic, with iron atoms octahedrally coordinated at the corners and face centres of the crystal. Disulfide atoms are at the centre of the crystal and at mid-distance of the cube edges and every sulfur atom, in turn, is coordinated to three iron atoms and one sulfur atom in a distorted tetrahedral configuration (Vaughan and Craig 1978).

The oxidative dissolution of pyrite is a complex electrochemical process that involves both chemical and biological factors, typically used to study the reactions that originate AMD (Singer and Stumm 1970, Rimstidt and Vaughan 2003).The generally accepted sequence for AMD generation starts when pyrite reacts with oxygen and water to produce Fe(II), sulfate and acidity (Equation 1). This reaction transfers 7 electrons from the pyrite surface to the oxidant (commonly either O_2 or Fe (III)).

Fe(II) is oxidised by oxygen to Fe(III) (Equation 2), which is the beginning of AMD autocatalytic reactions (Singer and Stumm 1970). Depending on the geochemical conditions, Fe(III) will form different secondary iron minerals (Equation 3) releasing additional acidity. At lower pH values, iron solubility is higher and the newly formed Fe(III) will oxidise more Fe(II) (Equation 4), triggering off the propagation cycle of AMD.

$$2FeS_2 + 7O_2 + 2H_2O \rightarrow 2\,Fe^{2+} + 4SO_4 + 4H^+ \quad (1)$$

$$4Fe^{2+} + O_2 + 4H^+ \rightarrow 4\,Fe^{3+} + 2H_2O \quad (2)$$

$$4Fe^{3+} + 12\,H_2O \rightarrow 4\,Fe(OH)_3 + 12\,H^+ \quad (3)$$

$$FeS_2 + 14\,Fe^{3+} + 8\,H_2O \rightarrow 15\,Fe^{2+} + 2\,SO_4^{2-} + 16\,H^+ \quad (4)$$

At low pH the oxidation of pyrite is mediated by acidophilic microorganisms (Colmer and Hinkle 1947), accelerating the oxidation process by a factor of 10^6 (Singer and Stumm 1970). Above pH 6.4, the rate of oxidation of pyrite rapidly increases as a function of pH, so that the bacterial contribution is negligible (Singer and Stumm 1970, Kirby et al. 1999), but it has been suggested that above pH 3.5 the oxidation of Fe(II) is no longer due to microbial activity (Hallberg 2010).

Other aspects that govern the oxidation of Fe(II) are the crystallography of the mineral (Bennett and Tributsch 1978, Malmström et al. 2000) and the morphology of the mineral, for example, particle size (Swoboda-Colberg and Drever 1993). The products of pyrite oxidation are the common iron minerals detected at AMD sites, including goethite (α-FeOOH), schwertmannite (ideally, $Fe_8O_8(OH)_6SO_4$), ferrihydrite ($5Fe_2O_3{\cdot}9H_2O$) hematite (Fe_2O_3) and jarosite ($KFe_3(SO_4)_2(OH)_6$) (Ferris et al. 1989, Bigham et al. 1996, Kim et al. 2002, Murad and Rojík 2003, Valente et al. 2013). These minerals occur in different morphologies and crystal structures and can provide electron acceptors for the anaerobic growth of Fe(III)-reducing bacteria (Cutting et al. 2009). Sulfide ores also contain diverse trace elements, the most important are As, Ba, Cd, Cu, Mn, Mo, Ni, Pb, Se, and Zn (Sullivan and Yelton 1988, Robins 1993). Those like As, Cd and Pb are highly toxic and are released into the environment during sulfide oxidation by Fe(III) or solubilised by microbial metabolism (Johnson 2003).

1.1.4 Microbial life in an extreme environment

Some of the most extreme conditions on Earth are found at AMD sites. These places have broad range of stresses such as high toxic metal content, temperature variations, and a high acidity at which proteins can be denatured. Nevertheless, because of their adaptability and diverse metabolic abilities, acidophilic microorganisms grow successfully in these environments (Johnson 1998, Hedrich et al. 2011).

An excellent example of such adaptation is *Acidithiobacillus ferrooxidans*, the first discovered pyrite-oxidising bacterium. This bacteria is also able of oxidising sulfur and reduced sulfur compounds and possesses the capacity of reducing Fe(III) in anoxic environments (Colmer et al. 1950, Roger et al. 2012). *A. ferrooxidans* was considered the most important microorganism for AMD generation for several years but more recently, thanks to the development of molecular microbiology techniques (DNA stable isotope probing and 16S rRNA gene cloning and sequencing) new and uncultured microbial species, have been identified such as *Leptospirillum* (Rawlings et al. 1999) and archaea (Bruneel et al. 2008) and have been suggested to be more active and

abundant in AMD sites. In addition, many prokaryotes e.g. yeasts and fungi (*Trichosporum, Rhodotorula, Penicillium*), flagellates (*Eutreptia* and/or *Bode spp.*), ciliates (*Cinetochilium sp.*) and amoebas (*Vahlkampfia sp.)* have also been detected (Baker and Banfield 2003, Baker et al. 2003).

The microbial ecology and interactions occurring at AMD are still poorly understood. Chemoautotrophic microorganisms are the most abundant in AMD sites and may form the base of an acidophilic food web in subterranean environments (Johnson 1995, Hallberg 2010, Ñancucheo and Johnson 2010), probably because at low pH (pH 2) the redox potential of the Fe(III)/Fe(II) pair is close to the value of the O_2/H_2O pair (770 mV and 816 mV, respectively), indicating that Fe(III) can be used as an electron acceptor during anaerobic respiration (Weber et al. 2006, Vaughan and Lloyd 2011). The microbial reduction of Fe(III) may require the direct contact of the microbial cells to the oxide surface (Caccavo et al. 1997). Because of this, Fe(III)–reducing bacteria such as Ge*obacter metallireducens* are able to detect the gradient of reduced metal ions originating from the dissolution of the Fe(III) oxyhydroxides and can express flagella and pili during growth on Fe(III) oxyhydroxides (Childers et al. 2002). Some microorganisms do not require direct contact with the mineral and may use electron-shuttling compounds, such as quinones, flavins and humic materials during the Fe(III) reduction (Nevin and Lovley 2000, Jiang and Kappler 2008). In addition, several forms of anaerobic respiration including Fe(III)-reduction and sulfate-reduction, are alkali-generating processes (Vile and Wieder 1993) that can potentially reverse acidification caused by pyrite oxidation.

1.1.5. The presence of organic matter in AMD environments

The organic matter (OM; carbon) content is generally considered low at AMD sites, on average, less than 10 mg/l of dissolved organic carbon (Johnson 2012). In such environments, chemoautotropic microorganisms may satisfy their carbon requirements using atmospheric CO_2, although other acidophilic microorganisms may exhibit the capacity to assimilate organic carbon (heterotrophs) or to assimilate both CO_2 and organic carbon (mixotrophs) (Wood and Kelly 1983, Harrison 1984, Johnson et al. 1992, Johnson and Bridge 2002).

Given that the metabolic pathway of a microorganism may offer an insight of its role in the ecosystem, it is not unlikely to hypothesize the involvement of OM in the processes of AMD generation/amelioration. However, it remains unclear exactly what type of organic matter is present at AMD sites and to what extend it is bioavailable during the

generation/amelioration of AMD; therefore the characterisation and a better understanding of the role of the OM naturally present at an AMD site is needed.

1.1.6 Organic molecular analyses

The composition of the OM present in AMD sediments can be complex and could require a variety of analytical methods for its characterisation at a molecular level. For example, the extractable OM fraction (lipids) of a sediment can be determined and quantified using Gas Chromatography Mass Spectrometry (GC-MS). Lipids represent an unambiguous link to specific organisms (Vestal and White 1989, Gaines et al. 2009) and provide useful information about the sediments because i) are widely distributed; ii) can be source-specific and iii) are easily identifiable.

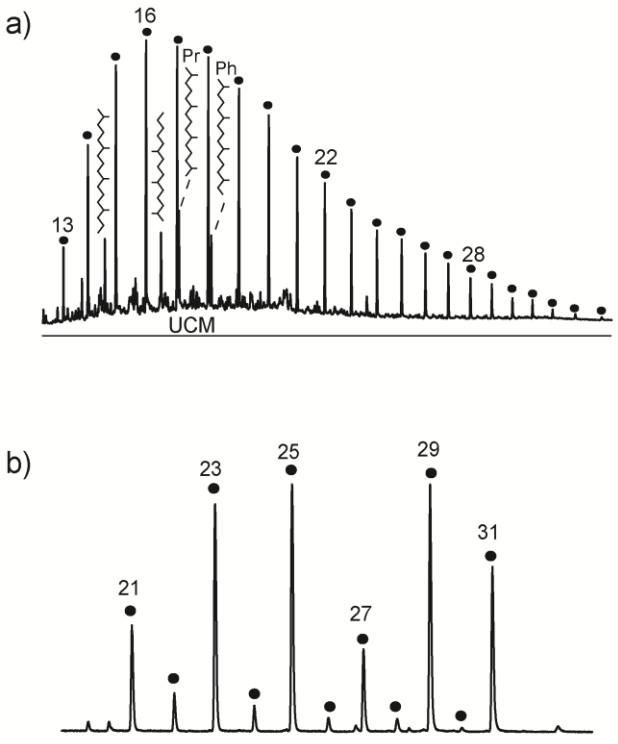

Figure 1.2. Comparison of the distribution pattern of saturated hydrocarbons of a) mature origin (petroleum derived; CPI=1.1) and b) recent origin (plant derived; CPI=11.1), detected in sediment samples from Mam Tor UK. Closed circles indicate *n*-alkanes; Pr=Pristane; Ph=Phytane; UCM= unresolved complex mixture. Numbers indicate carbon chain length.

From the lipid fraction, *n*-alkanes of high molecular weight (HMW; C>20) of plant origin have very specific distribution patterns and a high odd-over-even predominance of the carbon chain length (Eglinton and Hamilton 1963, 1967); if such a diagnostic pattern is observed in an AMD sediment, it can be directly linked to an OM input of recent origin (e. g. higher plants; Figure 1.2). On the other hand, when HMW *n*-alkanes are formed in an abiotic process due to "cracking" of OM deeper down in the sediments, the *n*-alkanes will not have a similar odd-over-even predominance as observed in plants and can be directly linked to mature OM (e.g. petroleum; Figure 1.2). Additionally, the presence of pristane (C_{19}), phytane (C_{20}) and an unresolved complex mixture (UCM) are clear indicators of a petroleum input (Volkman et al. 1992). These differences are helpful to distinguish the source and maturity of OM and can be expresed in the HMW *n*-alkane carbon preference index (CPI), where plant-derived HMW *n*-alkanes will give a CPI value greater than one while petroleum-derived HMW *n*-alkanes will give a CPI vale close to one (Figure 1.2).

A major problem with lipid analyses is that lipids only represent a relatively small fraction of the OM present in sediments. By far, the largest pool of OM (kerogen; ca. 95%) cannot be extracted (Forsman and Hunt 1958, Durand 1980) and cannot be analysed using only GC-MS. This implies that other techniques are required to obtain more information. Pyrolysis (Py) for instance, destroys macromolecular compounds applying temperatures above 300°C or 350°C that enable the separation of small or modified fractions of the macromolecules. When pyrolysis is coupled with a GC-MS system, the technique allows the identification and relative quantification of the resulting products (Vancampenhout et al. 2009). Lignocellulose is other important OM fraction in sediments that can be attacked by fungi and some bacteria (Hatakka 1994, Brown and Chang 2014) and requires the use of Py-GC-MS for its characterisation.

1.2. Aims and Objectives

1.2.1 Aims

The aims of this research are to:

i. Characterise and analyse the organic matter (OM), mineralogy and microbial communities present at the ARD generation site and acidic ponds of Mam Tor (UK), including the source rock and indigenous vegetation.
ii. Use the Mam Tor source rock in microcosm incubations to relate ARD generation to the degradation of OM present in the source rock.
iii. Use natural OM sources present *in situ* (plants and manures) in microcosm incubations to determine/monitor ARD attenuation, the mineralogy and microbial communities with the degradation of different OM sources.
iv. To compare the organic geochemical and mineralogical data from Mam Tor and Parys Mountain to determine the role of organic matter in ARD/AMD environments.

1.2.2 Objectives

i. To determine the OM sources naturally present in certain ARD or AMD environments.
ii. To investigate the relationship between the bioavailability of indigenous OM and source rock from Mam Tor and ARD generation.
iii. To investigate the relationship between mineralogy, microbial communities and bioavailability of different natural OM sources with the attenuation of ARD.
iv. To compare the relative importance of OM in ARD/AMD systems from Mam Tor and Parys Mountain.

1.3. Approach and thesis structure

This thesis consists of a general introduction (**Chapter 1**) followed by three chapters written in a scientific paper format, a summary chapter, and appendices summarising the methods used in this study. This allows each chapter to stand alone as a piece of research, regardless of the repetition between chapters. Each of these chapters **(Chapter 2, 3** and **4)** will soon be submitted for publication.

The presence/type of OM and the biodiversity of acidophilic bacteria in an acidic pond at Mam Tor, UK were assessed in **Chapter 2**. The organic analyses showed an abundant amount of petroleum-derived OM in the sediment while the DNA analysis suggested a predominance of bacteria with the potential to degrade such compounds. The results of the microcosm experiments suggested that the mature OM detected was not involved in the generation of acidity and supported the use of carbon dioxide as the main carbon source at ARD sites.

The characterisation of an ARD pond from the debris zone of the Mam Tor, UK, is presented in **Chapter 3**. A substantial contribution of OM from the local vegetation was determined in the sediment dominated by goethite. The data from microcosm experiments enriched with either plant- or manure, showed a higher bioavailability of plant material when compared to manure amendments but despite of the higher bioavailability, the plant material was apparently not involved in the ARD neutralisation. In contrast, the addition of different manure-types had a significant effect on the microbial Fe(III)-reduction and greatly ameliorated the ARD conditions up to near neutral pH. These results indicated that manure addition can make an interesting and non expensive electron donor for ARD/AMD treatments, although the specific organic components present in manure that drive this process remain unclear.

Mineralogical analyses of Mam Tor sediments (scarp and debris zones) before and after incubations (**Chapter 2** and **Chapter 3**) suggested that the particle size of the mineral substrate (e.g. goethite) is a determining factor for the mineral bioavailability, and that independently of the type of OM used in the microcosm experiments (**Chapter 3**), it can support the microbial Fe(III)-reduction.

The characterisation of AMD sediments from Parys Mountain, UK (**Chapter 4**) indicated the presence of plant-derived OM in the site, with a mismatch between the OM composition of vegetation/biofilm overlying the ponds and the OM composition of the sediment below those layers. The results suggested that the surface OM is only used by the surface microbial community for fermentation processes and is not available for

the microbial community that could be established deeper down in the ponds. The predominantly Fe(II)-oxidising environment and the fermentation products detected may further limit the microbial Fe(III)-reduction in the site.

Finally, **Chapter 5** presents overall conclusions from the previous chapters and outlines future work that could be carried out in this field.

1.4. Author's and co-author's contributions to each paper.

a) Paper 1 (Chapter 2).

Author, the lead investigator, sample collection, characterising bulk starter material, setting up and sampling aerobic microcosms, performing organic geochemical analyses, modelling and interpreting mineralogical data, performing data analyses and interpretation, writing up the manuscript.

David J. Vaughan, Jonathan R. Lloyd and *Bart E. van Dongen*, sample collection, full conceptual guidance and manuscript review.

b) Paper 2 (Chapter 3).

Author, the lead investigator, sample collection, characterising bulk starter material, setting up and sampling anaerobic microcosms, performing organic geochemical analyses, modelling and interpreting mineralogical data, performing data analyses and interpretation, writing up the manuscript.

Carolina V. Scarincci, sample collection (plant material), setting up and sampling of plant-amended microcosm experiments.

Adam Burke, Sample collection (manures), setting up and sampling of manure-amended microcosm experiments.

David J. Vaughan, Jonathan R. Lloyd and Bart E. van Dongen, sample collection, full conceptual guidance and manuscript review.

c) Paper 3 (Chapter 4).

Author, the lead investigator, sample collection, characterising the samples, performing and interpreting organic geochemistry analyses, writing up the manuscript.

David J. Vaughan, Jonathan R. Lloyd and *Bart E. van Dongen,* sample collection, conceptual guidance and manuscript review.

REFERENCES

Akcil, A. and S. Koldas (2006). "Acid Mine Drainage (AMD): causes, treatment and case studies." Journal of Cleaner Production **14**(12–13): 1139-1145.

Baker, B. J. and J. F. Banfield (2003). "Microbial communities in acid mine drainage." FEMS Microbiology Ecology **44**(2): 139-152.

Baker, B. J., P. Hugenholtz, S. C. Dawson and J. F. Banfield (2003). "Extremely Acidophilic Protists from Acid Mine Drainage Host Rickettsiales-Lineage Endosymbionts That Have Intervening Sequences in Their 16S rRNA Genes." Applied and Environmental Microbiology **69**(9): 5512-5518.

Banks, D., P. L. Younger, R.-T. Arnesen, E. R. Iversen and S. B. Banks (1997). "Mine-water chemistry: the good, the bad and the ugly." Environmental Geology **32**(3): 157-174.

Banks, S. B. and D. Banks (2001). "Abandoned mines drainage: impact assessment and mitigation of discharges from coal mines in the UK." Engineering Geology **60**(1–4): 31-37.

Bennett, J. and H. Tributsch (1978). "Bacterial leaching patterns on pyrite crystal surfaces." Journal of Bacteriology **134**(1): 310-317.

Bigham, J. M., U. Schwertmann, S. J. Traina, R. L. Winland and M. Wolf (1996). "Schwertmannite and the chemical modeling of iron in acid sulfate waters." Geochimica et Cosmochimica Acta **60**(12): 2111-2121.

Bowen, G. G., C. Dussek and R. M. Hamilton (1998). "Pollution resulting from the abandonment and subsequent flooding of Wheal Jane Mine in Cornwall, UK." Geological Society, London, Special Publications **128**(1): 93-99.

Brown, M. E. and M. C. Y. Chang (2014). "Exploring bacterial lignin degradation." Current Opinion in Chemical Biology **19**(0): 1-7.

Bruneel, O., N. Pascault, M. Egal, C. Bancon-Montigny, M. S. Goñi-Urriza, F. Elbaz-Poulichet, J. C. Personné and R. Duran (2008). "Archaeal diversity in a Fe–As rich acid mine drainage at Carnoulès (France)." Extremophiles **12**(4): 563-571.

Caccavo, F., P. C. Schamberger, K. Keiding and P. H. Nielsen (1997). "Role of Hydrophobicity in Adhesion of the Dissimilatory Fe(III)-Reducing Bacterium Shewanella alga to Amorphous Fe(III) Oxide." Applied and Environmental Microbiology **63**(10): 3837-3843.

Chen, A., C. Lin, W. Lu, Y. Wu, Y. Ma, J. Li and L. Zhu (2007). "Well water contaminated by acidic mine water from the Dabaoshan Mine, South China: Chemistry and toxicity." Chemosphere **70**(2): 248-255.

Childers, S. E., S. Ciufo and D. R. Lovley (2002). "Geobacter metallireducens accesses insoluble Fe(iii) oxide by chemotaxis." Nature **416**(6882): 767-769.

Choudhary, R. P. and A. S. Sheoran (2012). "Performance of single substrate in sulphate reducing bioreactor for the treatment of acid mine drainage." Minerals Engineering **39**(0): 29-35.

Cole, M., J. Wrubel, P. Henegan, C. Janzen, J. Holt and T. Tobin (2011). "Development of a small-scale bioreactor method to monitor the molecular diversity and environmental impacts of bacterial biofilm communities from an acid mine drainage impacted creek." Journal of Microbiological Methods **87**(1): 96-104.

Colmer, A. R. and M. Hinkle (1947). "The role of microorganisms in acid mine drainage: a preliminary report." Science **106**(2751): 253-256.

Colmer, A. R., K. L. Temple and M. E. Hinkle (1950). "An iron-oxidizing bacterium from the acid drainage of some bituminous coal mines." Journal of bacteriology **59**(3): 317.

Coulton, R., C. Bullen and C. Hallett (2003). "The design and optimisation of active mine water treatment plants." Land Contamination and Reclamation **11**(2): 273-280.

Coupland, K. and D. B. Johnson (2004). "Geochemistry and microbiology of an impounded subterranean acidic water body at Mynydd Parys, Anglesey, Wales." Geobiology **2**(2): 77-86.

Craig, J. R., F. M. Vokes and T. N. Solberg (1998). "Pyrite: physical and chemical textures." Mineralium Deposita **34**(1): 82-101.

Cutting, R. S., V. S. Coker, J. W. Fellowes, J. R. Lloyd and D. J. Vaughan (2009). "Mineralogical and morphological constraints on the reduction of Fe(III) minerals by Geobacter sulfurreducens." Geochimica et Cosmochimica Acta **73**(14): 4004-4022.

David, C. P. C. (2003). "Establishing the impact of acid mine drainage through metal bioaccumulation and taxa richness of benthic insects in a tropical Asian stream (the Philippines)." Environmental Toxicology and Chemistry **22**(12): 2952-2959.

Davis Jr, R. A., A. T. Welty, J. Borrego, J. A. Morales, J. G. Pendon and J. G. Ryan (2000). "Rio Tinto estuary (Spain): 5000 years of pollution." Environmental Geology **39**(10): 1107-1116.

Durand, B. (1980). Kerogen: Insoluble organic matter from sedimentary rocks, Editions technip.

Eglinton, G. and R. Hamilton (1963). "The distribution of alkanes." Chemical Plant Taxonomy **187**: 217.

Eglinton, G. and R. J. Hamilton (1967). "Leaf Epicuticular Waxes." Science **156**(3780): 1322-1335.

Ferris, F. G., K. Tazaki and W. S. Fyfe (1989). "Iron oxides in acid mine drainage environments and their association with bacteria." Chemical Geology **74**(3–4): 321-330.

Forsman, J. P. and J. M. Hunt (1958). "Insoluble organic matter (kerogen) in sedimentary rocks." Geochimica et Cosmochimica Acta **15**(3): 170-182.

Gaines, S. M., G. Eglinton and R. J. (2009). Echoes of Life: What Fossil Molecules Reveal About Earth History, New York: Oxford University Press.

Gibert, O., J. de Pablo, J. L. Cortina and C. Ayora (2005). "Sorption studies of Zn(II) and Cu(II) onto vegetal compost used on reactive mixtures for in situ treatment of acid mine drainage." Water Research **39**(13): 2827-2838.

Gordon, A. R. (1994). "Environmental Consequences of Coal Mine Closure." The Geographical Journal **160**(1): 33-40.

Grimalt, J. O., M. Ferrer and E. Macpherson (1999). "The mine tailing accident in Aznalcollar." Science of The Total Environment **242**(1–3): 3-11.

Hallberg, K. B. (2010). "New perspectives in acid mine drainage microbiology." Hydrometallurgy **104**(3–4): 448-453.

Hallberg, K. B. and D. B. Johnson (2005). "Biological manganese removal from acid mine drainage in constructed wetlands and prototype bioreactors." Science of The Total Environment **338**(1–2): 115-124.

Harrison, A. P. (1984). "The Acidophilic Thiobacilli and other acidophilic bacteria that share their habitat." Annual Review of Microbiology **38**(1): 265-292.

Harvey, R., R. Hannah and J. Vaughan (2011). "Selective precipitation of mixed nickel–cobalt hydroxide." Hydrometallurgy **105**(3–4): 222-228.

Hatakka, A. (1994). "Lignin-modifying enzymes from selected white-rot fungi: production and role from in lignin degradation." FEMS Microbiology Reviews **13**(2–3): 125-135.

Hedrich, S., M. Schlömann and D. B. Johnson (2011). "The iron-oxidizing proteobacteria." Microbiology **157**(6): 1551-1564.

Herrera, S. P., H. Uchiyama, T. Igarashi, K. Asakura, Y. Ochi, F. Ishizuka and S. Kawada (2007). "Acid mine drainage treatment through a two-step neutralization ferrite-formation process in northern Japan: Physical and chemical characterization of the sludge." Minerals Engineering **20**(14): 1309-1314.

Jiang, J. and A. Kappler (2008). "Kinetics of Microbial and Chemical Reduction of Humic Substances: Implications for Electron Shuttling." Environmental Science & Technology **42**(10): 3563-3569.

Johnson, D. B. (1995). "Selective solid media for isolating and enumerating acidophilic bacteria." Journal of Microbiological Methods **23**(2): 205-218.

Johnson, D. B. (1998). "Biodiversity and ecology of acidophilic microorganisms." FEMS Microbiology Ecology **27**(4): 307-317.

Johnson, D. B. (2003). "Chemical and microbiological characteristics of mineral spoils and drainage waters at abandoned coal and metal mines." Water, Air and Soil Pollution: Focus **3**(1): 47-66.

Johnson, D. B. (2012). "Geomicrobiology of extremely acidic subsurface environments." FEMS Microbiology Ecology **81**(1): 2-12.

Johnson, D. B. and T. A. M. Bridge (2002). "Reduction of ferric iron by acidophilic heterotrophic bacteria: evidence for constitutive and inducible enzyme systems in Acidiphilium spp." Journal of Applied Microbiology **92**(2): 315-321.

Johnson, D. B., M. A. Ghauri and M. F. Said (1992). "Isolation and characterization of an acidophilic, heterotrophic bacterium capable of oxidizing ferrous iron." Applied and Environmental Microbiology **58**(5): 1423-1428.

Kim, J., S. Kim and K. Tazaki (2002). "Mineralogical characterization of microbial ferrihydrite and schwertmannite, and non-biogenic Al-sulfate precipitates from acid mine drainage in the Donghae mine area, Korea." Environmental Geology **42**(1): 19-31.

Kirby, C. S., H. M. Thomas, G. Southam and R. Donald (1999). "Relative contributions of abiotic and biological factors in Fe(II) oxidation in mine drainage." Applied Geochemistry **14**(4): 511-530.

Lin, C., Y. Wu, W. Lu, A. Chen and Y. Liu (2007). "Water chemistry and ecotoxicity of an acid mine drainage-affected stream in subtropical China during a major flood event." Journal of Hazardous Materials **142**(1–2): 199-207.

Malmström, M. E., G. Destouni, S. A. Banwart and B. H. E. Strömberg (2000). "Resolving the Scale-Dependence of Mineral Weathering Rates." Environmental Science & Technology **34**(7): 1375-1378.

Matlock, M. M., B. S. Howerton and D. A. Atwood (2002). "Chemical precipitation of heavy metals from acid mine drainage." Water Research **36**(19): 4757-4764.

Mays, P. A. and G. S. Edwards (2001). "Comparison of heavy metal accumulation in a natural wetland and constructed wetlands receiving acid mine drainage." Ecological Engineering **16**(4): 487-500.

Mitsch, W. J. and K. M. Wise (1998). "Water quality, fate of metals, and predictive model validation of a constructed wetland treating acid mine drainage." Water Research **32**(6): 1888-1900.

Murad, E. and P. Rojík (2003). "Iron-rich precipitates in a mine drainage environment: Influence of pH on mineralogy." American Mineralogist **88**(11-12): 1915-1918.

Naicker, K., E. Cukrowska and T. S. McCarthy (2003). "Acid mine drainage arising from gold mining activity in Johannesburg, South Africa and environs." Environmental Pollution **122**(1): 29-40.

Ñancucheo, I. and D. B. Johnson (2010). "Production of Glycolic Acid by Chemolithotrophic Iron- and Sulfur-Oxidizing Bacteria and Its Role in Delineating and Sustaining Acidophilic Sulfide Mineral-Oxidizing Consortia." Applied and Environmental Microbiology **76**(2): 461-467.

Neal, C., P. G. Whitehead, H. Jeffery and M. Neal (2005). "The water quality of the River Carnon, west Cornwall, November 1992 to March 1994: the impacts of Wheal Jane discharges." Science of The Total Environment **338**(1–2): 23-39.

Nevin, K. P. and D. R. Lovley (2000). "Lack of Production of Electron-Shuttling Compounds or Solubilization of Fe(III) during Reduction of Insoluble Fe(III) Oxide by Geobacter metallireducens." Applied and Environmental Microbiology **66**(5): 2248-2251.

Nordstrom, D. K., C. N. Alpers, C. J. Ptacek and D. W. Blowes (1999). "Negative pH and Extremely Acidic Mine Waters from Iron Mountain, California." Environmental Science & Technology **34**(2): 254-258.

Pain, D. J., A. Sánchez and A. A. Meharg (1998). "The Doñana ecological disaster: Contamination of a world heritage estuarine marsh ecosystem with acidified pyrite mine waste." Science of The Total Environment **222**(1–2): 45-54.

Rawlings, D. E., H. Tributsch and G. S. Hansford (1999). "Reasons why 'Leptospirillum'-like species rather than Thiobacillus ferrooxidans are the dominant iron-oxidizing bacteria in many commercial processes for the biooxidation of pyrite and related ores." Microbiology **145**(1): 5-13.

Rimstidt, J. D. and D. J. Vaughan (2003). "Pyrite oxidation: a state-of-the-art assessment of the reaction mechanism." Geochimica et Cosmochimica Acta **67**(5): 873-880.

Robins, R. G. (1993). "Chemical Interactions in Sulfide Mineral Tailings∗." Mineral Processing and Extractive Metallurgy Review **12**(1): 1-17.

Roger, M., C. Castelle, M. Guiral, P. Infossi, E. Lojou, M. T. Giudici-Orticoni and M. Ilbert (2012). "Mineral respiration under extreme acidic conditions: from a supramolecular organization to a molecular adaptation in Acidithiobacillus ferrooxidans." Biochemical Society Transactions **40**(part 6): 1324-1329.

Rosenberg, C. E., B. N. Carpinetti and C. Apartín (2001). "Contenido de Metales Pesados en Tejidos de Sábalos (Prochilodus Lineatus) del Río Pilcomayo, Misión La Paz, Provincia de Salta." Natura Neotropicalis **2**(32): 141-145.

Schoeman, J. J. and A. Steyn (2001). "Investigation into alternative water treatment technologies for the treatment of underground mine water discharged by Grootvlei Proprietary Mines Ltd into the Blesbokspruit in South Africa." Desalination **133**(1): 13-30.

Singer, P. C. and W. Stumm (1970). "Acidic Mine Drainage: The Rate-Determining Step." Science **167**(3921): 1121-1123.

Smolders, A. J. P., R. A. C. Lock, G. Van der Velde, R. I. Medina Hoyos and J. G. M. Roelofs (2003). "Effects of mining activities on heavy metal concentrations in water, sediment, and macroinvertebrates in different reaches of the Pilcomayo River, South America." Archives of Environmental Contamination and Toxicology **44**(3): 0314-0323.

Solà, C., M. a. Burgos, Á. Plazuelo, J. Toja, M. Plans and N. s. Prat (2004). "Heavy metal bioaccumulation and macroinvertebrate community changes in a Mediterranean stream affected by acid mine drainage and an accidental spill (Guadiamar River, SW Spain)." Science of The Total Environment **333**(1–3): 109-126.

Sudilovskiy, P. S., G. G. Kagramanov and V. A. Kolesnikov (2008). "Use of RO and NF for treatment of copper containing wastewaters in combination with flotation." Desalination **221**(1–3): 192-201.

Sullivan, P. and J. Yelton (1988). "An evaluation of trace element release associated with acid mine drainage." Environmental Geology and Water Sciences **12**(3): 181-186.

Swoboda-Colberg, N. G. and J. I. Drever (1993). "Mineral dissolution rates in plot-scale field and laboratory experiments." Chemical Geology **105**(1–3): 51-69.

Tünay, O. and N. I. Kabdaşli (1994). "Hydroxide precipitation of complexed metals." Water Research **28**(10): 2117-2124.

Tutu, H., T. S. McCarthy and E. Cukrowska (2008). "The chemical characteristics of acid mine drainage with particular reference to sources, distribution and remediation: The Witwatersrand Basin, South Africa as a case study." Applied Geochemistry **23**(12): 3666-3684.

Valente, T., J. A. Grande, M. L. de la Torre, M. Santisteban and J. C. Cerón (2013). "Mineralogy and environmental relevance of AMD-precipitates from the Tharsis mines, Iberian Pyrite Belt (SW, Spain)." Applied Geochemistry **39**(0): 11-25.

Vancampenhout, K., K. Wouters, B. De Vos, P. Buurman, R. Swennen and J. Deckers (2009). "Differences in chemical composition of soil organic matter in natural ecosystems from different climatic regions – A pyrolysis–GC/MS study." Soil Biology and Biochemistry **41**(3): 568-579.

Vaughan, D. J. and J. R. Craig (1978). Mineral chemistry of metal sulfides, Cambridge University Press Cambridge.

Vaughan, D. J. and J. R. Lloyd (2011). "Mineral-organic-microbe interactions: Environmental impacts from molecular to macroscopic scales." Comptes Rendus Geoscience **343**(2–3): 140-159.

Vestal, J. R. and D. C. White (1989). "Lipid Analysis in Microbial Ecology." BioScience **39**(8): 535-541.

Vile, M. and R. K. Wieder (1993). "Alkalinity generation by Fe(III) reduction versus sulfate reduction in wetlands constructed for acid mine drainage treatment." Water, Air, and Soil Pollution **69**(3-4): 425-441.

Volkman, J. K., D. G. Holdsworth, G. P. Neill and H. J. Bavor Jr (1992). "Identification of natural, anthropogenic and petroleum hydrocarbons in aquatic sediments." Science of The Total Environment **112**(2–3): 203-219.

Weber, K. A., L. A. Achenbach and J. D. Coates (2006). "Microorganisms pumping iron: anaerobic microbial iron oxidation and reduction." Nature Reviews Microbiology **4**(10): 752-764.

Whitehead, P. G. and H. Prior (2005). "Bioremediation of acid mine drainage: an introduction to the Wheal Jane wetlands project." Science of The Total Environment **338**(1–2): 15-21.

WHO (2012). UN-water global annual assessment of sanitation and drinking-water (GlAAS) 2012 report: the challenge of extending and sustaining services, World Health Organization.

Wood, A. P. and D. P. Kelly (1983). "Autotrophic and mixotrophic growth of three thermoacidophilic iron-oxidizing bacteria." FEMS Microbiology Letters **20**(1): 107-112.

Younger, P. L. (1997). "The longevity of minewater pollution: a basis for decision-making." Science of The Total Environment **194–195**(0): 457-466.

Younger, P. L. (2001). "Mine water pollution in Scotland: nature, extent and preventative strategies." Science of The Total Environment **265**(1–3): 309-326.

Zhou, J.-M., Z. Dang, M.-F. Cai and C.-Q. Liu (2007). "Soil heavy metal pollution around the Dabaoshan Mine, Guangdong Province, China." Pedosphere **17**(5): 588-594.

Zinck, J. and W. Griffith (2013). Review of mine drainage treatment and sludge management operations. Canada, Mine Environment Neutral Drainage (MEND) Program.

CHAPTER 2

Paper 1: The potential metabolism of petroleum-derived hydrocarbons in acid rock drainage systems

This chapter contains the following paper which is under preparation to be submitted to the journal: Journal of Applied Geochemistry.

Martha E. Jiménez-Castañeda[1]; Jonathan R. Lloyd[1]; David J. Vaughan[1]; Bart E. van Dongen[1,*]

[1] School of Earth, Atmospheric and Environmental Sciences, Williamson Research Centre for Molecular Environmental Science, University of Manchester, Manchester, UK.
* Corresponding author: Tel.: +44 161 3067460; fax: +44 161 3069361.
E-mail address: Bart.vanDongen@manchester.ac.uk

Abstract

The potential use of mature petroleum derived organic matter during the ARD generation was investigated on an acidic pond at Mam Tor, UK. This ARD-generating site is located on an active landslide where the continuous motion is permanently exposing fresh pyrite to the weather action, leading to the production of acidic waters for over 3000 years.

Substantial amounts of mature petroleum-derived organic matter were detected in the sediment hosting a range of acidophilic bacteria with the potential to degrade petroleum-related compounds. Mössbauer analyses suggested that jarosite was the product of microbial Fe(II)-oxidation while organic analyses indicated that the mature petroleum-derived organic matter was not degraded under aerobic and acidic conditions. Therefore, this type of carbon input may not be involved in the reactions and/or microbial metabolism related to ARD generation, consistent with a pivotal role for chemolithotrophic bacteria in mediation of Fe(II)-oxidation.

Key words: ARD, AMD, petroleum degradation, mature organic matter, Mössbauer, GC-MS, Py-GC-MS.

2.1. Introduction

Acid rock (or mine) drainage is an extreme environmental condition, characterised by waters of low pH and elevated concentrations of ferrous and ferric iron, sulfur and other dissolved metals. This phenomenon threatens human health (Chen et al. 2007, Zhou et al. 2007, Corkhill et al. 2008), has severe ecological effects (Grimalt et al. 1999, Solà et al. 2004) and also considerable treatment/remediation costs (Zinck and Griffith 2013). Acid mine drainage (AMD) is particularly associated with active and abandoned mine working, although acidic streams commonly arise from the weathering of naturally exposed pyrite (acid rock drainage, ARD).

The breakdown of pyrite during aqueous oxidation is a relatively complex multistage process (Rimstidt and Vaughan 2003) which can be simplistically represented by the overall reaction (Singer and Stumm 1970):

$$4FeS_2+15O_2+14H_2O \rightarrow 4\ Fe(OH)_3+8SO_4^{-2}+16H^+$$

This reaction is accelerated by a factor of 10^6 in presence of extremophilic acidophilic or acid tolerant microorganisms such as *Acidithiobacillus ferrooxidans* (Singer and

Stumm 1970). These bacteria fix atmospheric CO_2 as a carbon source and grow using energy obtained from the oxidation of reduced sulfur compounds and/or ferrous iron (Ingledew 1982, Jones and Kelly 1983).

The metabolism of *A. ferrooxidans* is not surprising because at AMD-generating sites Fe(II) is rather stable and available, even in the presence of atmospheric oxygen (Roger et al. 2012) and the carbon concentration is scarce (Johnson 2012); In consequence, the microbial populations are expected to be predominantly chemoautotrophs. Heterotrophic and mixotrophic bacteria have also been identified in association with chemoautotrophs (Wood and Kelly 1983, Harrison 1984, Johnson et al. 1992, Johnson and Bridge 2002), raising questions about the potential use of carbon sources to mediate some microbial processes. For example, petroleum-derived hydrocarbons naturally seeping into shallow sediments from deeper, more thermally mature sediments have been shown to act as a carbon source in the arsenic mobilisation within South East Asian aquifers (Rowland et al. 2006, Postma et al. 2007, Rowland et al. 2007, van Dongen et al. 2008). Petroleum-derived hydrocarbons may also occur naturally in the source rocks of ARD sites (Pering and Ponnamperuma 1969, Nooner et al. 1973, Pering 1973) and could stimulate microbial processes that ultimately lead to the ARD generation.

In particular, the biodegradation of petroleum-derived compounds under near neutral conditions is well documented (Leahy and Colwell 1990, Atlas 1991, Sivagurunathan et al. 2003, Obuekwe et al. 2009, Horel and Schiewer 2014) but few works have studied the biodegradation of certain petroleum-derived compounds, such as aromatic hydrocarbons at low pH (Stapleton et al. 1998, Uyttebroek et al. 2007). A study that considered the presence of petroleum-derived hydrocarbons in an acid-sulfate soil, similar to those of ARD environments, was carried out by Hamamura et al. (2005). They studied the microbial diversity of the site and reported alkane degradation by an acidophilic microorganism (isolate *C197*) relevant in the hydrocarbon-rich acidic soil environment, but it is presently unclear whether the occurrence of petroleum-derived hydrocarbons (mature organic matter) at ARD generating environments is involved in the microbial processes that lead to the ARD generation itself. In this work the presence of mature organic matter at an ARD site was determined and their influence in the ARD generation was tested.

2.2. MATERIALS AND METHODS

2.2.1 Study site and sample collection

The Mam Tor landslide (Derbyshire, UK), initially formed at least 3200 years ago (Donnelly 2006, Rutter and Green 2011), is comprised of a sequence of shales, siltstones and fine-grained, sole-marked sandstones (the Mam Tor beds) overlying dark pyritic shales and dark gray mudstones (Edale Shales) with the high ground south of Mam Tor formed by limestone (Skempton et al. 1989, Waltham and Dixon 2000) (Figure 2.1). Some of these layers are fossiliferous (Jackson 1925) and have been associated with petroleum-derived hydrocarbons (Pering and Ponnamperuma 1969, Nooner et al. 1973, Pering 1973). Mam Tor is still moving at a velocity of 7 cm/y in the edges and 0. 5 m/y in the middle section (Skempton et al. 1989, Waltham and Dixon 2000, Rutter and Green 2011) producing the constant breakdown of the source rock and therefore, continuously generating ARD (Vear and Curtis 1981).

A sample of ARD sediment was collected from the surface of an acidic pond in the Mam Tor scarp zone (Figure 2.1), using a stainless steel scoop and transferred into clean (acid washed and prefurnaced) glass jars to minimise contamination. Subsamples for DNA isolation were frozen at -80ºC upon return to the laboratory. Other subsamples were separated and anaerobically dried for Mössbauer analysis or freeze-dried for *n*-alkane characterisation, X-Ray (powder) diffraction (XRD) and X-Ray Fluorescence (XRF) analyses. The remaining ARD sediment was stored in the dark at -4°C to minimise any microbial activity until use in microcosm experiments.

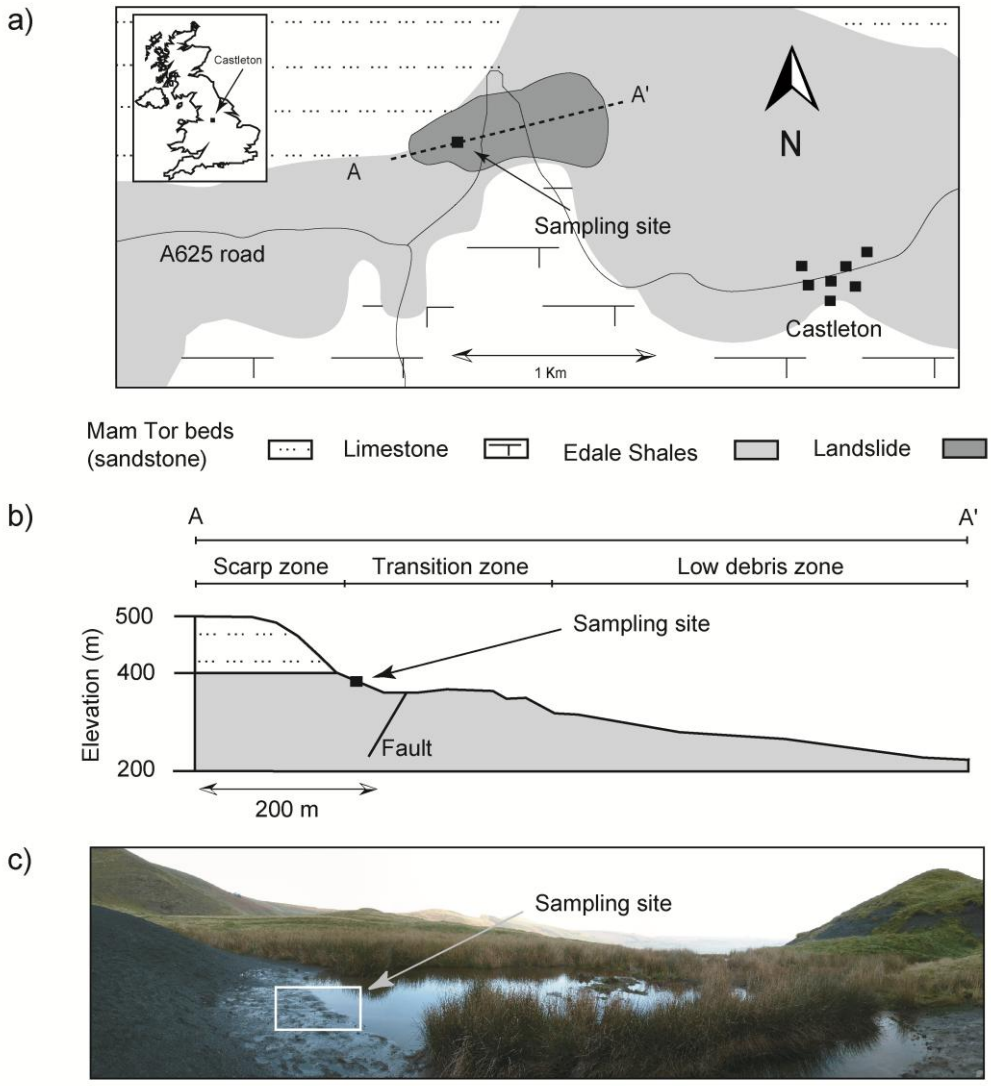

Figure 2.1. a) Location and geological map of Mam Tor. b) Cross section along the A-A' line, showing the vertical structure of Mam Tor and horizontal divisions. c) Picture of the sampling pond at the scarp zone, next to the fresh crushed source rock. Figure modified from Skempton et al. (1989) and Waltham and Dixon (2000).

2.2.2 Aerobic microcosms

To test the potential use of petroleum-derived hydrocarbons in the ARD generation, series of aerobic microcosms were set up using the ARD sediment and the 9K liquid medium for acidophilic microorganisms (Silverman and Lundgren 1959, Johnson 1995). To differentiate abiotic processes, a series of control samples were also prepared using heat sterilised sediment (121ºC; 30 min). Both conditions, the aerobic microcosm and the control experiment, were prepared in triplicate using 250 ml of the 9K medium

and 2.5 g of either fresh ARD sediment or sterilised ARD sediment, respectively. The 9K medium was prepared by mixing carefully the filter sterilised (0.22 μm) iron source (Johnson 1995), the heat sterilised basal salts (121°C; 30 min) and acidifying the medium to pH ~2 (Table 2.1). All microcosms were incubated for 28 days at 20°C using a shaking incubator at 100 rpm.

Table 2.1. 9K medium for acidophilic microorganisms

Reagents	Amount
Basal salts	
$(NH_4)_2SO_4$	3 g
KCl	0.1 g
K_2HPO_4	0.5 g
$MgSO_4.7H_2O$	0.5 g
$Ca(NO_3)_2$	0.01 g
Distilled H_2O	700 ml
$FeSO_4.7H_2O$	20 mM
Distilled H_2O	300 ml
H_2SO_4	To reach pH 2

Slurry samples from the aerobic and control microcosms were taken at times t_0, t_7, t_{14} and t_{28} (0, 7, 14 and 28 incubation days, respectively) for pH, Eh and iron content measurements. The pH and Eh were measured on a Basic Denver pH/ORP meter (Denver Instrument Company) with 3M KCl liquid-filled electrode Ag/AgCl reference. The Fe(II)-oxidation rate was monitored from the optical absorbance (562 nm) of the samples using the ferrozine method (Stookey 1970) on a Jenway 6715 UV/visible spectrophotometer with total iron concentration determined after hydroxylamine hydrochloride reaction (Lovley and Phillips 1987). Subsamples taken at t_0 and t_{28} were immediately filtered (0.22 μm) for Volatile Organic Compounds (VOCs) determination by Ion Chromatography. After incubation (t_{28}), the triplicates were mixed into clean glass jars and subsamples taken for DNA and Mössbauer analyses storing them at -80°C or anaerobically dried, respectively. The rest of the slurries were freeze-dried for organic and XRD analyses.

2.2.3 Analyses of Mam Tor sediment and microcosms slurries

2.2.3.1 Mineralogy and geochemistry

The mineralogy and geochemistry of the ARD sediment (t_o) was determined using Mössbauer Spectroscopy along with XRF and XRD analyses performed at the University of Manchester facilities. For XRF analysis, a pressed pellet prepared with 12 g of pulverised sediment and 3 g of wax binder was used for quantification of major, minor and trace elements on an Axios Sequential XRF Spectrometer (PANalytical, Almelo, Netherlands). XRD data was obtained on a Bruker D8 Advanced Instrument with $CuK_{\alpha 1}$ radiation, over a range of 5°2θ to 7°2θ, using a step size of 0.02° each 2 s. Mössbauer data was collected at room and near liquid nitrogen temperature on a FAST ComTeC 1024-multichannel analyser system, using a constant acceleration drive with a ~25 mCi ^{57}Co/Rh γ-ray source and metallic iron foil for calibration. The spectra were fitted using the Lagarec/Rancourt Recoil software (Intelligent Scientific Applications Inc., Ottawa, ON, Canada; v. 1.0). Mineralogical analyses of the microcosm slurries after incubation (t_{28}) were accomplished using Mössbauer spectroscopy and XRD analyses as described above.

2.2.3.2 Organic matter content

To quantify any changes on the total organic matter content due to microbial activity, subsamples of the control (control t_{28}) and the microcosm experiment (sediment t_{28}), taken in triplicate, were used for the sequential loss on ignition method (Heiri et al. 2001, Beaudoin 2003). Here, 500 mg of freeze-dried slurries were weighed accurately, using constant weight vials. The vials containing the samples were heated at 105°C for 12 h, cooled down into a desiccator, weighed and ignited at 350°C for 16 h. Subsequently, they were cooled down into desiccator and weighed again. The content of organic matter was the weight difference of the samples at 105°C and at 350°C, expressed in percentage abundance.

2.2.3.3 Gas Chromatography Mass Spectrometry (CG-MS) analyses

To characterise the saturated hydrocarbons, a subsample of the sediment t_o (40 g) was freeze dried, homogenised and extracted using a Soxleth apparatus with a dichloromethane/methanol solution (DCM/MeOH, 2:1, v/v) for 24 h to obtain the total lipid extract (TLE). TLEs from the control t_{28} and sediment t_{28} slurries, were ultrasonic extracted (3x) from 3 g of freeze-dried samples, using the modified Bligh-Dyer extraction method (White et al. 1979, Frostegård et al. 1991) with a single phase

mixture of chloroform:methanol:water buffered with KH_2PO_4 to pH ~7.2 (1:2:0.8 v/v/v; 18 ml).

The lipid fractions were collected every time, washed using water buffered with KH_2PO_4, combined and concentrated using rotary evaporation and nitrogen blowing down. Subsequently, the TLEs were re-dissolved in DCM and desulfurised using activated copper prepared according Blumer (1957). Small amounts of activated Cu were added to the TLEs, sonicated until no more reaction, filtered over glass wool columns and concentrated using a smooth nitrogen flow. After the addition of the internal standard (tetracosane-d50), the desulfurised aliquots were fractionated according to the method described in Dickson et al. (2009). Briefly, the aliquots were passed through a silica column using 10 ml of a solution of $CHCl_3$ saturated with NH_3OH to obtain the simple lipids. Subsequently this fraction was eluted on an aluminium column using 6 ml of a hexane/DCM solution (9:1, v/v) to obtain the hydrocarbon fraction (*n*-alkanes). To ensure that no contamination was introduced during extraction and fractionation procedures, blanks were also prepared and analysed. The saturated hydrocarbon fractions were concentrated in 50 µl of hexane for Gas Chromatography Mass Spectrometry (GC-MS) analysis.

GC-MS analyses were carried out on an Agilent 7890A GC system equipped with an Agilent 7683B auto-sampler and programmable temperature vaporization (PVT) inlet, interfaced to an Agilent 5975C MSD mass spectrometer operated in electron ionization mode (scanning a range, *m/z* 50–600 at 2.7 scans/s; ionisation energy, 70 eV; solvent delay of 3 min) using helium as the carrier gas at a constant flow (1 mL/min). The heated interface and PTV temperatures were set to 280°C; the mass source, at 230°C and the mass spectrometer quadrupole, at 150°C. The analytical separation of the saturated hydrocarbons was accomplished using a 30 m x 0.25 mm (i. d.) HP-5 MS capillary column (Agilent; (5%-Phenyl)-methylpolysiloxane) programmed from 70°C to 130°C at 20°C/min, then to 320 °C at 4 °C/min and kept at isothermally for 10 min. Individual compounds were identified by comparison of their molecular mass (*m/z*) with The National Institute of Standards and Technology (NIST) library. Quantitative data were determined by comparison of individual peak areas with a known concentration of the internal standard.

The high molecular weight (HMW) *n*-alkane odd-over-even predominance was expressed in the carbon preference index (CPI), using the following equation (van Dongen et al. 2008):

$CPI_{i-n}=0.5[(X_i+X_{i+2}+...+X_n)/(X_{i-1}+X_{i+1}+...+X_{n-1})]+0.5[(X_i+X_{i+2}+...+X_n)/(X_{i+1}+X_{i+3}...+X_{n+1})]$

where X is the *n*-alkane concentration in the range from *i* to *n*.

The average chain length (ACL) of the HMW *n*-alkanes was calculated using the following equation (van Dongen et al. 2008):

$ACL= \Sigma(iX_i + ... + nX_n)/\Sigma(X_i + ... +X_n)$,

where X is the *n*-alkane concentration in the range from *i* to *n*.

2.2.3.4 Pyrolysis (Py)-GC-MS analyses

To determine changes in the macromolecular composition of the samples, subsamples of the freeze-dried slurries (control and sediment; t_{28}), were analysed by Py-GC-MS. To avoid interferences due the presence of iron oxides (Tessier et al. 1979, Horsfield and Douglas 1980, Baldock and Skjemstad 2000), the subsamples were demineralised following a modification on the Gélinas et al. (2001) method. For this, 0.25 g of freeze-dried slurries were mixed with 30 ml of 1M HCl into sterile universal plastic tubes and agitated at room temperature (60 min) using a magnetic stirrer. After centrifuging (2700 rpm; 15 min) for HCl removal, the residues were digested in a solution of HCl/HF (10% HF in 1M HCl; v/v; 12 h). The products of the digestion were rinsed with distilled water (3x; 3.5 ml) and freeze-dried. Hereafter, the demineralised subsamples were ready for Py-GC-MS analysis.

Triplicates (1.2 µg each) of the demineralised slurries were pyrolysed in a quartz tube at 600°C (10s) on a Chemical Data System 5200 Series Pyroprobe Pyrolysis Unit coupled to the GC-MS system described earlier. In the GC-MS system, helium was the carrier gas used in split mode (ratio 5:1; constant flow, 1 ml/min) and the HP-5 MS capillary column used was the same HP-5 MS column as described above. The pyrolysis transfer line and injector temperatures were set at 350°C; the heated interface, at 280°C; the electron ionization source, at 230°C, and the mass spectrometer quadrupole, at 150°C. The oven was programmed from 40°C for 3 min to 300°C at 4°C/min for 15 min. The macromolecular compounds were identified by comparison of their molecular mass (*m/z*) with the NIST library.

A total of 84 different chemical compounds were identified in each pyrolysed sample. Their relative contribution was quantified as the percentage of the peak area of each compound out of the summed area of the 84 compounds (100%). To determine the

extent of biodegradation, those compounds were grouped into three classes: polysaccharides (ketones and cyclic hydrocarbons), aromatic compounds (benzenes and naphtalenes) and bipolymer compounds (*n*-alkanes, branched *n*-alkanes and *n*-alkenes).

2.2.3.5 Bacterial analysis

The bacterial communities present in Mam Tor sediment were identified by DNA analysis, isolated from 0.2 g of surface sediment (t_0) and 0.2 ml of microcosm slurry (sediment t_{28}) using the MoBio PowerLyzer™ UltraClean Microbial DNA Isolation Kit (MoBio Laboratories, Inc., Carlsbad, CA, USA). The bacterial primers 27F (Lane 1991) and 338R (Hamady et al. 2008), targeting the V1-V2 hypervariable region of the bacterial 16S rRNA gene, were applied in the PCR for amplicon pyrosequencing. This run was performed at the University of Manchester sequencing facility, on a Roche 454 Life Sciences GS Junior system. The pyrosequencing reads were analysed using QIIME v. 1.8.0 (Caporaso et al. 2010), for data denoising and chimera removal, during operational taxonomic unit (OTU) picking (at 97% sequence similarity) with USEARCH (Edgar 2010). QIIME was also applied for the taxonomic classification of all reads using the Ribosomal Database Project (RDP) at 80% confidence threshold (Cole et al. 2009) and to create the curves of bacterial population distribution. The closest GenBank match for the most representative sequence for each OTU was identified by BLASTN nucleotide search.

2.3. RESULTS AND DISCUSSION

2.3.1 Characterisation of the ARD sediment

The XRF analysis of the sediment t_0 showed a predominance of silica (60%), alumina (23.8%) and iron oxides (9%) components with a wide range of other elements in trace amounts (Table 2.2) most likely from phyllosilicate origin (Allen 1960, Ford et al. 1993). In accordance with the elemental composition, XRD diffractograms confirmed the presence of quartz (SiO_2) and a significant contribution of clays like montmorillonite ($(Na,Ca)_{0.33}(Al,Mg)_2Si_4O_{10}(OH)_2 \cdot nH2O$), and kaolinte ($Al_2Si_2O_5(OH)_4$) and mica such as muscovite ($KAl_2(AlSi_3O_{10})(F,OH)_2$).

Table 2.2. Elemental composition of the ARD sediment (t_0)

Major oxides (%)*		Trace element concentration (ppm)			
SiO_2	60.0	Ba	462	Cu	35
Al_2O_3	23.8	V	146	Nd	34
Fe_2O_3	9.0	W	143	Y	30
K_2O	2.7	Zr	140	Pb	21
SO_3	2.0	Rb	115	Ga	28
MgO	1.1	Ce	109	Nb	24
TiO_2	1.0	Cr	108	Co	25
CaO	0.1	Sr	98	Ni	21
Na_2O	0.3	Mn	62	Zn	18
		La	57	Mo	18
Total	100	As	51	Sc	14

* variation<0.1%

Mössbauer spectroscopy provided detailed information about the iron phases contained in the sediment t_0. At room temperature (Table 2.3), the Mössbauer spectrum was fitted with a doublet (isomer shift, δ/Fe=0.39 mm/s; quadrupole splitting, Δ=1.46 mm/s) interpreted as arising from jarosite and two associated doublets (δ/Fe=0.36 mm/, Δ=0.52 mm/s and δ/Fe=1.36 mm/s, Δ=2.34 mm/s) arising from Fe-containing clay minerals, probably illite. The parameters of the second doublet (Δ=0.52 mm/s) could also arise from goethite.

At near liquid nitrogen temperature (Table 2.3), the iron contributions were more clearly shown. Two sextets were fitted (δ/Fe=0.49 mm/s, magnetic field, H=467 kOe and δ/Fe=0.5 mm/s, H=425 kOe) and attributed to goethite. The reduced magnetic field of goethite (425 KOe; Table 2.3) may have several interpretations. This value could have arisen due the presence of surface atoms that produce magnetic hyperfine fields different from the bulk material (Morrish and Haneda 1983, Shinjo 1991, Bødker et al. 1994). Fine sized particles of goethite (van der Kraan and van Loef 1966, Bocquet et al. 1992) and some impurities, such as Al (Golden et al. 1979, Goodman and Lewis 1981), could also produce reduced magnetic field values.

A doublet that is present (δ/Fe=0.37 mm/s; Δ= 0.76 mm/s) may correspond to an amorphous iron oxide component, similar to those reported by Davison and Dickson (1984), plus a contribution from fine particles of goethite. Spectral contributions of jarosite (δ/Fe=0.49 mm/s; Δ=1.22 mm/s) and ferrous iron containing illite (δ/Fe=1.49 mm/s; Δ=2.58 mm/s) were also confirmed. The Mössbauer parameters of Mam Tor sediment t_0 are shown in Table 2.3.

Table 2.3. Mössbauer hyperfine parameters of the sediment before incubation (t_o)

T	δ/Fe (mm/s)	Δ (mm/s)	H (kOe)	Probable mineral	Values reported/References
RT	0.36	0.52		Goethite/ Fe-substituted mica (illite)	Goethite 0.34 –0.38; 0.5–0.70 Vandenberghe et al. (1986) 0.36–0.38; 0.56–0.65 Olowe et al. (1990) 0.38;0.58 Music et al. (1986) Illite 0.31;0.54 Malathi et al. (1969) 0.34–0.37; 0.49–0.62 Saporoschenko et al. (1980)
RT	0.39	1.15		Jarosite	0.36–0.43; 1.0–1.24 Russell and Montano (1978) 0.39; 1.13 Kovács et al. (2009) 0.38; 1.15–1.29 Nomura et al. (2007) 0.34–0.35; 1.1–1.3 Gancedo et al. (1992)
RT	1.36	2.34		Fe-substituted mica (illite)	1.01–1.31; 2.50–2.68 Russell and Montano (1978) 1.23–1.34; 2.4–2.7 Gancedo et al. (1992) 1.15; 2.86) Saporoschenko et al. (1980) 1.14–1.15; 2.15–2.69 Heller-Kallai and Rozenson (1981) 1.39; 2.34 Audley et al. (1986)

T= temperature.
δ/Fe= isomer shift relative to metallic iron.
Δ= Quadrupole splitting.
H=Magnetic field.

Table 2.3 (continuation). Mössbauer hyperfine parameters of the sediment before incubation (t_o)

T	δ/Fe (mm/s)	Δ (mm/s)	H (kOe)	Probable mineral	Values reported/References
LNT	0.38	0.76		Amorphous iron oxide?	Davison and Dickson (1984)
LNT	0.49	1.23		Jarosite	0.49–0.52; 1.10–1.15 Huggins et al. (1983) 0.48–0.49;1.16–.30 Nomura et al. (2007) 0.45–0.51; 1.10–1.22 Herbert (1997)
LNT	1.47	2.58		Fe-substituted mica (illite)	1.47; 2.56 Russell and Montano (1978) 1.23–1.31; 2.66–2.87 Huggins et al. (1983)
LNT	0.49		467	Goethite	0.47–0.51; 449–495 Huggins et al. (1983) 0.48; 483–493 Vandenberghe et al. (1986)
LNT	0.50		425	Goethite fine particle size/ Al-substituted	The reduced H may be related to small particle size effect. Al-substitution 0.48–0.49; 432–469 Goodman and Lewis (1981)

T= temperature.
δ/Fe= isomer shift relative to metallic iron.
Δ= Quadrupole splitting.
H=Magnetic field.

In terms of carbon content, different forms of mature organic matter (bitumens) have been reported in the Windy Knoll, located to the west of Mam Tor (Pering 1973). To determine if such compounds were present in the ARD sediment, the saturated hydrocarbon fraction was analysed. The results indicated that the *n*-alkanes were present and were dominated by the C_{15}–C_{31} homologous series, maximising at the C_{17} *n*-alkane (C_{max}; Figure 2.2). No clear odd-over-even predominance was visible and this was reflected in the CPI_{15-31} value of one. The hydrocarbon fraction also contains an unresolved complex mixture (UCM) and substantial amounts of isoprenoidal hydrocarbons including pristine and phytane (Figure 2.2). Such distribution is typical of the presence of petroleum and indicated the mature character of the organic matter (Volkman et al. 1992). The presence of an UCM also indicates that the sediment has undergone some biodegradation.

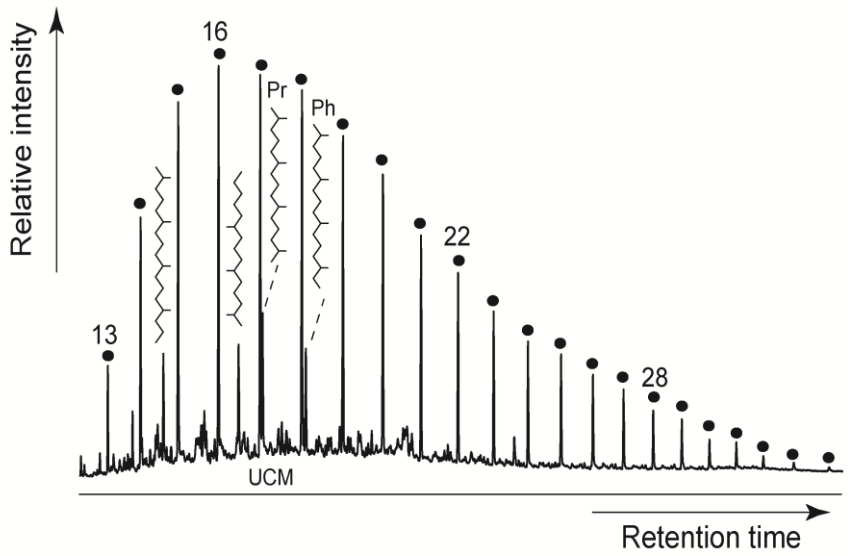

Figure 2.2. Partial gas chromatogram of the saturated hydrocarbon fraction obtained from the Mam Tor sediment. Closed circles indicate *n*-alkanes; Pr=Pristane; Ph=Phytane; UCM=unresolved complex mixture; numbers indicate carbon chain length.

In the case of the bacteria present in the ARD sediment (t_o; Figure 2.3; Figure 2.6), bacterial populations were characterised by DNA analysis. The data obtained indicated that the most heavily represented bacterial classes were *Gammaproteobacteria* (23.5%), *Nitrospira* (11.8%), *Betaproteobacteria* (5.8%) and *Bacilli* (3.3%). The *Gammaproteobacteria* class was dominated by two microorganisms closely related to the facultative anaerobe, thermo-tolerant, *Acidiferrobacter thiooxydans (m-1 DSM 2392*) that oxidises iron and sulfur but not hydrogen and is able to tolerate high salt concentrations (Hallberg et al. 2011, Hedrich et al. 2011). The *Nitrospira* class included an iron-oxidising microorganism most closely related to *Leptospirillum ferrooxidans (C2-3)*. *L. ferrooxidans* is one of the most abundant AMD microorganisms and is considered one of the main bacteria responsible for AMD generation (Schrenk et al. 1998).

Microorganisms related to *Acidovorax valerianelle (CFBP 4730)* and *Thauera sp. (G3DM-88)* were the dominant representatives of the *Betaproteobacteria* detected. Members of the *Acidovorax* genus have been reported to degrade polycyclic aromatic hydrocarbons (PAHs) under aerobic and nitrate-reducing conditions (Eriksson et al. 2003), although the microorganism identified in the Mam Tor sediment may also be a metal oxidiser, due to its similarity to *Leptothrix discophora*, a model Mn(II)-oxidising

bacterium (Boogerd and De Vrind 1987). Some *Thauera* species (e.g. strain *DNT-1)* have been reported to use toluene as a sole carbon source under aerobic or anaerobic conditions (Shinoda et al. 2004) and have been implicated in phenol degradation (Silva et al. 2010) and the dissimilatory reduction of Fe(III) under anaerobic conditions (Heinnickel et al. 2010).

The bacterial characterisation of the ARD sediment provided useful insights into the community responsible of acid generation, suggesting that some bacteria have degradative capabilities for petroleum-related compounds, although the dominant species are more likely to be iron and sulfur (metal) oxidisers.

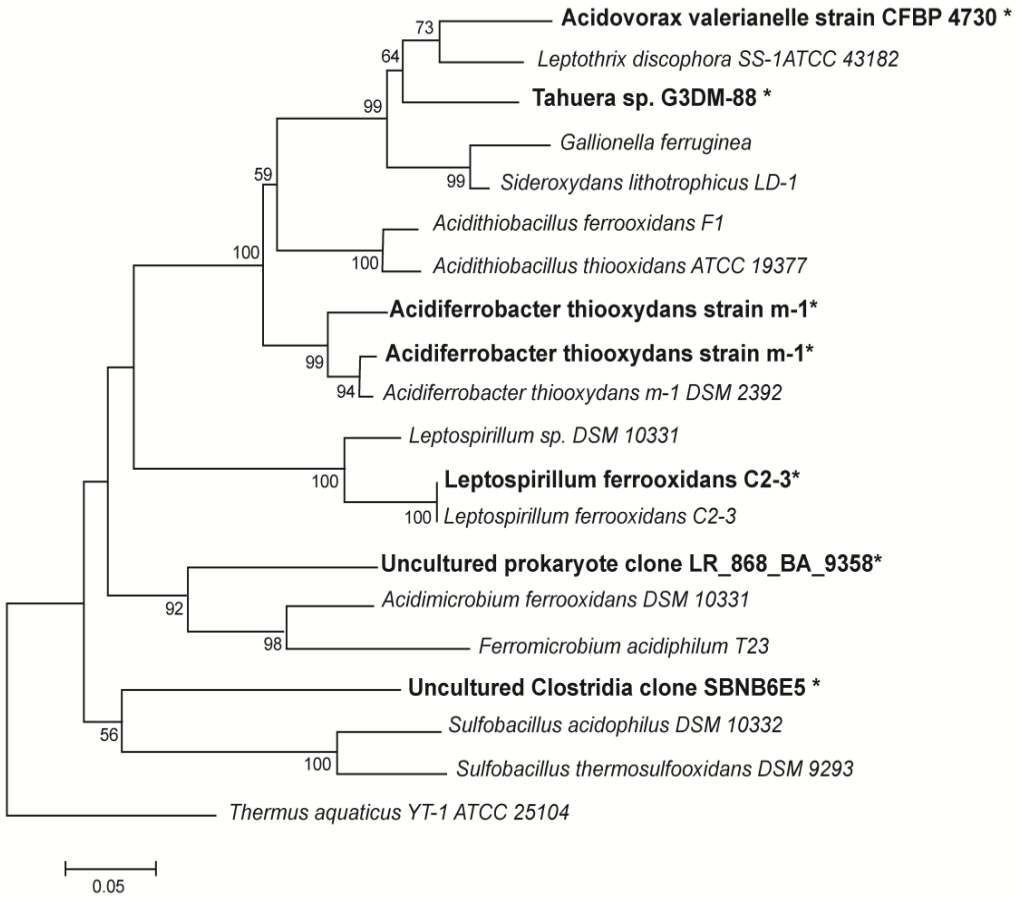

Figure 2.3. Phylogenetic tree obtained from Mam Tor communities. Names in bold and with * indicate the closest match for Mam Tor bacteria (scale in fixed mutations per site).

2.3.2 Characterisation of microcosm experiments

Before proceeding to examine the organic changes of the microcosm-based experiments, it is necessary to present the geochemical and mineralogical conditions of such systems. The major changes on the system occurred within the first 7 incubation days and after that, the variations were minimal (Figure 2.4).

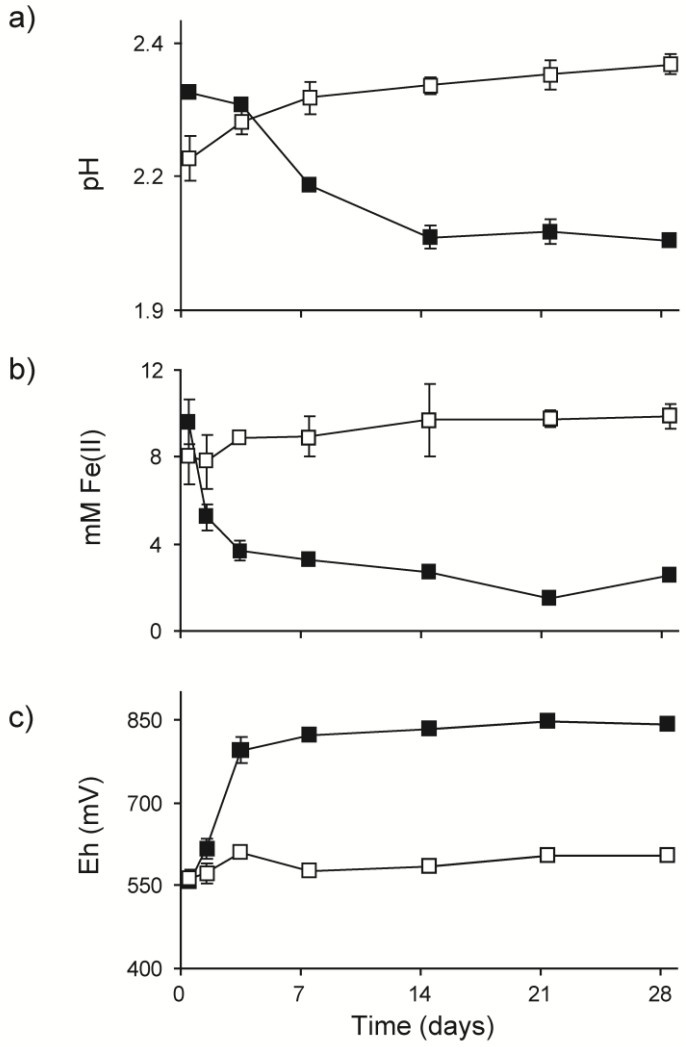

Figure 2.4. Geochemical analyses of the aerobic microcosm using Mam Tor ARD sediment. a) Slurry pH. B) Bioavailable Fe(II) concentration, c) Slurry Eh. Closed squares represent the aerobic microcosm; open squares the control experiment; bars indicate the error, when they are not visible the error is smaller than the symbol used.

In terms of acidity, the pH of the experiment (sediment) decreased from pH 2.3 to pH 2.0, indicating that the ARD-generating process was still ongoing (Figure 2.4a; Table 2.4). After 28 days incubation, the Fe(II) concentration decreased from 9.6 mM to 2.5 mM and the system became more oxidative, from 556.9 mV to 841.7 mV (Figure 2.4c; Table 2.4). High concentrations of dissolved sulfate (~11 mM) in subsamples filtered at t_o and t_{28} for VOCs determination, along with the trace amount of VOCs produced, made difficult the identification of each individual compound; however, it was possible to determine the total concentration at t_o and t_{28}, based on their summed peak areas. From this data, changes on the total concentration of VOCs were negligible (Table 2.4). In contrast to the aerobic microcosm, the pH, Eh and Fe(II) concentration did not change significantly in the sterile control, indicating that the processes that occurred in the experimental treatments were biologically mediated (Table 2.4).

Table 2.4. Geochemical and organic parameters of the microcosm experiments

	Initial conditions, t_o		**Final conditions, t_{28}**	
	Control	Sediment	Control	Sediment
pH	2.2[a]	2.3 [a]	2.3 [a]	2.0 [a]
Fe II (mM)	8.0±1.3	9.6±1.0	10.5±2.4	1.9±0.3
Eh (mV)	562±20	557±3	804±3	841±6
Sulfate (mM/l)	13.5±0.2	11.0±0.1	14.6±0.1	11.1±0.03
VOC[b]	0.04	0.01	0.04	0.01
%Organic matter	4.8 ±0.5[d]		5.4[a]	5.5 [a]
n-alkanes (µg/g sed) [c]	16.3[d]		16.0	16.5
C_{max}	17[d]		20	17
ACL_{15-31}	19.9[d]		22.6	20.9

[a] Variation <0.1, measured in triplicates.
[b] VOCs could not be identified individually due to a high sulfate concentration.
[c] ΣC15-31
[d] Values calculated from the bulk sediment sample.

At t_{28}, the bacterial diversity decreased probably because the experimental conditions were optimal only for more specialised microorganisms (Figure 2.5).

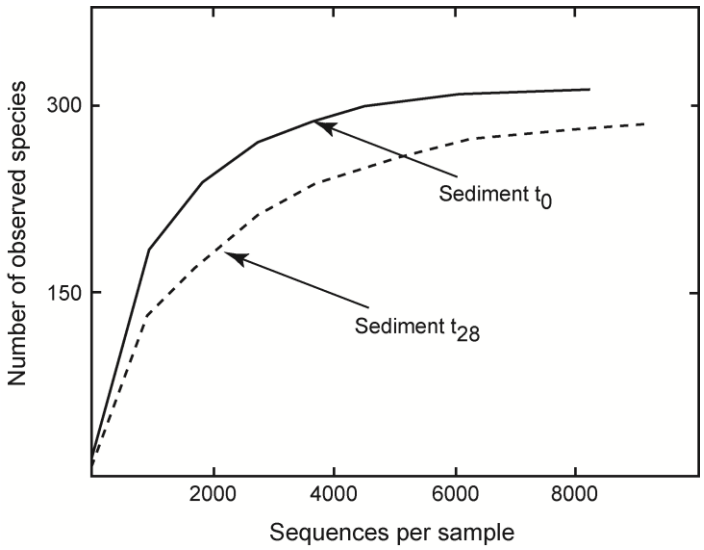

Figure 2.5. Curves of microbial diversity of Mam Tor sediment before (t_0) and after incubation (t_{28}).

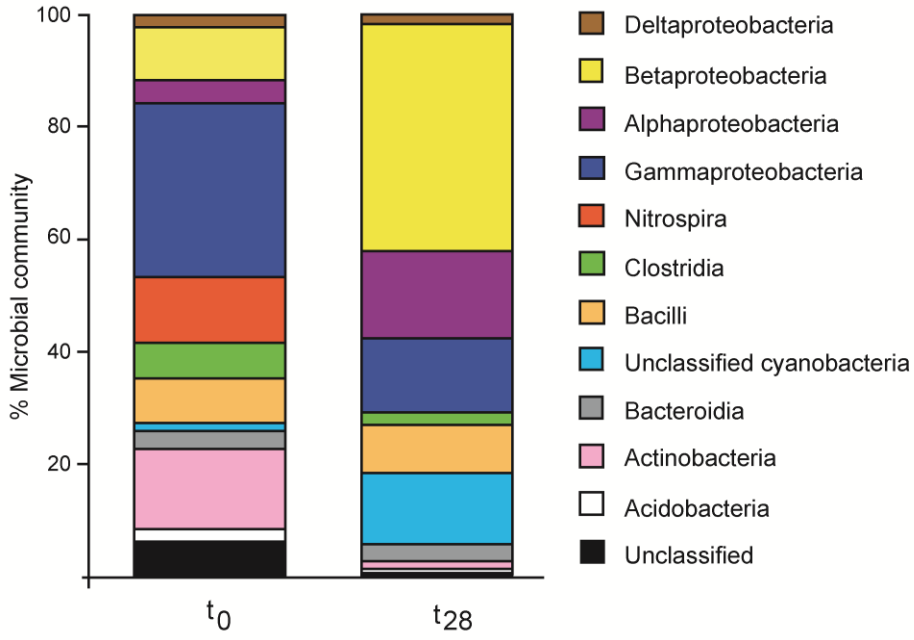

Figure 2.6. Comparison of microbial populations detected in Mam Tor sediments. After 28 days incubation the population of *Betaproteobacteria* and A*lfaproteobacteria* increased substantially. *Clostridia* communities decreased significantly whereas *Nitrospira* communities were not detected.

After 28 days incubation *Betaproteobacteria* and *Alphaproteobacteria* were the dominant bacterial communities (Figure 2.6). The *Betaproteobacteria* included microorganisms related to *Ralstonia eutropha (NH9), Burkholderia phenoliruptrix (BR3459a), Burkholderia ferrariae (FeG101), Thauera sp. (G3DM88), Dyella koreensis (BB4), Pseudomonas* sp. (*W15Feb34)* and a microorganism closely related to *Acidovorax valerianelle (CFBP4730).*

Ralstonia eutropha is a common aerobic hydrogen-oxidising soil bacterium (Friedrich et al. 1981) that is capable of degrading phenol at neutral pH (Dursun and Tepe 2005). *R. eutropha* strain NH9, has the ability of degrading chlorinated aromatic hydrocarbons (Ogawa et al. 1999). Organisms affiliated with *Burkholderia* and *Psedudomonas* in the *Betaproteobacteria* class, have also been suggested to be involved in hydrocarbon degradation (Leahy and Colwell 1990, Hamamura et al. 2006, Obuekwe et al. 2009). For example *P. aeruginosa* is capable of degrading *n*-alkanes (Belhaj et al. 2002, Striebich et al. 2014) while *P. fluorescens* (Sivagurunathan et al. 2003). *Burkholderia G4* (Mars et al. 1996) have the potential for toluene degradation while *Burkholderia cepacia (ES1)* has been considered an aliphatic degrader and strains of *Burkholderia multivorans* (*NG1* and *HN1*) have been related to the degradation of aromatic compounds (Chakraborty et al. 2010).

Some unclassified *Cyanobacteria* were also enriched for during incubation; in contrast, the *Acidobacteria* class, identified in the sediment t_o, decreased in relative abundance and the *Nitrospira* class were not detected after 28 days of incubation (Figure 2.6). The *Deltaproteobacteria*, *Bacilli* and *Bacteroidia* populations remained stable. The closest match of the bacteria detected after 28 days incubation is shown in Figure 2.7.

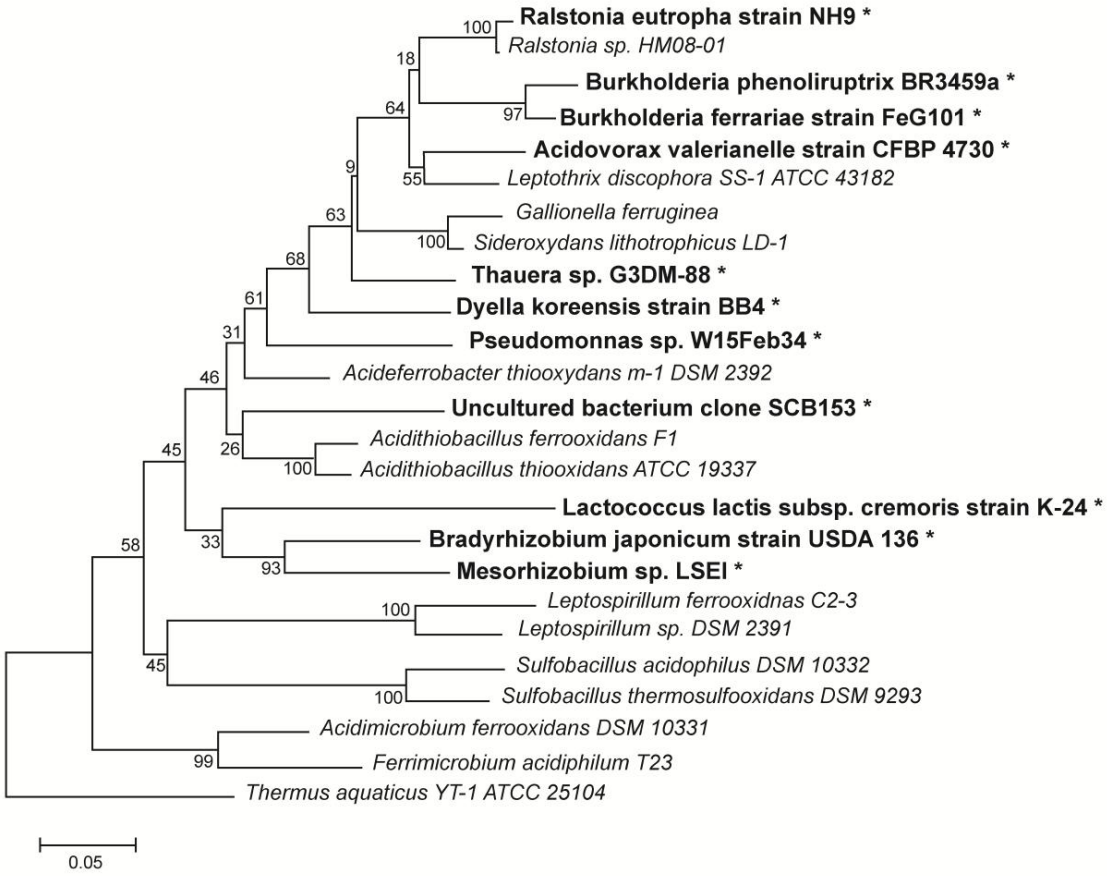

Figure 2.7. Phylogenetic tree of Mam Tor sediment after incubation (t_{28}). Names in bold and with * indicate the closest match for the bacteria detected in the microcosm (scale in fixed mutations per site).

Respect to the Mössbauer analyses of the sediment t_{28}, the iron phases detected were similar to those of the start material (Figure 2.8; Table 2.3) and could be fitted with a doublet (δ/Fe=1.35 mm/s; Δ=2.39 mm/s) assigned to jarosite and two associated doublets (δ/Fe=0.38 mm/s; Δ=0.53 mm/s and δ/Fe=1.36 mm/s; Δ=2.34 mm/s) from illite and goethite. At liquid nitrogen temperatures the determined values (δ/Fe=0.59 mm/s; H=475 kOe) were consistent with the values reported for normal goethite, with a more defined superparamagnetic doublet (δ/Fe=0.41 mm/s; Δ=0.54 mm/s) arising from fine particles. Jarosite (δ/Fe=0.45 mm/s; Δ= 1.14 mm/s) and ferrous illite (δ/Fe=1.39 mm/s; Δ= 2.54 mm/s) contributions were also detected. The results of the Mössbauer measurements are summarized in Table 2.5 and compared with the data from the literature there in. The comparison of the Mössbauer spectra before and after incubation is shown in Figure 2.8.

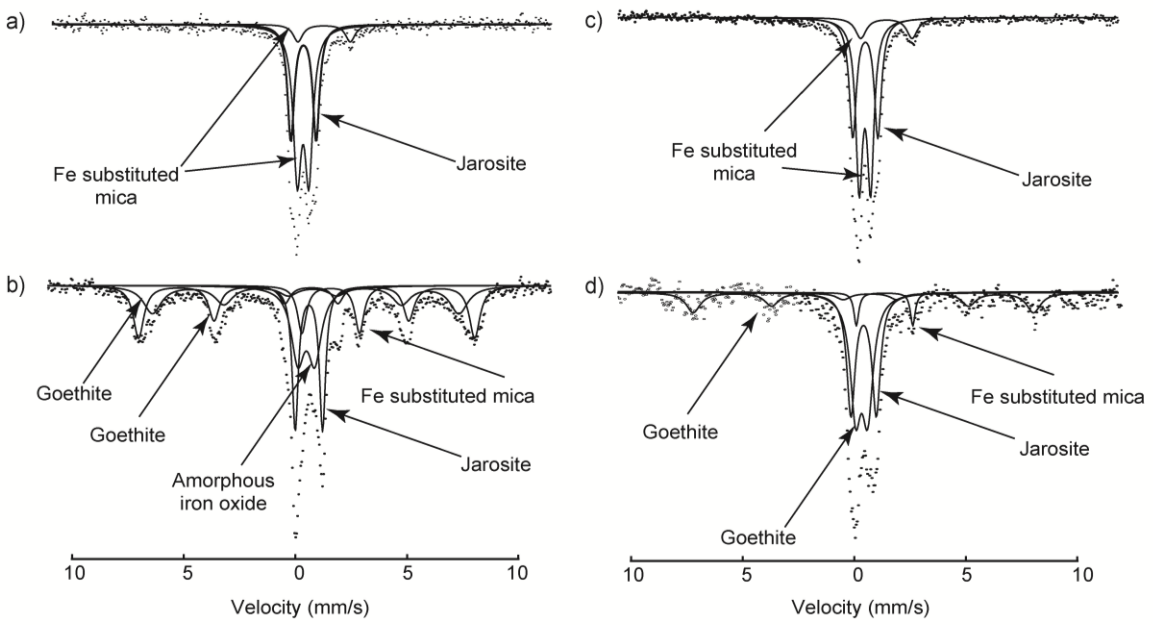

Figure 2.8. Mösbauer spectra of the initial sediment, t_0: a) at room temperature; b) at near liquid nitrogen temperature. Spectra of the sediment after incubation, t_{28}: c) at room temperature; d) at near liquid nitrogen temperature.

The spectral contribution of the amorphous iron oxide, detected in the ARD sediment (t_0; Table 2.3), disappeared after incubation. It is probable that this iron phase was converted to jarosite through incubation (Norlund et al. 2010), in accordance with the increase of Fe(III) in the microcosm and the XRD data (Figure 2.9). The contribution of goethite in fine particles also decreased, (Figure 2.8) which may indicate the bioavailability of this iron form.

Table 2.5. Mössbauer hyperfine parameters of the sediment after incubation (t_{28})

T	δ/Fe	Δ	H	Probable mineral	Values reported/References
RT	0.38	0.53		Goethite/Fe-substituted mica (illite)	Goethite 0.34—0.38; 0.5-0.70 Vandenberghe et al. (1986) 0.36—0.38; 0.56—0.65 Olowe et al. (1990) 0.38;0.58 Music et al. (1986) Illite 0.31;0.54 Malathi et al. (1969) 0.34—0.37; 0.49—0.62 Saporoschenko et al. (1980)
RT	0.40	1.15		Jarosite	0.36—0.43; 1.0—1.24 Russell and Montano (1978) 0.39; 1.13 Kovács et al. (2009) 0.38; 1.15—1.29 Nomura et al. (2007) 0.34—0.35; 1.1—1.3 Gancedo et al. (1992)
RT	1.35	2.39		Fe-substituted mica (illite)	1.01-1.31; 2.50-2.68 Russell and Montano (1978) 1.23—1.34; 2.4—2.7 Gancedo et al. (1992) 1.15; 2.86) Saporoschenko et al. (1980) 1.14—1.15; 2.15—2.69 Heller-Kallai and Rozenson (1981) 1.39; 2.34 Audley et al. (1986)
LNT	0.41	0.54		Goethite	0.41; 0.44—0.45 Vandenberghe et al. (1986) 0.37— 0.39; 0.54—0.58 Herbert (1997)
LNT	0.45	1.14		Jarosite	0.49—0.52; 1.10—1.15 Huggins et al. (1983) 0.48—0.49;1.16—1.30 Nomura et al. (2007) 0.45-0.51; 1.10–1.22 Herbert (1997)
LNT	1.39	2.54		Fe-substituted mica (illite)	1.47; 2.56 Russell and Montano (1978) 1.23–1.31; 2.66–2.87 Huggins et al. (1983)
LNT	0.59		475	Goethite	0.47–0.51; 449–495 Huggins et al. (1983) 0.48; 483–493 Vandenberghe et al. (1986) 0.36–0.56; 480–535 Eissa et al. (1974) 0.61- 0.62; 500–502 Brož et al. (1990)

T= temperature.
δ/Fe= isomer shift relative to metallic iron; mm/s.
Δ= Quadrupole splitting; mm/s.
H=Magnetic field; kOe.

In accordance with the XRF data, the XRD diffractograms (Figure 2.9a) indicted the presence of clay material and micas. The diffractograms obtained from samples of the sediment taken before incubation and at t_{28} are similar, but the signals arising from jarosite are stronger after incubation (Figure 2.9b). This result is consistent with the Mössbauer data that indicated the presence of jarosite, and is also accordingly to the increase of Fe(III) detected by the ferrozine method (Figure 2.4).

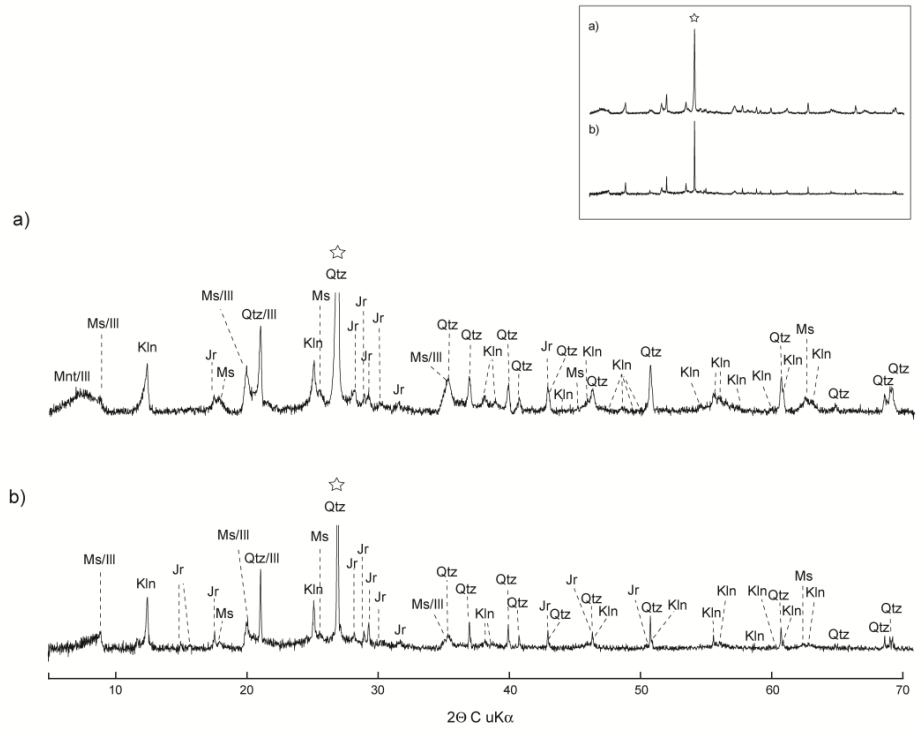

Figure 2.9. X-ray diffractograms of a) Mam Tor sediment before incubation, t_o b) Sediment after 28 days incubation, t_{28}. The small square represents the full diffractograms with high quartz peaks. The star was added for reference. Ms=muscovite; Mnt=Montmorillonite; Kln=kaolinte, Jr=jarosite; Qtz=quartz; Ill=Illite.

Regarding to the saturated hydrocarbons contained in the sediment after incubation (t_{28}; Figure 2.10), the data showed that this fraction was dominated by the C_{15}—C_{31} homologous series, with no clear odd-over-even carbon chain predominance ($CPI_{15\text{-}31}$=1). The $ACL_{15\text{-}31}$ was 20.9 and the C_{17} *n*-alkane, the most abundant compound (C_{max}). The hydrocarbons present in the control experiment (Figure 2.10), were dominated as well, by the C_{15}—C_{31} homologous series with a $CPI_{15\text{-}31}$=1, $ACL_{15\text{-}31}$ =22.6 and C_{max}= C_{20} *n*-alkane. The summed concentration of the C_{15}—C_{31} *n*-alkanes in the microcosm and control experiment were comparable, 16.6 and 16.1 $\mu g/g_{sediment}$, respectively. An UCM was also detected in both experiments. Small differences in the distribution patterns of the microcosm and control experiment were observed as illustrated in the values of the ACL and C_{max} (Figure 2.10). Those changes indicated that the homologue series of the microcosm slurry were dominated by relatively shorted-chain-length *n*-alkanes if compared to the control experiment, although it remains unclear how this could be caused by bacterial activity.

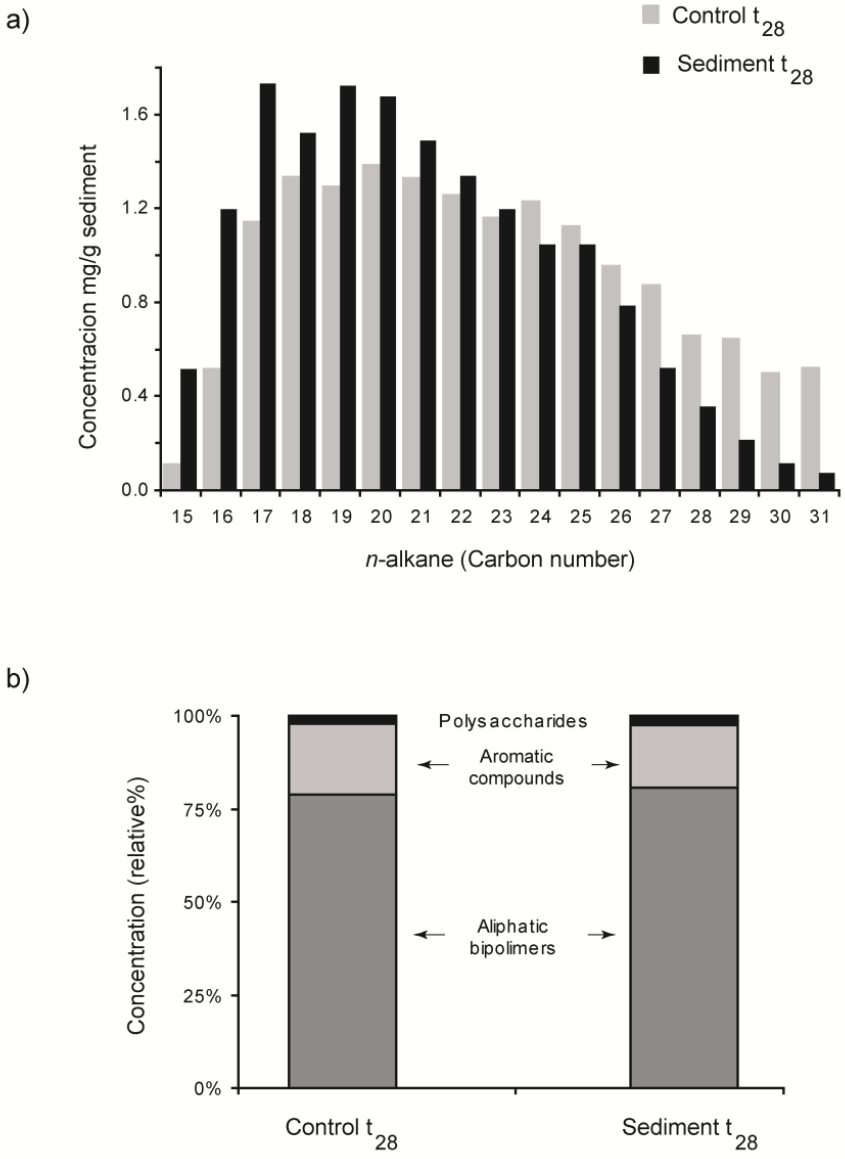

Figure 2.10. a) Abundance of C_{15}—C_{31} n-alkanes after 28 days of aerobic incubation in microcosms (black bars) and sterile control (gray bars). b) Relative macromolecular composition based on Py-GCMS analyses.

For example, Hamamura et al. (2006) examined the microbial response to hydrocarbon mixture contamination in diverse soil types under anaerobic conditions. They indicated that a range of hydrocarbons could be degraded sequentially when a microbial succession occurred; when this succession was not observed, the dominant bacteria were able to degrade a broad hydrocarbon range of different chain lengths. Previous research has suggested the bacterial degradation of mature organic matter at the Windy Knoll (Pering 1973), but the combined results of our experiments indicate that it is unlikely that the bacterially-mediated differences in pH, Eh and Fe(II)

concentration observed in the microcosms experiments, were promoted by the mature hydrocarbons present in the ARD sediment.

Besides the saturated hydrocarbons, other carbon fractions, such as macromolecular compounds, could have enhanced the ARD generation. The macromolecular analyses of the sediment t_{28} and control t_{28} experiment indicated a comparable composition (Figure 2.10b), being dominated by aliphatic bipolymeric structures (~78%) followed by aromatic compounds (~17%) and small proportion of polysaccharide derived moieties (2.4%). Comparably with the hydrocarbon analyses, the use of macromolecular organic compounds could not be detected.

Overall, the results indicated that although the acidophilic microbial populations have the potential capability of hydrocarbon degradation, the presence of petroleum-derived hydrocarbons is not involved in the generation of ARD and is therefore likely that the main carbon source in the Mam Tor system is most likely atmospheric CO_2.

2.4. Conclusions

In acid drainage environments the organic matter (OM) contributions have not been extensively studied, particularly during AMD/ARD generation. This work highlights the presence of petroleum-derived compounds as a potential OM (carbon) source naturally occurring at an ARD environment. Besides the presence of substantial amounts of mature petroleum-derived OM, the Mam Tor sediment hosts acidophilic bacterial populations including Fe(II) oxidisers. Some of these microorganisms have the potential capability to degrade petroleum-derived compounds. The microcosm experiments suggest that during ARD generation, jarosite was formed as a product of microbial Fe(II) oxidation. It was also noticed that the contribution of goethite in fine particle size decreased after incubation. After 28 days incubation, the microbial population was less diverse and a bacterial community with more defined hydrocarbon-degrading capabilities was identified. However, organic analyses show that mature petroleum derived-hydrocarbons and other OM sources present in the sediment were not degraded under aerobic and acidic conditions.

These experiments confirm that the ARD generation is an inorganic process, microbially catalysed. Our results indicate that the presence of mature organic matter is not involved in the reactions and/or bacterial metabolism related to ARD generation and support the use of atmospheric carbon dioxide as the main carbon source in ARD-generating environments.

Acknowledgements

We gratefully acknowledge the receipt of a PhD studentship for M. E. Jiménez-Castañeda, funded by the National Council of Science and Technology of México (CONACyT). We thank to C. Boothman (University of Manchester) for his assistance in the bacterial analyses; P. Lythgoe (University of Manchester), for his support in the XRF analyses and especially to A. Bewsher (University of Manchester) for his invaluable assistance during VOC's determination.

REFERENCES

Allen, J. R. L. (1960). "The Mam Tor Sandstones: A "turbidite" facies of the namurian deltas of Derbyshire, England." Journal of Sedimentary Research **30**(2).

Atlas, R. M. (1991). "Microbial hydrocarbon degradation—bioremediation of oil spills." Journal of Chemical Technology & Biotechnology **52**(2): 149-156.

Audley, G. J., G. S. Pyne, M. J. Tricker, T. E. Cranshaw and B. J. Laundy (1986). "A new approach to the determination of pyrite in coals by Mössbauer spectroscopy." Fuel **65**(8): 1103-1107.

Baldock, J. A. and J. Skjemstad (2000). "Role of the soil matrix and minerals in protecting natural organic materials against biological attack." Organic Geochemistry **31**(7): 697-710.

Beaudoin, A. (2003). "A comparison of two methods for estimating the organic content of sediments." Journal of Paleolimnology **29**(3): 387-390.

Belhaj, A., N. Desnoues and C. Elmerich (2002). "Alkane biodegradation in Pseudomonas aeruginosa strains isolated from a polluted zone: identification of alkB and alkB-related genes." Research in Microbiology **153**(6): 339-344.

Blumer, M. (1957). "Removal of elemental sulfur from hydrocarbon fractions." Analytical Chemistry **29**(7): 1039-1041.

Bocquet, S., R. Pollard and J. Cashion (1992). "Dynamic magnetic phenomena in fine-particle goethite." Physical Review B **46**(18): 11657.

Bødker, F., S. Mørup and S. Linderoth (1994). "Surface effects in metallic iron nanoparticles." Physical Review Letters **72**(2): 282-285.

Boogerd, F. C. and J. P. De Vrind (1987). "Manganese oxidation by Leptothrix discophora." Journal of Bacteriology **169**(2): 489-494.

Brož, D., J. Straková, J. Šubrt, J. Vinš, B. Sedlák and S. I. Reiman (1990). "Mössbauer spectroscopy of goethite of small particle size." Hyperfine Interactions **54**(1-4): 479-482.

Caporaso, J. G., J. Kuczynski, J. Stombaugh, K. Bittinger, F. D. Bushman, E. K. Costello, N. Fierer, A. Pena González, J. K. Goodrich, J. I. Gordon, G. A. Huttley, S. T. Kelley, D. Knights, J. E. Koenig, R. E. Ley, C. A. Lozupone, D. McDonald, B. D. Muegge, M. Pirrung, J. Reeder, J. R. Sevinsky, P. J. Turnbaugh, W. A. Walters, J. Widmann, T. Yatsunenko, J. Zaneveld and R. Knight (2010). "QIIME allows analysis of high-throughput community sequencing data." Nature Methods **7**(5): 335-336.

Chakraborty, S., S. Mukherji and S. Mukherji (2010). "Surface hydrophobicity of petroleum hydrocarbon degrading Burkholderia strains and their interactions with NAPLs and surfaces." Colloids and Surfaces B: Biointerfaces **78**(1): 101-108.

Chen, A., C. Lin, W. Lu, Y. Wu, Y. Ma, J. Li and L. Zhu (2007). "Well water contaminated by acidic mine water from the Dabaoshan Mine, South China: Chemistry and toxicity." Chemosphere **70**(2): 248-255.

Cole, J. R., Q. Wang, E. Cardenas, J. Fish, B. Chai, R. J. Farris, A. Kulam-Syed-Mohideen, D. M. McGarrell, T. Marsh and G. M. Garrity (2009). "The Ribosomal Database Project: improved alignments and new tools for rRNA analysis." Nucleic acids research **37**(suppl 1): D141-D145.

Corkhill, C. L., P. L. Wincott, J. R. Lloyd and D. J. Vaughan (2008). "The oxidative dissolution of arsenopyrite (FeAsS) and enargite (Cu3AsS4) by Leptospirillum ferrooxidans." Geochimica et Cosmochimica Acta **72**(23): 5616-5633.

Davison, W. and D. P. E. Dickson (1984). "Mössbauer spectroscopic and chemical studies of particulate iron material from a seasonally anoxic lake." Chemical Geology **42**(1–4): 177-187.

Dickson, L., I. D. Bull, P. J. Gates and R. P. Evershed (2009). "A simple modification of a silicic acid lipid fractionation protocol to eliminate free fatty acids from glycolipid and phospholipid fractions." Journal of Microbiological Methods **78**(3): 249-254.

Donnelly, L. (2006). The Mam Tor Landslide, geology & mining legacy around Castleton, Peak District National Park, Derbyshire, UK. Engineering Geology for Tomorrow's Cities, Proceedings of the 10th Congress of The International Association for Engineering Geology and The Environment, Nottingham, UK.

Dursun, A. Y. and O. Tepe (2005). "Internal mass transfer effect on biodegradation of phenol by Ca-alginate immobilized Ralstonia eutropha." Journal of Hazardous Materials **126**(1–3): 105-111.

Edgar, R. C. (2010). "Search and clustering orders of magnitude faster than BLAST." Bioinformatics **26**(19): 2460-2461.

Eissa, N. A., H. A. Sallam, S. S. Gomaa, S. A. Saleh and Z. Miligy (1974). "Mössbauer study of Egyptian goethite." Journal of Physics D: Applied Physics **7**(15): 2121.

Eriksson, M., E. Sodersten, Z. Yu, G. Dalhammar and W. W. Mohn (2003). "Degradation of polycyclic aromatic hydrocarbons at low temperature under aerobic and nitrate-reducing conditions in enrichment cultures from northern soils." Applied and Environmental Microbiology **69**(1): 275-284.

Ford, T., W. Sarjeant and M. Smith (1993). "Minerals of the Peak District." Bulletin of the Peak District Mines Historical Society **12**(1): 1.

Friedrich, B., C. Hogrefe and H. Schlegel (1981). "Naturally occurring genetic transfer of hydrogen-oxidizing ability between strains of Alcaligenes eutrophus." Journal of bacteriology **147**(1): 198-205.

Frostegård, Å., A. Tunlid and E. Bååth (1991). "Microbial biomass measured as total lipid phosphate in soils of different organic content." Journal of Microbiological Methods **14**(3): 151-163.

Gancedo, J. R., M. Gracia, A. Martínez-Alonso, J. L. Miranda and J. M. D. Tascón (1992). "Mössbauer study of the effect of acidic treatment on iron minerals during the demineralization of coals." Hyperfine Interactions **71**(1-4): 1403-1406.

Gélinas, Y., J. A. Baldock and J. I. Hedges (2001). "Demineralization of marine and freshwater sediments for CP/MAS 13C NMR analysis." Organic Geochemistry **32**(5): 677-693.

Golden, D. C., L. H. Bowen, S. B. Weed and J. M. Bigham (1979). "Mössbauer studies of synthetic and soil-occurring aluminum-substituted goethites." Soil Science Society of America Journal **43**(4): 802-808.

Goodman, B. A. and D. G. Lewis (1981). "Mössbauer spectra of aluminous goethites (α-FeOOH)." Journal of Soil Science **32**(3): 351-364.

Grimalt, J. O., M. Ferrer and E. Macpherson (1999). "The mine tailing accident in Aznalcollar." Science of The Total Environment **242**(1–3): 3-11.

Hallberg, K., S. Hedrich and D. B. Johnson (2011). "Acidiferrobacter thiooxydans, gen. nov. sp. nov.; an acidophilic, thermo-tolerant, facultatively anaerobic iron- and sulfur-oxidizer of the family Ectothiorhodospiraceae." Extremophiles **15**(2): 271-279.

Hamady, M., J. J. Walker, J. K. Harris, N. J. Gold and R. Knight (2008). "Error-correcting barcoded primers for pyrosequencing hundreds of samples in multiplex." Nature Methods **5**(3): 235-237.

Hamamura, N., S. H. Olson, D. M. Ward and W. P. Inskeep (2005). "Diversity and functional analysis of bacterial communities associated with natural hydrocarbon

seeps in acidic soils at Rainbow Springs, Yellowstone National Park." Applied and Environmental Microbiology **71**(10): 5943-5950.

Hamamura, N., S. H. Olson, D. M. Ward and W. P. Inskeep (2006). "Microbial population dynamics associated with crude-oil biodegradation in diverse soils." Applied and Environmental Microbiology **72**(9): 6316-6324.

Harrison, A. P. (1984). "The Acidophilic Thiobacilli and other acidophilic bacteria that share their habitat." Annual Review of Microbiology **38**(1): 265-292.

Hedrich, S., M. Schlömann and D. B. Johnson (2011). "The iron-oxidizing proteobacteria." Microbiology **157**(6): 1551-1564.

Heinnickel, M. L., F. M. Kaser and J. D. Coates (2010). Hydrocarbon degradation coupled to metal reduction. Handbook of Hydrocarbon and Lipid Microbiology. K. Timmis, Springer Berlin Heidelberg**:** 947-955.

Heiri, O., A. Lotter and G. Lemcke (2001). "Loss on ignition as a method for estimating organic and carbonate content in sediments: reproducibility and comparability of results." Journal of Paleolimnology **25**(1): 101-110.

Heller-Kallai, L. and I. Rozenson (1981). "The use of Mössbauer spectroscopy of iron in clay mineralogy." Physics and Chemistry of Minerals **7**(5): 223-238.

Herbert, R. B. (1997). "Properties of goethite and jarosite precipitated from acidic groundwater, Dalarna, Sweden." Clays and Clay Minerals **45**(2): 261-273.

Horel, A. and S. Schiewer (2014). "Influence of inocula with prior hydrocarbon exposure on biodegradation rates of diesel, synthetic diesel, and fish-biodiesel in soil." Chemosphere **109**(0): 150-156.

Horsfield, B. and A. G. Douglas (1980). "The influence of minerals on the pyrolysis of kerogens." Geochimica et Cosmochimica Acta **44**(8): 1119-1131.

Huggins, F. E., G. P. Huffman and M. C. Lin (1983). "Observations on low-temperature oxidation of minerals in bituminous coals." International Journal of Coal Geology **3**(2): 157-182.

Ingledew, W. J. (1982). "Thiobacillus Ferrooxidans the bioenergetics of an acidophilic chemolithotroph." Biochimica et Biophysica Acta (BBA) - Reviews on Bioenergetics **683**(2): 89-117.

Jackson, J. W. (1925). "The relation of the Edale Shales to the Carboniferous Limestone in North Derbyshire." Geological Magazine **62**(06): 267-274.

Johnson, D. B. (1995). "Selective solid media for isolating and enumerating acidophilic bacteria." Journal of Microbiological Methods **23**(2): 205-218.

Johnson, D. B. (2012). "Geomicrobiology of extremely acidic subsurface environments." FEMS Microbiology Ecology **81**(1): 2-12.

Johnson, D. B. and T. A. M. Bridge (2002). "Reduction of ferric iron by acidophilic heterotrophic bacteria: evidence for constitutive and inducible enzyme systems in Acidiphilium spp." Journal of Applied Microbiology **92**(2): 315-321.

Johnson, D. B., M. A. Ghauri and M. F. Said (1992). "Isolation and characterization of an acidophilic, heterotrophic bacterium capable of oxidizing ferrous iron." Applied and Environmental Microbiology **58**(5): 1423-1428.

Jones, C. A. and D. P. Kelly (1983). "Growth of Thiobacillus ferrooxidans on ferrous iron in chemostat culture: Influence of product and substrate inhibition." Journal of Chemical Technology and Biotechnology. Biotechnology **33**(4): 241-261.

Kovács, K., E. Kuzmann, Z. Homonnay, A. Vértes, L. Gunneriusson and A. Sandström (2009). Mössbauer study of synthetic jarosites. ICAME 2007. N. S. Gajbhiye and S. K. Date, Springer Berlin Heidelberg**:** 951-955.

Lane, D. J. (1991). "16S/23S rRNA sequencing." Nucleic acid techniques in bacterial systematics: 125-175.

Leahy, J. G. and R. R. Colwell (1990). "Microbial degradation of hydrocarbons in the environment." Microbiological Reviews **54**(3): 305-315.

Lovley, D. R. and E. J. Phillips (1987). "Rapid assay for microbially reducible ferric iron in aquatic sediments." Applied and Environmental Microbiology **53**(7): 1536-1540.

Malathi, N., S. P. Puri and I. P. Saraswat (1969). "Mössbauer studies of iron in illite and montmorillonite." Journal of the Physical Society of Japan **26**(3): 680-683.

Mars, A. E., J. Houwing, J. Dolfing and D. B. Janssen (1996). "Degradation of toluene and trichloroethylene by Burkholderia cepacia G4 in growth-limited fed-batch culture." Applied and Environmental Microbiology **62**(3): 886-891.

Morrish, A. H. and K. Haneda (1983). "Surface magnetic properties of fine particles." Journal of Magnetism and Magnetic Materials **35**(1–3): 105-113.

Music, S., I. Czakó-Nagy, S. Popovic, A. Vértes and M. Tonkovic (1986). "Mössbauer-spectroscopy, X-ray-diffraction and IR spectroscopy of oxide precipitates formed from FeSO4 solution." Croatica Chemica Acta **59**(4): 833-851.

Nomura, K., M. Takeda, T. Iiyama and H. Sakai (2007). Mössbauer studies of Jarosite, Mikasaite and Yavapaiite, and implication to their Martian counterparts. ICAME 2005. P. E. Lippens, J. C. Jumas and J. M. R. Génin, Springer Berlin Heidelberg**:** 657-664.

Nooner, D. W., W. S. Updegrove, D. A. Flory, J. Oro and G. Mueller (1973). "Isotopic and chemical data of bitumens associated with hydrothermal veins from Windy Knoll, Derbyshire, England." Chemical Geology **11**(3): 189-202.

Norlund, K. L. I., C. Baron and L. A. Warren (2010). "Jarosite formation by an AMD sulphide-oxidizing environmental enrichment: Implications for biomarkers on Mars." Chemical Geology **275**(3–4): 235-242.

Obuekwe, C. O., Z. K. Al-Jadi and E. S. Al-Saleh (2009). "Hydrocarbon degradation in relation to cell-surface hydrophobicity among bacterial hydrocarbon degraders from petroleum-contaminated Kuwait desert environment." International Biodeterioration & Biodegradation **63**(3): 273-279.

Ogawa, N., S. M. McFall, T. J. Klem, K. Miyashita and A. M. Chakrabarty (1999). "Transcriptional activation of the chlorocatechol degradative genes of Ralstonia eutropha NH9." Journal of Bacteriology **181**(21): 6697-6705.

Olowe, A. A., P. Refait and J. M. R. Génin (1990). "Superparamagnetic behaviour of goethite prepared in sulphated medium." Hyperfine Interactions **57**(1-4): 2037-2043.

Pering, K. and C. Ponnamperuma (1969). "Alicyclic hydrocarbons from an unusual deposit in Derbyshire, England—A study in possible diagenesis." Geochimica et Cosmochimica Acta **33**(4): 528-532.

Pering, K. L. (1973). "Bitumens associated with lead, zinc and flnorite ore minerals in North Derbyshire, England." Geochimica et Cosmochimica Acta **37**(3): 401-417.

Postma, D., F. Larsen, N. T. Minh Hue, M. T. Duc, P. H. Viet, P. Q. Nhan and S. Jessen (2007). "Arsenic in groundwater of the Red River floodplain, Vietnam: Controlling geochemical processes and reactive transport modeling." Geochimica et Cosmochimica Acta **71**(21): 5054-5071.

Rimstidt, J. D. and D. J. Vaughan (2003). "Pyrite oxidation: a state-of-the-art assessment of the reaction mechanism." Geochimica et Cosmochimica Acta **67**(5): 873-880.

Roger, M., C. Castelle, M. Guiral, P. Infossi, E. Lojou, G.-O. Marie-Therese and M. Ilbert (2012). "Mineral respiration under extreme acidic conditions: from a supramolecular organization to a molecular adaptation in Acidithiobacillus ferrooxidans." Biochemical Society Transactions **40**(part 6): 1324-1329.

Rowland, H. A. L., R. L. Pederick, D. A. Polya, R. D. Pancost, B. E. Van Dongen, A. G. Gault, D. J. Vaughan, C. Bryant, B. Anderson and J. R. Lloyd (2007). "The control of organic matter on microbially mediated iron reduction and arsenic release in shallow alluvial aquifers, Cambodia." Geobiology **5**(3): 281-292.

Rowland, H. A. L., D. A. Polya, J. R. Lloyd and R. D. Pancost (2006). "Characterisation of organic matter in a shallow, reducing, arsenic-rich aquifer, West Bengal." Organic Geochemistry **37**(9): 1101-1114.

Russell, P. E. and P. A. Montano (1978). "Magnetic hyperfine parameters of iron containing minerals in coals." Journal of Applied Physics **49**(8): 4615-4617.

Rutter, E. H. and S. Green (2011). "Quantifying creep behaviour of clay-bearing rocks below the critical stress state for rapid failure: Mam Tor landslide, Derbyshire, England." Journal of the Geological Society **168**(2): 359-372.

Saporoschenko, M., H. Twardowska, G. V. Smith, C. C. Hinckley, R. H. Shiley and W. A. White (1980). "Mössbauer studies of illites and heat-treated illite as related to coal-conversion processes." Fuel **59**(11): 767-771.

Schrenk, M. O., K. J. Edwards, R. M. Goodman, R. J. Hamers and J. F. Banfield (1998). "Distribution of Thiobacillus ferrooxidans and Leptospirillum ferrooxidans: implications for generation of acid mine drainage." Science **279**(5356): 1519-1522.

Shinjo, T. (1991). "Interface magnetism." Surface Science Reports **12**(2): 51-98.

Shinoda, Y., Y. Sakai, H. Uenishi, Y. Uchihashi, A. Hiraishi, H. Yukawa, H. Yurimoto and N. Kato (2004). "Aerobic and anaerobic toluene degradation by a newly isolated denitrifying bacterium, Thauera sp. Strain DNT-1." Applied and Environmental Microbiology **70**(3): 1385-1392.

Silva, C. C., A. F. Viero, A. Dias, F. D. Andreote, E. C. Jesus, S. O. De Paula, A. Torres, V. Santiago and V. M. Oliveira (2010). "Monitoring the bacterial community dynamics in a petroleum refinery wastewater membrane bioreactor fed with a high phenolic load." Journal of microbiology and biotechnology **20**(1): 21-29.

Silverman, M. P. and D. G. Lundgren (1959). "Studies on the chemoautotrophic iron bacterium Ferrobacillus ferrooxidans: I. An improved medium and a harvesting procedure for securing high cell yields." Journal of bacteriology **77**(5): 642.

Singer, P. C. and W. Stumm (1970). "Acidic Mine Drainage: the rate-determining step." Science **167**(3921): 1121-1123.

Sivagurunathan, M., A. M. Martin and R. J. Helleur (2003). "Biological waste-treatment of hydrocarbon residues: effects of humic acids on the degradation of toluene." Applied Energy **75**(3–4): 267-273.

Skempton, A. W., A. D. Leadbeater and R. J. Chandler (1989). "The Mam Tor Landslide, North Derbyshire." Philosophical Transactions of the Royal Society of London. Series A, Mathematical and Physical Sciences **329**(1607): 503-547.

Solà, C., M. a. Burgos, Á. Plazuelo, J. Toja, M. Plans and N. s. Prat (2004). "Heavy metal bioaccumulation and macroinvertebrate community changes in a Mediterranean stream affected by acid mine drainage and an accidental spill (Guadiamar River, SW Spain)." Science of The Total Environment **333**(1–3): 109-126.

Stapleton, R. D., D. C. Savage, G. S. Sayler and G. Stacey (1998). "Biodegradation of aromatic hydrocarbons in an extremely acidic environment." Applied and environmental microbiology **64**(11): 4180-4184.

Stookey, L. L. (1970). "Ferrozine- a new spectrophotometric reagent for iron." Analytical Chemistry **42**(7): 779-781.

Striebich, R. C., C. E. Smart, T. S. Gunasekera, S. S. Mueller, E. M. Strobel, B. W. McNichols and O. N. Ruiz (2014). "Characterization of the F-76 diesel and Jet-A aviation fuel hydrocarbon degradation profiles of Pseudomonas aeruginosa and Marinobacter hydrocarbonoclasticus." International Biodeterioration & Biodegradation **93**(0): 33-43.

Tessier, A., P. G. C. Campbell and M. Bisson (1979). "Sequential extraction procedure for the speciation of particulate trace metals." Analytical Chemistry **51**(7): 844-851.

Uyttebroek, M., S. Vermeir, P. Wattiau, A. Ryngaert and D. Springael (2007). "Characterization of cultures enriched from acidic polycyclic aromatic hydrocarbon-contaminated soil for growth on pyrene at low pH." Applied and Environmental Microbiology **73**(10): 3159-3164.

van der Kraan, A. M. and J. J. van Loef (1966). "Superparamagnetism in submicroscopic α-FeOOH particles observed by the Mössbauer effect." Physics Letters **20**(6): 614-616.

van Dongen, B. E., H. A. L. Rowland, A. G. Gault, D. A. Polya, C. Bryant and R. D. Pancost (2008). "Hopane, sterane and n-alkane distributions in shallow sediments hosting high arsenic groundwaters in Cambodia." Applied Geochemistry **23**(11): 3047-3058.

Vandenberghe, R., E. De Grave, G. De Geyter and C. Landuydt (1986). "Characterization of goethite and hematite in a Tunisian soil profile by Mössbauer spectroscopy." Clays and Clay Minerals **34**(3): 275-280.

Vear, A. and C. Curtis (1981). "A quantitative evaluation of pyrite weathering." Earth Surface Processes and Landforms **6**(2): 191-198.

Volkman, J. K., D. G. Holdsworth, G. P. Neill and H. J. Bavor Jr (1992). "Identification of natural, anthropogenic and petroleum hydrocarbons in aquatic sediments." Science of The Total Environment **112**(2–3): 203-219.

Waltham, A. C. and N. Dixon (2000). "Movement of the Mam Tor landslide, Derbyshire, UK." Quarterly Journal of Engineering Geology and Hydrogeology **33**(2): 105-123.

White, D. C., W. M. Davis, J. S. Nickels, J. D. King and R. J. Bobbie (1979). "Determination of the sedimentary microbial biomass by extractible lipid phosphate." Oecologia **40**(1): 51-62.

Wood, A. P. and D. P. Kelly (1983). "Autotrophic and mixotrophic growth of three thermoacidophilic iron-oxidizing bacteria." FEMS Microbiology Letters **20**(1): 107-112.

Zhou, J.-M., Z. Dang, M.-F. Cai and C.-Q. Liu (2007). "Soil heavy metal pollution around the Dabaoshan Mine, Guangdong Province, China." Pedosphere **17**(5): 588-594.

Zinck, J. and W. Griffith (2013). Review of mine drainage treatment and sludge management operations. Canada, Mine Environment Neutral Drainage (MEND) Program.

CHAPTER 3

Paper 2: Importance of organic matter in the microbial reduction of Fe(III) at an acid rock drainage environment

This chapter contains the following paper which is under preparation to be submitted to the journal: Science of the Total Environment.

Jiménez-Castañeda, M. E.[2]; Scarincci, C. [1]; Burke, A. [1]; Vaughan, D. J., Lloyd, J. R[1]; van Dongen, B. E.[1]*.

[2] School of Earth, Atmospheric and Environmental Sciences, Williamson Research Centre for Molecular Environmental Science, University of Manchester, Manchester, UK.

* Corresponding author: Tel.: +44 161 3067460; fax: +44 161 3069361.
E-mail address: Bart.vanDongen@manchester.ac.uk

ABSTRACT

Microcosms based experiments were performed using sediment from an old Acid Rock Drainage (ARD) site, stimulated with local plants and manures, to elucidate the role of organic matter (OM) in promoting Fe(III) reduction at an ARD environment. Changes in the mineralogical, organic and microbiological composition were monitored through a 100 incubation days period. This study shows that natural sources of OM may occur at an ARD site, influencing the microbial diversity and the mineralogical composition of the sediment. The mineralogical results suggest that goethite in fine particles, can make a bioavailable mineral substrate to support the growth of Fe(III)-reducing bacteria. The evidence from this study also suddests that the saturated hydrocarbon fraction from plant material is more degradable than those from manure additions, but it does not have a substantial role in stimulating microbial Fe(III)-reduction, especially in presence of acetate, which is inhibitory. In contrast, OM from the manure amendments greatly stimulated the microbial reduction of Fe(III) and consequently increased the pH of the systems up to near neutral conditions offering a potential remediation strategy for AMD- and ARD- impacted environments.

Keywords: acid drainage, ARD, AMD, bacteria, iron reduction, organic matter, goethite, jarosite.

3.1. INTRODUCTION

Acid Mine Drainage (AMD), or its general term, Acid Rock Drainage (ARD), is one of the most widespread forms of water pollution in the world, characterised by water streams with low pH and high concentrations of iron, sulfur and other dissolved metals. The discharge of AMD causes serious problems to the aquatic life, wild life, crops and in consequence, threatens human health (Rosenberg et al. 2001, Lin et al. 2007). An example of its environmental impact occurred in 1998, when the Agrio and Guadiamar Rivers (Spain) received 4 million m^3 of AMD and 2 million m^3 of toxic mud from the Aznalcollar spill (Solà et al. 2004). This ecological disaster affected the Doñana Park, the largest reserve of birds in Europe, and had a high negative impact on the economy of the region (Pain et al. 1998, Grimalt et al. 1999).

Across the UK several accidents have also taken place, for example the case of the Wheal Jane mine in 1992, that delivered a very toxic and dramatic AMD plume in the

Fal estuary (Neal et al. 2005, Younger et al. 2005) and the drainage works carried out at Parys Mountain (UK) in 2003, that released several tons of copper, manganese and zinc to the Irish Sea (Coupland and Johnson 2004). The financial cost derived of the treatment and attempts of remediation of AMD sites are elevated (Zinck and Griffith 2013) and had led to the bankruptcy many mining companies.

Acid drainage can be spontaneously generated when sulfide minerals are weathered; for simplicity, those reactions are better explained on the aqueous breakdown of pyrite (Singer and Stumm 1970, Rimstidt and Vaughan 2003). Briefly, the reactions start when pyrite is oxidised, producing sulfuric acid and Fe(II). Consequently, Fe(II) is oxidised to Fe(III), which in turn catalyses the oxidation of new Fe(II), generating different secondary iron minerals and releasing a wide range of metals contained in the pyritic ores (Corkhill et al. 2008, Valente and Leal Gomes 2009, Nordstrom 2011, Valente et al. 2013). The overall representation of the AMD/ARD cycle is (Singer and Stumm 1970):

$$4FeS_2+15O_2+14H_20\rightarrow 4Fe(OH)_3+8SO_4^{-2}+16H^+$$

The oxidation of sulfide minerals is catalysed by highly specialised microorganisms such as *Acidithiobacillus ferrooxidans* and *Leptospirillum ferrooxidans* (Johnson 1995) but other bacteria and prokaryotes have also been identified and considered important for the AMD cycle (Johnson 1998, Hallberg and Johnson 2001, Bruneel et al. 2008). Ferrihydrite ($5Fe_2O_3{\cdot}9H_2O$), magnetite (Fe_3O_4), hematite (Fe_2O_3), goethite (α-FeOOH), jarosite ($KFe_3(SO_4)_2(OH)_6$) or schwertmannite ($Fe_8O_8(OH)_6SO_4$) are amongst the minerals formed from pyrite oxidation (Murad and Rojík 2003), and can be used in microbial metabolic processes, for example during Fe(III) reduction (Johnson 1998, Cutting et al. 2009).

The reduction of Fe(III) is known to take place in "healthier" anaerobic sediments coupled to the oxidation of organic matter (Lovley and Phillips 1986); similarly, under acidic conditions this process could be considered, although has not been extensively studied. Due to the assumption that the organic matter will also act as electron donors the terms "organic matter", "carbon source" and "electron donor" will be used synonymously in the text with the precise choice of word varying due to context.

In ARD/AMD environments the concentration of Fe(III) exceeds that of other electron acceptors (Lovley and Phillips 1986), and consequently the mechanisms of microbial respiration involve the transformations of iron minerals, based on the redox potential of the Fe(II)/Fe(III) couple, 770 mV (Johnson and Bridge 2002, Weber et al. 2006,

Vaughan and Lloyd 2011). In such sites, the concentration of organic matter is considered low (<10 mg/l of dissolved organic carbon) (Johnson 2012) but different sources could be potentially present, such as petroleum seeps and spills, plant litter or animal waste.

The presence of OM may play an important role for the microbial communities and mineralogical processes occurring. This was shown in Adams et al. (2007) where the addition of glycerol and complex electron donors increased the pH of the ARD experiments while stimulated the microbial reduction of Fe(III). Those results opened questions about the implication of natural sources of OM in the amelioration of ARD sites. Thus, the aim of this work is to better understand the potential role of organic matter in the natural attenuation of ARD, monitoring the attenuation, mineralogical transformations and microbial communities with the use/degradation of natural organic matter in microcosm-based experiments amended with natural carbon sources (plants and manures).

3.2. MATERIALS AND ANALYTICAL METHODS

3.2.1 Study site

Mam Tor (Castleton, UK) is a landslide of rotational type (Vear and Curtis 1981, Green et al. 2010) formed approximately 3200 years ago (Skempton et al. 1989, Arkwright et al. 2003) when a section of the Mam Tor beds overlying Edale Shales collapsed (Skempton et al. 1989, Rutter et al. 2003, Donnelly 2006, Dixon and Brook 2007).

Mam Tor is part of several landslides but is the one that is still moving at a velocity of 7 cm/y in the edges and 0. 5 m/y in the middle section (Waltham and Dixon 2000, Rutter and Green 2011) with the consequent breakdown of the pyritic rocks and generation of ARD (Vear and Curtis 1981).

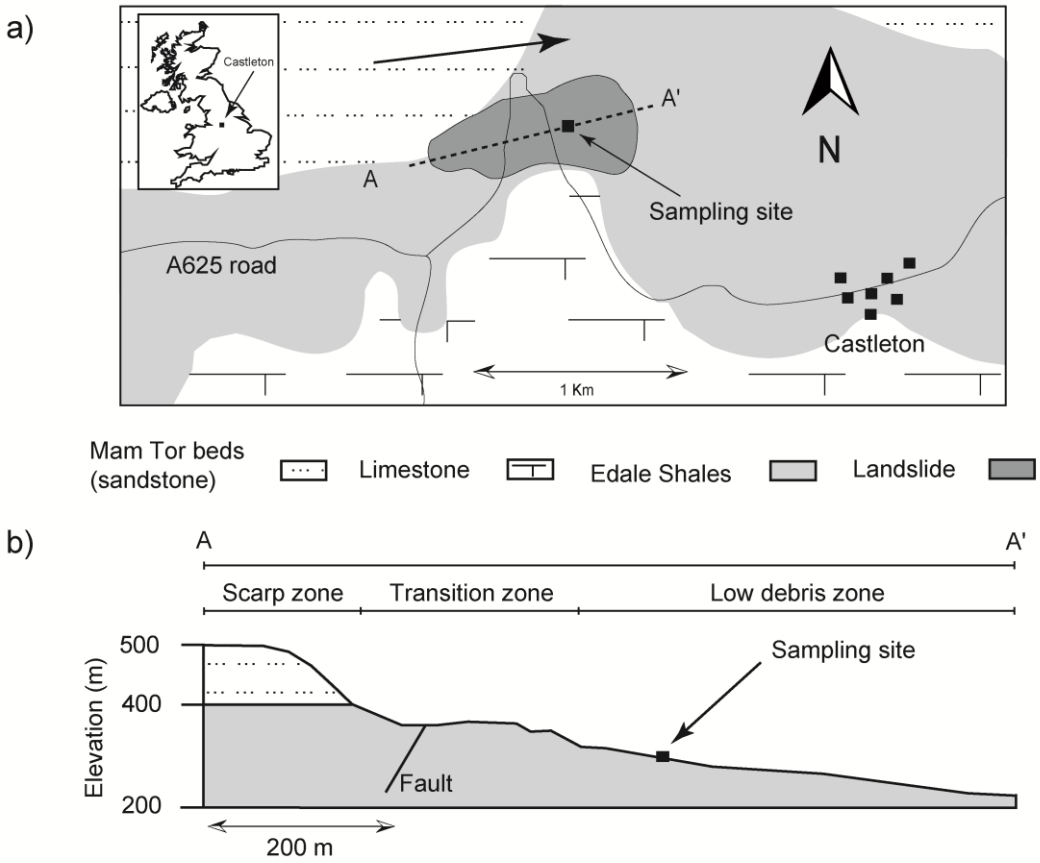

Figure 3.1. a) Location map and relevant geology of the Mam Tor landslide. The bold arrow indicates the general direction of the landslide. b)The cross section A-A' shows the Mam Tor beds and the Edale Shales; the scarp zone, transition zone and low debris zones of the landslide are also indicated. The scarp zone comprises the head scar and the scree slope. Figure modified from Skempton et al. (1989) and Waltham and Dixon (2000).

According to Waltham and Dixon (2000), the structure of the landslide is composed of three different zones: i) the scarp zone, that comprises the head scar and the slope; ii) the transition zone, that includes the fault that cuts through the landslide (Vear and Curtis 1981) and iii) the low debris zone where ARD streams emerge (Figure 3.1). The acidic ponds formed are ideal environments for well-adapted Fe(III)-reducing bacteria and for the study of the role of organic inputs in the amelioration of an acid drainage site.

3.2.2 Sample collection

Surface sediment samples from an acidic pond at the lower debris zone of Mam Tor (Figure 3.1) were collected using a stainless steel scoop and transferred into clean glass jars (acid washed and pre-furnaced), to minimise the risk of contamination. Samples of local plants (fern, reed and moss) were collected into pre-furnaced aluminium foil bags; acidic pond water (pH~3) was collected into clean plastic bottles and manure samples were collected into clean glass jars at Mam Tor (sheep manure) and at Tatton Park (Chesire, UK; pig and cow manures). The sediment and water samples were stored in the dark at -4°C to minimise any microbial activity while plant and manure samples were stored at -20°C until freeze-drying.

3.2.3 Experimental set up

Six series of microcosm experiments were prepared in quadruplicate, using 100 ml sterile serum bottles, 30 g of sediment, 60 ml of acidic pond water and 1 g of either plants or manures, as carbon sources. Two experiment controls were set up in triplicate using a sediment:water proportion 1:2, adding either glycerol (50 mM) as a positive control (Adams et al. 2007) or without external carbon sources (unamended sediment). All the microcosm bottles were sealed using butyl rubber stoppers and aluminium clamps, and bubbled with nitrogen for 15 min to create anaerobic conditions.

Three out of four microcosms were incubated at 20°C for 100 days; the fourth microcosm of each series was sampled immediately for pH, Eh and iron content, and stored after sampling at -20°C to preserve the initial conditions (t_0). Slurry samples of the incubated microcosms were anaerobically taken at 0, 7, 14, 28, 50 and 100 days for pH and Eh measurements using a Basic Denver pH/ORP meter (Denver Instrument Company) with a 3M KCl liquid-filled electrode (Ag/AgCl reference). Subsamples were filtered (0.22 μm) and acidified (2% w/v, HNO_3) for elemental analysis on an Optima 5300 dual view ICP-AES (PerkinElmer, US). The concentration of Volatile Organic Compounds (VOCs) was quantified on filtered (0.22 μm) but no acidified subsamples on a Bio High Pressure Liquid Chromatograph (Dionex, US) equipped with an IonPac ICE-AS1 ion-exclusion column (Dionex, US).

The bioavailable Fe(II) and total iron contents were measured in triplicate by reading the optical absorbance (at 562 nm) of subsamples treated according the ferrozine assay (Stookey 1970) and the hydroxylamine hydrochloride reaction (Lovley and Phillips 1987) on a Jenway 6715 UV/visible spectrophotometer. After 100 days

incubation (t_{100}), all the microcosms were anaerobically opened and the triplicates were combined into clean glass jars. Subsamples for Mössbauer analyses were anaerobically dried and the remaining of the combined slurries was freeze-dried for XRD and organic analyses.

3.2.4 Mineralogical and geochemical analyses

The mineralogy and geochemistry of Mam Tor sediment and microcosm slurries was monitored using Mössbauer Spectroscopy along with X-Ray Fluorescence (XRF) and X-Ray (powder) Diffraction (XRD) analyses. XRF analysis was performed to determine the elemental composition of the Mam Tor sediment using pressed pellets prepared with 12 g of pulverised surface sediment and 3 g of wax binder were used for quantification of major, minor and trace elements by XRF on an Axios Sequential XRF Spectrometer (PANalytical, Almelo, Netherlands).

XRD data were obtained from freeze-dried subsamples, on a Bruker D8 Advanced Instrument with $CuK_{\alpha 1}$ radiation, over a range of $5^{o}2\theta$ to $7^{o}2\theta$, using a step size of 0.02° each 2 s. Mössbauer data were collected on anaerobically dried samples at room and near liquid nitrogen temperature, on a FAST ComTeC 1024-multichannel analyser system, using a constant acceleration drive with a ~25 mCi $^{57}Co/Rh$ γ-ray source, and metallic iron foil for calibration. The spectra were modelled and fitted using the Lagarec/Rancourt Recoil software (Intelligent Scientific Applications Inc., Ottawa, ON, Canada; v. 1.0).

3.2.5 Organic analyses

The total organic matter content was quantified using the sequential loss on ignition method (Heiri et al. 2001, Beaudoin 2003). Glass vials were set at constant weight using an oven programmed at 375°C for 3 h to minimise any organic interference. Triplicates of the freeze-dried, pulverised sediments (500 mg each) were accurately weighed into the vials and heated at 105°C for 12 h, allowed to cool down into a desiccator and weighed. Subsequently, the samples were ignited at 350°C for 16 h, allowed to cool down into a desiccator and weighed again. The organic matter content, present in the sample, was determined calculating the difference in weight before and after ignition, expressed in percentage.

For lipid analysis, 40 g of surface sediment, 5 g of microcosm slurries or 5 g of local plants were extracted using a Soxhlet apparatus for 24 h with a solution of dichloromethane/methanol (2:1; v/v). The obtained Total Lipid Extracts (TLEs) were collected by rotary evaporation, concentrated by nitrogen blowing down and treated

with active copper (Blumer 1957) to remove elemental sulfur. Aliquots of the desulfurised TLEs were further fractionated using the method described by Dickson et al. (2009). After the addition of known amounts of internal standards (tetracosane-d50 and 2-hexadecanol), the aliquots were eluted on a silica column using 10 ml of a solution of chloroform saturated with ammonium hydroxide. The obtained extracts were further separated into hydrocarbon and alcohol fractions, via aluminium column chromatography using 6 ml of a solution of hexane/dichloromethane (9:1, v/v) and 6 ml of a solution of dichloromethane/methanol (1:1, v/v), respectively. The concentrated alcohol fractions were dissolved in bis(trimethylsilyl) trifluroacetamide (BSTFA) and heated at 70°C for 60 minutes to convert the alkanols into their correspondent trimethylsilyl ethers. Blanks were also prepared and analysed to ensure that no contamination was introduced during the extraction and fractionation procedures. Finally, all the hydrocarbon and alcohol fractions were concentrated in 50 µl of hexane for Gas Chromatography Mass Spectroscopy (GC-MS) analysis.

Lignocellulosic materials may also be used as a carbon source to determine whether the macromolecular compounds of the plant and manure enrichments were used, a pyrolysis (Py) analysis of subsamples taken at t_0 and t_{100} was carried out. The Soxhlet extracted residues of the microcosms slurries, were demineralised following the method described in Gélinas et al. (2001). This method consisted on the digestion of 250 mg of a sample in 30 ml of HCl (1 M) during 60 min with constant agitation; centrifugation for HCl removal, and a subsequent digestion for 12 h with a HCl:HF solution (10% HF in 1M HCl, v/v; 20 ml) using a shaker for complete reaction. The recovered material was rinsed with distilled water (3x, 3.5 ml) and freeze-dried for Py-GC-MS analysis. Samples of the local plants were also analysed by Py-GC-MS.

The lipid fractions were analysed on an Agilent 7890A gas chromatography system equipped with an Agilent 7683B auto-sampler and programmable temperature vaporisation (PVT) inlet interfaced to an Agilent 5975C MSD mass spectrometer operated in electron ionization mode (scanning a range of *m/z* 50 to 600 at 2.7 scans/s; ionisation energy, 70 eV; solvent delay, 3 min). The heated interface and PTV temperatures were set at 280°C; the mass source, at 230°C and the mass spectrometer quadrupole at 150°C. The analytical separations of the lipid fractions were accomplished using a HP-5 MS capillary column (Agilent; (5%-phenyl)-methylpolysiloxane; 30 m x 0.25 mm, i.d.), programmed from 70°C to 130°C at 20°C/min, then to 320°C at 4°C/min and kept isothermally for 10 min. The samples were run using He as a carrier gas at a constant flow (1 ml/min). Individual compounds were identified by comparison of their molecular mass (*m/z*) with The

National Institute of Standards and Technology (NIST) library and relevant literature (Goad and Akihisa 1997).

To fragment the macromolecular components, triplicates (1 μg each) of the demineralised samples and were pyrolysed in a quartz tube at 600°C (10s) using a Chemical Data System (CDS) 5200 Series Pyroprobe Pyrolysis Unit, coupled to the Agilent GCMS system described above. The pyrolysis transfer line and injector temperatures were set at 350°C; the heated interface, at 280°C; the electron ionization source, at 230°C and the mass spectrometer quadrupole, at 150°C. The samples were injected using He as carrier gas in split mode (ratio 5:1; constant flow, 1 ml/min) and the fragments were analysed using the HP-5 MS capillary column described above. The oven was programmed to hold 40°C for 3 min and then to 300°C at 4°C/min, and kept isothermally for 15 min. Individual compounds were identified by comparison of the molecular mass (*m/z*) with The NIST library and relevant literature (Saiz-Jimenez and De Leeuw 1986, Ralph and Hatfield 1991, Vancampenhout et al. 2009, del Río et al. 2012, Yassir and Buurman 2012). Over 40 different compounds were identified in the samples of the local material and samples of the microcosm experiments taken at t_0 and t_{100}. The sum of the 40 peak areas was set at 100% and the relative contribution of each compound was calculated. To determine the extent of biodegradation, those compounds were grouped into aromatic compounds (benzenes), lignin compounds (guaicol, syringol, methoxyphenols), phenolic compounds (other than methoxyphenols) and nitrogen compounds (amines and N-containing compounds). Polysaccharide compounds included furans, furfurals, ketones, cyclic hydrocarbons and glucopyranose compounds, but the group was represented only by the 5 more abundant compounds after levoglucosan; because levoglucosan contributed up to 38% of the overall concentration and the less abundant polysaccharides represented a negligible contribution, all those compounds were considered for identification purposes.

3.2.6 Microbial analyses

To determine the potential capacity to couple the reduction of Fe(III) to the oxidation of organic matter, the microbial diversity of Mam Tor sediment was studied using the sequence of 16S ribosomal RNA genes (16S rRNA). Samples taken from the Mam Tor sediment at t_0, and from the microcosm experiments at t_{100} were used to study the microbial changes occurring due to the addition of different natural carbon sources. The DNA from bacterial communities was isolated from 0.2 g of sediment and 0.2 ml of microcosm slurries, using the MoBio PowerLyzer™ UltraClean Microbial DNA

Isolation Kit (MoBio Laboratories, Inc., Carlsbad, CA, USA). The bacterial primers 27F (Lane 1991) and (Hamady et al. 2008), targeting the V1-V2 hypervariable region of the bacterial 16S rRNA gene, were applied in the PCR for amplicon pyrosequencing. This run was performed at the University of Manchester sequencing facility, on a Roche 454 Life Sciences GS Junior system. The pyrosequencing reads were analysed using QIIME v. 1.8.0 (Caporaso et al. 2010), for data denoising and chimera removal, during operational taxonomic unit (OTU) picking (at 97% sequence similarity) with USEARCH (Edgar 2010). QIIME was also applied for the taxonomic classification of all reads using the Ribosomal Database Project (RDP) at 80% confidence threshold (Cole et al. 2009). The closest GenBank match for the most representative sequence for each OTU, was identified by BLASTN nucleotide search.

3.3. RESULTS AND DISCUSSIONS

3.3.1 Inorganic characterisation of Mam Tor sediment

The elemental analysis of the Mam Tor sediment, indicated a predominance of Fe_2O_3 (89%) and SO_3 (8.4%) with minor amounts of other minerals probably from phyllosilicate origin (Allen 1960, Ford et al. 1993). Mn (53 ppm) and W (47 ppm) were the most abundant trace elements that could be associated to some tungstates such as wolframite (Fe, Mn)WO_4 and Mn sulfides. Zn contribution (39 ppm) can be related to the presence of sphalerite (ZnS), whereas Ni (12 ppm) and Cu (9 ppm) can be attributed to some nickel sulphides such as millerite (NiS) or to the dissolution of chalcocite (Cu_2S) or chalcopyrite ($CuFeS_2$), respectively (Table 3.1).

Table 3.1. Elemental composition of Mam Tor sediment

Oxides (%)[a]		Other elements (ppm)	
SiO_2	1.5	Mn	53
Al_2O_3	0.5	W	47
Fe_2O_3	89.0	Zn	39
CaO	0.1	Ni	12
SO_3	8.4	Cu	9
		Br	4
		Ba	3
Total	99.5	Mo, Sr, Co	1

[a] variation <0.1%

The presence of poorly crystallized iron oxides is typical of AMD sites (Ferris et al. 1989), in line with this, the mineralogical analysis by XRD (Figure 3.2) confirmed that the Mam Tor sediment was dominated by iron oxides, in the form of a poorly crystalline goethite (α-FeOOH).

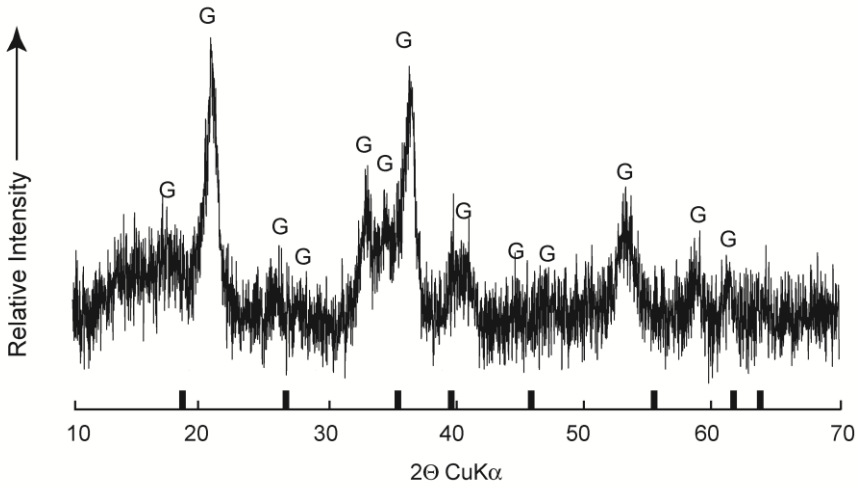

Figure 3.2. X-Ray diffractogram showing goethite (G) as the dominant mineral phase in Mam Tor sediment. The bold lines indicated the 2θ angles typically used for schwertmannite identification.

In accordance with XRD data and the XRF analysis, the Mössbauer spectrum at room temperature (Figure 3.3a), was fitted using a single doublet with an isomer shift, δ/Fe=0.38 mm/s and quadrupole splitting, Δ=0.56 mm/s identified as goethite. At near liquid nitrogen temperature (Figure 3.3b), two six-line patterns (δ/Fe=0.48 mm/s, H= 431 kOe; δ/Fe=0.49 mm/s, 462 kOe) and a central doublet (δ/Fe=0.46 mm/s, Δ= 0.73 mm/s) were observed and attributed to goethite (Table 3.2).

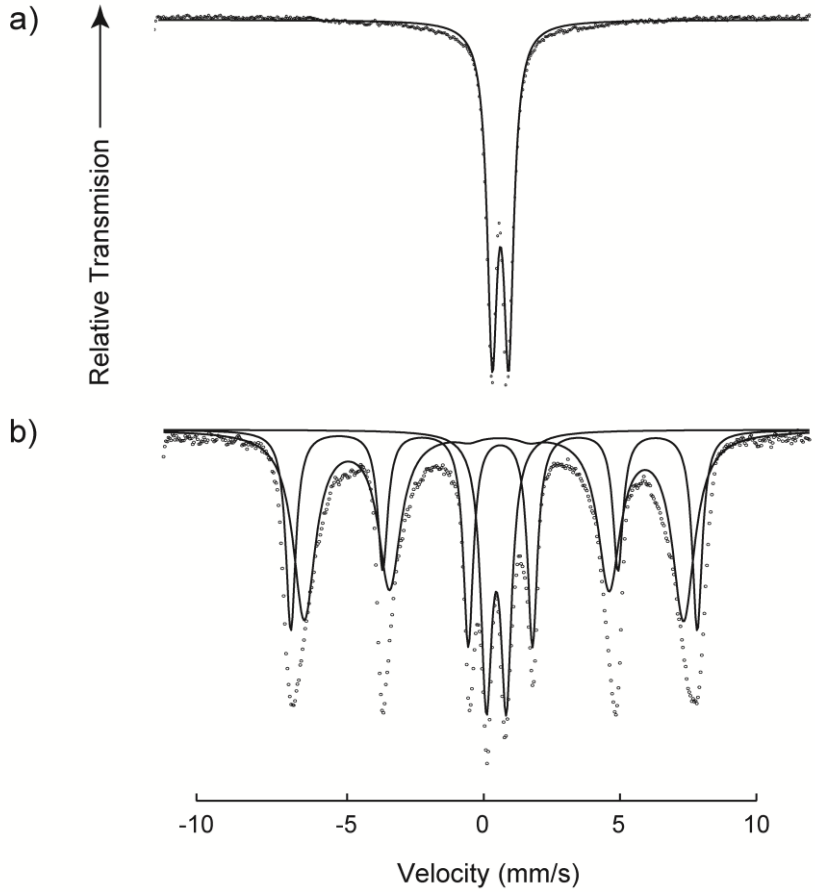

Figure 3.3. a) A single doublet of goethite is observed from Mössbauer analysis at room temperature. b) The Mössbauer spectrum at near liquid nitrogen temperature shows the magnetic behaviour of goethite with the central doublet produced by superparamagnetism of small size particles.

There are two possible explanations for this spectrum, first, the coexistence of a magnetic sextet and a doublet of the same iron phase may occur when the superparamagnetic blocking temperature is not reached (Mørup et al. 1983). Second, at low temperature, the hyperfine magnetic field, H, of the normal goethite is approximately of 500 kOe (Eissa et al. 1974, Murad 1989, Bocquet et al. 1992), therefore the reduced value of 431 kOe may be related to an impurity (such as Al) or to small particle size (van der Kraan and van Loef 1966, Golden et al. 1979, Mørup et al. 1982). The effect due to impurities or small particle size are practically indistinguishable (Bocquet et al. 1992). In this work such behaviour was attributed to small particle effect based on the Scherrer relation that gave a crystallite size of 40.1±3.5 nm and on the low aluminium content of the surface sediment (0.5%), although it is also possible the presence of carbon impurities in the mineral (Yapp and

Poths 1986). Data from Table 3.2 can be compared with data in Table 3.5 which shows the Mössbauer parameters of microcosm experiments.

Table 3.2. Mössbauer hyperfine parameters of Mam Tor sediment

T	δ/Fe (mm/s)	Δ (mm/s)	H (kOe)	Values reported for α-FeOOH	References
RT	0.38	0.56		δ/Fe=0.34-0.38 mm/s	Vandenberghe et al. (1986)
				Δ= 0.5-0.7 mm/s	Olowe et al. (1990)
				δ/Fe=0.38 mm/s	
				Δ= 0.58 mm/s	Herbert (1997)
				δ/Fe=0.37-0.39 mm/s	
				Δ=0.54-0.58 mm/s	
LN	0.46	0.73		δ/Fe=0.47-0.50 mm/s	Larese-Casanova et al. (2010)
				Δ=0.65-0.79 mm/s	
	0.48		431	δ/Fe=0.48-0.49 mm/s	Goodman and Lewis (1981)
				H= 432-469 kOe	
	0.49		462	δ/Fe=0.47-0.51 mm/s	Huggins et al. (1983)
				H= 449-495 kOe	

T= temperature.
RT= room temperature.
LN= near liquid nitrogen temperature.
δ/Fe= isomer shift relative to metallic iron.
Δ= quadrupole splitting
H=Magnetic hyperfine field.

The presence of schwertmannite ($Fe_8O_8(OH)_6SO_4$) may also be considered, but this mineral was not detected by XRD analysis, probably because if it was occurring, its signal was masked by those of goethite (Murad and Rojik 2005); for reference, the 2θ angles for the XRD spectra of schwertmannite are indicated in Figure 3.2. Additionally, although sulfur could be present on schwertmannite, it was more probable that sulfur was part of sulfides or sulfosalts that involve some of the other minerals detected by XRF analysis (e.g. ZnS, NiS, Cu_2S).

3.3.2 Organic analyses of Mam Tor sediment and plant contributions

Several organic analyses were carried out to examine the organic inputs present in the Mam Tor sediment. The lipid analysis indicated that the hydrocarbon fraction of the Mam Tor sediments was dominated by a homologous series of High Molecular Weight (HMW) *n*-alkanes with predominance of odd-numbered homologous and the C_{23} *n*-alkane being the most abundant homologue (C_{max}) (Figure 3.4a; Table 3.3). The

carbon preference index, (CPI, defined in Table 3.3) was 5.6; the summed concentration, 2.3 μg/g sediment; and the Average Chain Length (ACL, defined in Table 3.3) 23.6. Such parameters suggested that the hydrocarbon fraction of the sediment had a high influence of plant derived organic matter (Figure 3.4a; Table 3.3).

Table 3.3. Analysis of the hydrocarbon fractions of the Mam Tor sediment and local plants

Sample	*n*-alkanes				
	$\Sigma C_{20\text{-}31}$[a]	$CPI_{20\text{-}31}$[b]	$ACL_{20\text{-}31}$[c]	C_{max}[d]	P_{aq}
Sediment	7.4	8.1	24.7	23	0.77
Moss	11.9	27.3	24.2	23	0.97
Fern	35.5	11.1	26.1	29	0.53
Reed	50.2	13.9	28.8	29	0.08

[a] Summed concentration over the range C_{20}-C_{31} expressed in μg/g sediment.
[b] CPI= carbon preference index over the range C_{20}-C_{31} (van Dongen et al. 2008) $0.5[(X_{21+}X_{23}+...X_{31})/(X_{20}+X_{22}+...X_{30})]+0.5[(X_{21}+X_{23}+...X_{31})/(X_{22}+X_{24}+...X_{30})]$, where X is concentration.
[c] Average chain length over the range C_{20}-C_{31}, ACL= $\Sigma(20X_{20} + ... + 31X_{31})/\Sigma(X20 + ... +X_{30})$, where X is concentration.
[d] Chain length of the *n*-alkane with highest concentration.
$P_{aq}=(X_{23}+X_{25})/(X_{23}+X_{25}+X_{29}+X_{31})$ (Ficken et al. 2000), where X is concentration.

The predominant vegetation of the study site was characterised by the presence of reeds (*Juncus effusus* and *Juncus acutiflorus*), ferns (*Pteridium aquilinum)* and *Sphagnum* moss. Comparable with the sediment content, all plant hydrocarbon fractions were dominated by homologous series of HMW *n*-alkanes with predominance of odd-numbered *n*-alkanes, clearly reflected in a CPI ranging from 11.1 to 27.3 (Figure 3.4; Table 3.3). The hydrocarbon fraction of *Sphagnum* moss was dominated by the C_{23} and C_{25} homologues, typical feature of different species of *Sphagnum* (Nott et al. 2000, Bingham et al. 2010), but with a considerably lower concentration of the other HMW *n*-alkanes (Figure 3.4b; Table 3.3). The ratio C_{23}/C_{25} of this sample was of 1.11, which may suggest a relationship with *S. capillifolium,* but is also similar to those reported for *S. angustifolium, S. palustre* and *S. recurvum* (Bingham et al. 2010).

The hydrocarbon fraction of the reeds ranged from the C_{21} to the C_{31} *n*-alkanes with a predominance of odd-numbered *n*-alkanes (CPI= 13.9), maximising at the C_{29} and C_{31} homologues with an ACL of 28.8 (Figure 3.4c; Table 3.3), whereas the distribution patter of the *n*-alkanes from the fern sample, showed a typical distribution of higher plants (Eglinton and Hamilton 1963, 1967) with *n*-alkanes ranging from the C_{21} to C_{31}

homologues maximising at C_{23} and C_{25} and also in C_{29} and C_{31} n-alkanes and ACL of 26.1 (Figure 3.4d; Table 3.3).

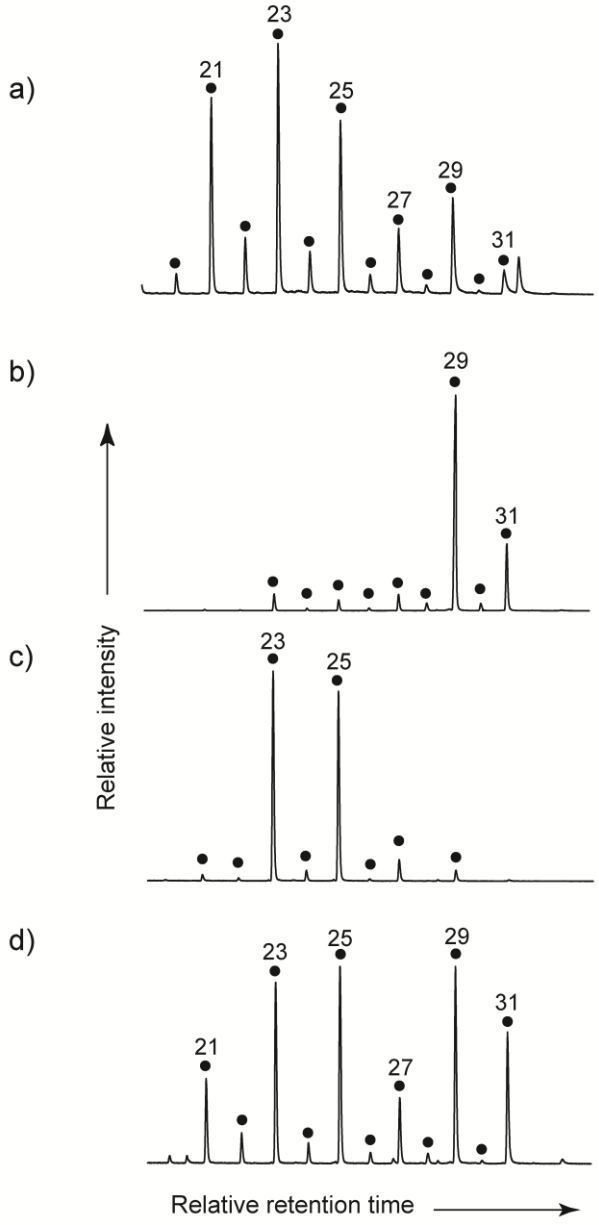

Figure 3.4. Comparison of the partial ion current chromatograms (*m/z 57*) of a) the Mam Tor sediment and local plants: b) reeds, c) mosses d) ferns. Closed circles indicate *n*-alkanes. Numbers indicate carbon chain length.

To better estimate the relative contribution of the different plants in the Mam Tor sediment, the P_{aq} proxy (defined in Table 3.3) was calculated. The value obtained for the *Sphagnun* sample was P_{aq}=0.97; for reed, P_{aq}=0.08 and fern P_{aq}=0.53. The sediment yielded a P_{aq} value of 0.77, which along to the hydrocarbon distribution

pattern indicated a mixed plant input with a predominant contribution of *Sphagnum* moss and fern (Table 3.3).

Regarding to the Py-GC-MS analyses (Figure 3.5), the macromolecular composition of the sediment indicated a relative predominance of polysaccharides (43.7%); lignin compounds (19.4%); nitrogen compounds (17.2%); phenols (12.3%) and aromatic compounds (7.4%). The most abundant macromolecular groups (at relative abundance) in the *Sphagnum* sample were the polysaccharides, representing 61.5%, and phenolic compounds, representing 20.8%. Nitrogen compounds contributed with 11.9%; aromatic compounds, with 4.8 % and lignin with ~1%. The characteristic *Sphagnum* compound at *m/z 134* (McClymont et al. 2011) was also detected in the sample. Kirk and Farrell (1987) indicated that lignin is found in higher plants, including ferns, but not in mosses. However, other works have suggested that *Sphagnum* moss indeed contain lignin (Farmer and Morrison 1964, Bland et al. 1968). In the Mam Tor sample, the lignin contributions were related to the presence of a compound at *m/z 135,* identified as 4-vinylguaiacol (*m/z* 135, 150) and to the contribution of 4-methyl guaiacol (*m/z* 138, 123).

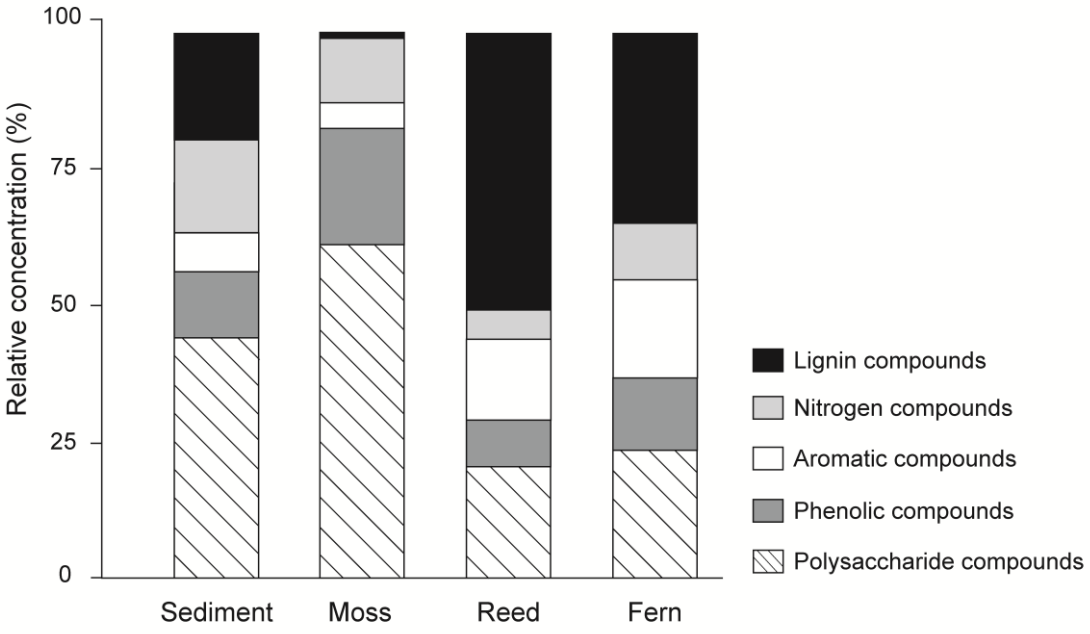

Figure 3.5. Macromolecular characterisation of Mam Tor sediment and local vegetation.

The reeds contained 50.4% of lignin; the polysaccharide fraction represented 21.2% and the aromatic compounds, 14.8% (Figure 3.5). Phenols and nitrogen compounds contributed with 8.1% and 5.4% of the sample, respectively. The lignin and polysaccharide contributions in this sample were different from those reported in

Benner et al. (1984) for *Juncus roemerianus*, which have a polysaccharide composition of 75% and 25% lignin. This may be explained because *J. roemerianus* was taken from a salt marsh while reeds growing in acid drainage environments (i. e. *Juncus bulbosus*) may have developed adaptive mechanisms to survive (Chabbi 1999, Fyson 2000).

Ferns growing at Mam Tor posses a range of toxic chemicals within its tissues which can prevent it being eaten or decaying (Fenwick 1989). Pyrolysis data showed a (relative) lignin content of 34.7%, followed by 23.7% of polysaccharides and 17.4% of aromatic compounds. Phenols and nitrogen compounds represented 13.8% and 10.4% respectively (Figure 3.5). Collectively, the organic results indicate that Mam Tor sediment is not carbon limited (14.3% of organic matter) and that the organic matter inputs, such as the saturated hydrocarbons and the macromolecular markers, are derived from the local plants, mainly from moss and ferns.

3.3.3. The bacterial community

The characterisation of the microbial population from the acidic ponds of Mam Tor was important to determine its potential involvement in the use of different natural electron donors. The 16S rRNA gene sequences amplified from the bacterial population growing in the surface sediment, indicated that the bacterial population comprised approximately 30% of unclassified microorganisms and four main phylogenetic divisions; *Solibacteres* (17.7%), *Alphaproteobacteria* (16.7%), *Gammaproteobacteria* (16.7%) and *Acidobacteria* (5.6%).

The *Solibacteres* were mainly represented by microorganisms closely related to the uncultured bacterial clone *W2-75* (Barreto et al. unpublished), identified in a sample obtained from an abandoned mine. The dominant *Alphaproteobacteria* included microorganisms closely related to the uncultured bacterial clone *RS-G2* (8.9%), detected in rivers contaminated with AMD (Li and Sun unpublished). A second member of the *Alphaproteobacteria* was related to the uncultured *Acidisphaera sp. clone SBLE1E7* (4.4%) identified in a sulfate-reducing community (Meier et al. unpublished). The third most abundant member of the *Alphaproteobacteria* was closely related to *Acidiphilum sp. NO-17 (1%)*, which has 95% sequence similarity to *A. rubrum* and 94% *to A. cryptum (Johnson et al. 2001)*. Some *Acidiphilium* species are capable of coupling the reduction of Fe(III) to the complete oxidation of a large variety of substrates such as glucose and H_2 (Küsel et al. 1999).

The *Gammaproteobacteria* were represented by a clone closely related to the uncultured proteobacterial clone *BHL3-310I-54* (16.7%), that has been implicated in the reduction of Fe(III) in an alkaline environment (Whittleston et al. 2011). The *Acidobacteria* genus included microorganisms mostly related to the uncultured bacterial clone *WER18* (Männistö et al. 2013). Collectively, these results are consistent with the microbial communities detected in a range of AMD/ARD sites worldwide (Bond et al. 2000a, Bond et al. 2000b, Johnson et al. 2001, Johnson and Hallberg 2003, Kuang et al. 2013).

3.3.4 Fe(III)-reduction and microcosm geochemistry

Several series of anaerobic microcosms were set up using different natural carbon sources but for simplicity, they were grouped into plant- or manure amended microcosms when necessary.

The most significant neutralisation effect was produced using the manure amendment which increased the pH of the system immediately after its addition (from pH 3.1 to pH 4.5) and thereafter, kept increasing up to near neutral conditions (pH 5.8) (Table 3.4; Figure 3.6a). The manure addition also yielded the highest Fe(III) -reduction rate (43 mM, Fe(II)) concomitantly with a decrease in the redox potential (-102 mV) and elevated sulfate concentration (91.5 mM/l; Table 3.4; Figure 3.6b). The accumulation of lactate (118 mg/l), and the decrease of acetate (from 18 mg/l to below detection limit) is likely to be related to the presence of fermentative microorganisms such as *Paludibacter sp.* and to the stimulation *Desulfovibrio sp.* (Table 3.4; Figure 3.8). An elevated Mg concentration (from 10 mg/l to 14 mg/l) was also observed using manure enrichments (Table 3.4).

In the glycerol amended microcosms, the pH improved moderately, from pH 3.2 to pH 3.8, producing a Fe(II) concentration of approximately 40 mM, (Table 3.4; Figure 3.6a) consistent with a previous study (Adams et al. 2007). High levels of sulfate (132.3 mM/l) were also recorded, but no substantially amounts of volatile organic compounds could be detected. For the sediment stimulated with local plants, the pH became more acidic over incubation (pH 3.0) and therefore, no significant effect of AMD remediation was demonstrated (Table 3.4; Figure 3.6a). The sulfate concentration of these systems was on average 66.7 mM and the Fe(II) concentration, 34 mM. The acetate accumulation (455 mg/l), was observed, probably due to the hydrolysis and fermentation of cellulose compounds by microorganisms closely affiliated to *Clostridia* populations (Figure 3.8).

Table 3.4. Geochemical parameters of microcosms

Type	UM t_0	UM t_{100}	Glycerol t_0	Glycerol t_{100}	Plants t_0	Plants t_{100}	MA t_0	MA t_{100}
Fe II (Mm)	0.5 ±0.1	14 ±0.2	0.5 ±0.1	40 ±5	0.8 ±0.4	34 ±2	0.4 ±1	43 ±4
pH	3.1[a]	2.7[a]	3.2 [a]	3.8 ±0.2	3.3 [a]	3.0 [a]	4.5 ±0.1	5.8 ±0.4
Eh (mV)	563 ±172	495 ±146	414 ±0.6	591 ±5	403 ±5	494 ±3	517 ±87	-102 ±13
Sulfate (mM/l)	9.3 ±0.2	44.8 ±1.4	8.2 ±0.8	132.3 ±22.0	12.5 ±0.4	66.7 ±3.0	14.8 ±3	91.5 ±27
Lactate (mg/l) *	<0.01	151 ±6	<0.01	<0.01	<0.01	<0.01	<0.01	118 ±12
Acetate (mg/l) *	<0.01	<0.01	<0.01	<0.1	<0.1	455 ±7	18 ±10	<0.1
Mg (mg/l)	5 ±0.3	6 ±0.8	47 ±0.2	44 ±0.8	60 ±0.5	59 ±7.0	10 ±0.7	14 ±2
Mn (mg/l)	1.2[a]	1.5[a]	11[a]	12[a]	14 [a]	17 ±1.3	1.1 ±0.4	1.7 ±0.6

UM=unamended sediment.
MA=manure amended microcosms.
* values below the typical routine detection limits (0.01 – 0.1 mg/l) reported as <0.01
[a] value variation <0.1 units
t_0=Initial conditions of experiments.
t_{100}=Final conditions of experiments, after 100 incubation days.

Studies performed using sediment samples taken from lakes contaminated with AMD (pH ranging from 3.1 to 5.6), indicated that the addition of lactate to did not stimulate the formation of Fe(II) and acetate was not consumed but inhibited its formation (Küsel and Dorsch 2000). Blodau and Peiffer (2003) also indicate that the hydrolysis/fermentation of organic matter is a limiting factor for sulfate and Fe(III)-reduction in acidic lakes (pH 3 – 8). In a similar way, our experiments showed a low Fe(III)-reduction rate in presence of acetate and both the highest and the lowest Fe(III)-reduction rates in presence of lactate. These findings further support the idea that acetate is an inhibitory addition and that the lactate is not an effective electron donor.

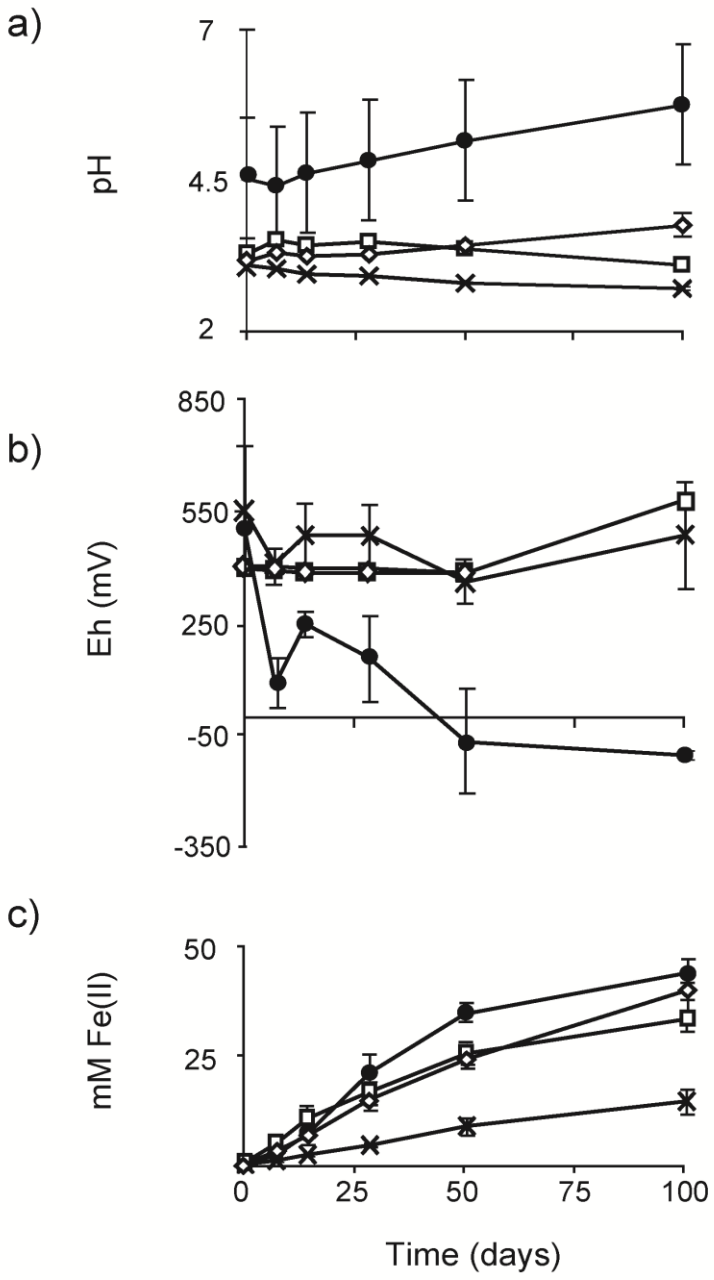

Figure 3.6. a) Changes in pH using different electron donors over 100 days incubation. b) Slurries Eh. c) Time course of Fe(II) concentrations obtained using different electron donors. Closed circles indicate manure microcosms; open squares, plants addition; open diamonds, glycerol addition; crosses, unamended microcosms.

3.3.5 Characterisation of the sediment after incubation

After 100 days of stimulating the ARD sediment using different natural carbon sources, the XRD analyses of the microcosm slurries indicated that goethite was the dominant mineral phase in all the experiments. In accordance with this, the Mössbauer spectra of all the microcosm slurries were fitted using two sextets interpreted as arising from goethite (Table 3.5; Figure 3.7). The hyperfine magnetic field values of the slurries were higher than those calculated for the starter sediment (see Table 3.2), probably related to an increase in the particle size or the formation of particle clusters (Tamura and Mizushima 2002).

Table 3.5. Mössbauer hyperfine parameters of the Mam Tor sediment stimulated using different amendments after 100 days incubation.

T	Microcosm type	δ/Fe (mm/s)	H (kOe)	Values reported for α-FeOOH	References
LN	Plant amended	0.51	472	δ/Fe=0.36-0.56 mm/s H= 482-535 kOe	Eissa et al. (1974)
		0.48	444	δ/Fe=0.45-0.46 mm/s H= 497-504 kOe	Berquó et al. (2007)
LN	Manure amended	0.49	457	δ/Fe=0.48 mm/s H=502 kOe	Bocquet et al. (1992)
		0.50	481	δ/Fe= 0.61-0.62 mm/s H= 500-502 kOe	Brož et al. (1990)
LN	Glycerol amended	0.51	477	δ/Fe=0.63-0.69 mm/s H=495-510 kOe	Dézsi and Fodor (1966)
		0.48	451	H=434-441 kOe	Murad and Bowen (1987)

T= temperature.
LN= near liquid nitrogen temperature.
δ/Fe= isomer shift relative to metallic iron.
H=Magnetic hyperfine field.

The calculus of the crystallite size provided evidence for the increase of the particle size, with a considerable change using manure (from 41 nm to 59 nm) and only a slight size variation using plant material (from 40 nm to 45 nm). Consistently, the reduced hyperfine magnetic field value of the plant amended microcosms was of 444 kOe (Table 3.5).

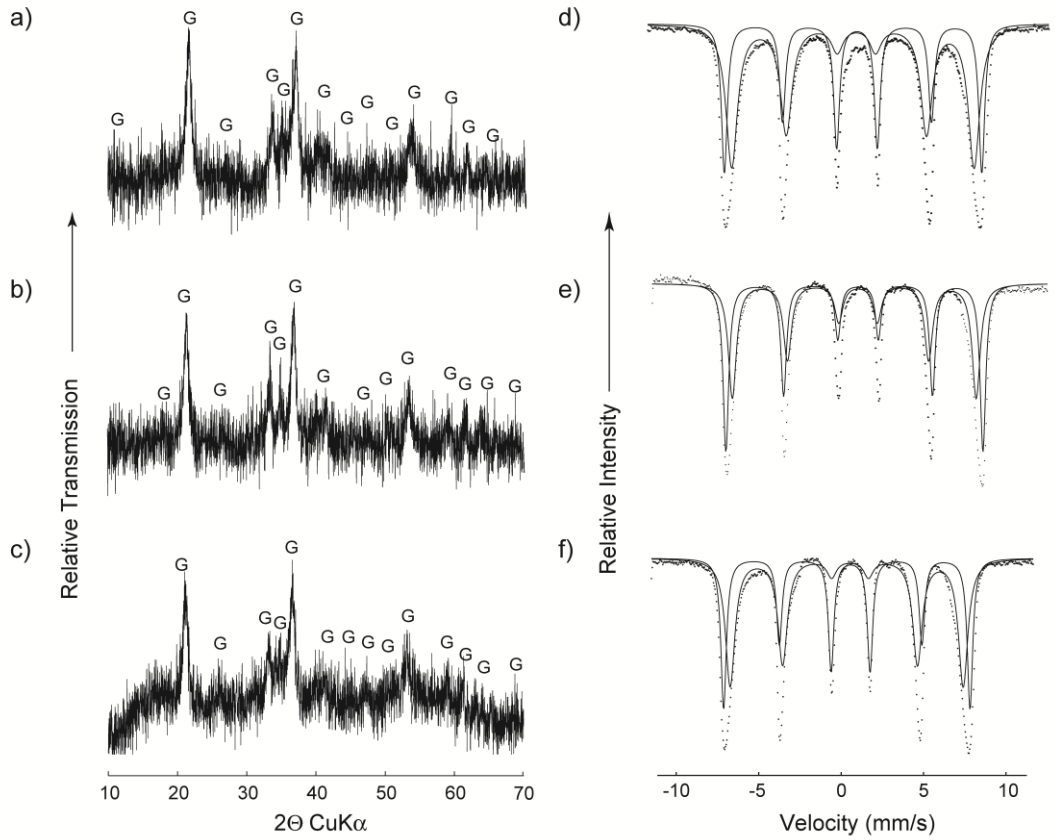

Figure 3.7. Changes after 100 days of incubation in microcosms amended with different carbon sources. Left, X-Ray diffractograms of a) plant amended microcosms b) manure amended microcosms, c) glycerol amended microcosms. Goethite (G) was the dominant iron phase. Right, Mössbauer spectra (at near liquid nitrogen temperature) of d) plant amended microcosms, e) manure-amended microcosms and f) glycerol amended microcosms.

An interesting observation was that the central doublet attributed to fine particles of goethite (Figure 3.3), disappeared after incubation (Figure 3.7). Prior studies have indicated that iron hydroxides in fine particles are more bioavailable than the bulk mineral (Pédrot et al. 2011). It has also been shown, for example, that the microbial reduction of hematite depends on the size and shape of the nanoparticles involved (Bose et al. 2009, Dehner et al. 2010). Considering this, the absence of the contribution of goethite in fine particles suggested that this iron fraction was bioavailable and was used during the microbial Fe(III)-reduction. The Mössbauer parameters of the sediment after 100 days of incubation are presented in Table 3.5 and compared with the data from the literature therein.

3.3.6 Bacterial communities stimulated using natural carbon sources

Regarding to the bacterial populations stimulated using different natural electron donors, the 16S rRNA gene sequences amplified from the bacterial community of the microcosm slurries, showed the following results. After 100 days incubation, the sediment without any external electron donor added (unamended sediment t_{100}), contained abundant bacterial sequences affiliated to the *Gammaproteobacteria* and the *Alphaproteobacteria* classes, comprising the 37.2% and 17.3% of the bacterial sequences, respectively (Figure 3.8).

Microorganisms closely related to the uncultured proteobacterial clone *BHL3-310I-54* (detected at t_0) doubled in relative abundance and seemed to have replaced the *Solibacteres* (not detected at t_{100}). The data may suggest that the organisms related to *BHL3-310I-54* may have been involved in the redox reactions of the system. Whittleston et al. (2011) detected the *BHL3-310I-54* in a hyperalkaline Fe(II)-containing soil where chromate reduction had taken place; this may indicate that such microorganisms have the capacity of adapting to different environments where metals are present at high concentrations, possibly participating on the Fe(III) - reduction.

Two microorganisms were representative of the *Alphaproteobacteria*, one affiliated with the uncultured *Acidisphaera sp. clone SBLE1E7* (5.1%) detected in sulfate reducing community (Meier et al. unpublished) and the second affiliated with the uncultured bacterial clone *RS-G26* (1.8%), detected in river sediments affected by mine activity (Li and Sun unpublished). A large proportion of the sequences (35%), was composed of unclassified microorganisms with an abundance of ~1%, each, of the total number of sequences.

The plant t_{100} sample was dominated by *Clostridia* (70.4%) and *Alphaproteobacteria* (12.6%; Figure 3.8). *Clostridia* comprise microorganisms capable to ferment or degrade plant polysaccharides, involving the use of enzymes such as cellulases and xylanases (Cornet, 1983; Kato et al, 2004; Thomas 2014). Some members of this genus have been recently used in the production of biofuels (Joungmin et al., 2012; Thomas et al 2014).

In the plant t_{100} sample, *Clostridia* were chiefly represented by microorganisms closely related to the mesophilic and obligated anaerobe *Clostridium nitrophenolicum strain 1D*. This bacterium grows at a temperature range between 20°C and 45°C and at a pH range from pH 6.5 to pH 8.0. It is also capable of degrading p-nitrophenol under anaerobic conditions, and to produce (from glucose) end products such as acetate, formate and pyruvate (Suresh et al. 2007). Members of the *Clostridia* have also been

detected in acid drainage environments; here, microorganisms identified as *C. scatologenes SL1*, have shown the capacity of use side chains of aromatic compounds (Küsel et al. 2000).

On the other hand, Ramond et al. (2014) suggested that some *Clostridia* may have been involved in the neutralization of AMD. Such results are not consistent with those of this study, but it is necessary to consider that Ramond's experiments were based on synthetic AMD, using glucose as the carbon source. In the plant t_{100} sample, a microorganism closely related to the *Alphaproteobacterium Desulfosporosinus sp. enrichment culture clone K1* (Sánchez-Andrea et al. 2013) was also detected (7.7%). Members of the genus *Desulfosporosinus* are strictly anaerobic, spore-forming bacteria (Sánchez-Andrea et al. 2013) that are able to degrade incompletely organic compounds to acetate (Alazard et al. 2010). The fermentative pathway of microorganisms like *Clostridium sp*. and *Desulfosporosinus sp.* may explain the accumulation of acetate reported in Table 3.4. Other *Alphaproteobacteria* (2%) were closely related to the uncultured bacterial clone *W7-62* (Barreto et al. unpublished) while approximately 4.6% of the total sequences were unclassified microorganisms.

The sample of the microcosm glycerol t_{100} (Figure 3.8) was dominated by *Gammaproteobacteria* (16%) with microorganisms mostly related to the uncultured *Proteobacterial* clone *BHL3-310I-54* (Whittleston et al. 2011), which was also found in the unamended t_o sample (at an abundance of 16.7%). The addition of glycerol also favoured selection of *Deltaprotobacteria* (12%), represented by microorganisms closely related to the uncultured bacterial clone *CN2m-bac_h7*, detected in acidic lakes (Santofimia et al. 2013).

Another bacterial class detected at significant loadings was the *Acidobacteria*, with a summed abundance of 17.3%, including 8.8% of microorganisms related to the uncultured bacterial clone *W7-15* (Barreto et al. unpublished); 3.8% of bacteria related to the *Acidisphaera sp. clone SBLE1E7* (Meier et al. unpublished) and 2.7% of the bacteria related to the uncultured bacterial clone *WER18* (Männistö et al. 2013).

Bacilli closely affiliated to the uncultured *Alicyclobacillus sp. clone DAAP3B4* represented approximately 5% of the total sequences*;* this bacterium is closely related to *Alicyclobacillus ferrooxidans (NR_044413)* and *Alicyclobacillus K23_bac* (EF464642) (Kay et al. 2013). Unclassified bacteria represented 21% of the total sequences, but their abundance was less than 3% each. Within this percentage, the most abundant microorganisms were closely related to the uncultured bacterial clone

GB7N87003GH4UR (Yergeau et al. 2012) and to the uncultured bacterial clone *T4_42* (Imfeld and Richnow unpublished), representing the 2.9% and 2.5% of the genes sequenced, respectively (Figure 3.8).

In the sample from the manure-amended microcosm taken at t_{100}, the *Bacteroidia* class comprised the largest portion of the 16S rRNA gene library (Figure 3.8). The most abundant sequence belonged to microorganisms closely related to an uncultured *Paludibacter sp. clone 17-13* (32%), detected in a sulfate-reducing community (Meier et al. unpublished). Other members of this genus have also been identified in acid mine environments (Sánchez-Andrea et al. 2013) and in AMD bioreactors amended with complex organic substrates such as peat, spent brewing grain and municipal biosolids (Lindsay et al. 2011). *Paludibacter sp*. are fermentative bacteria, for example, *P. propionicigenes* has the capacity of fermenting a variety of sugars, forming propionate and acetate as the end products (Ueki et al. 2006).

Although less abundant (14%), *Bacilli* were the second most highly represented group characterised by the uncultured *Alicyclobacillus sp. clone DAAP3B4* (Kay, 2013) (8.9% of the total sequences). Members of this genus are able to reduce Fe(III) (Bridge and Johnson 1998) and others such as *Alicyclobacillus Y004* are non-Fe(II) oxidising bacteria (Johnson et al. 2003). *Alicyclobacillus Y004* is a strictly heterotroph, able to grow at temperatures ranging from 40°C to 81°C and pH values ranging from 2.1 to 2.9 although can be found at pH 1 (Johnson et al. 2003). Other uncultured bacillus mostly closed to the prokaryote clone *6B_3951* (Mendez-Garcia et al. 2014), represented 2.9% of the 16S rRNA gene library while the sequences affiliated with the *Deltaproteobacteria* represented 9.5%. A microorganism closely related to *Desulfovibrio idahonensis strain CY2* was the most highly represented (5.6%). *Desulfovibrio* members can tolerate extreme environmental conditions (Abildgaard et al. 2006) and are able to use a wide range of electron donors (Reichenbecher and Schink 1997, Hernandez-Eugenio et al. 2000). *D. idahonensis CY2* can reduce Fe(III), although this process does not support its growth. The strain is also unable to use acetate, and was found to contain *c*-type cytochromes and to reduce different forms of sulfur using lactate as an electron donor. The optimal growth for this bacterium are temperatures between 10°C and 37°C and the pH range from pH 6.5 to pH 7.5 (Sass et al. 2009).

Microorganisms, closely related to the uncultured *Geobacteraceae clone M22_1334* (Holmes et al. 2007), represented 1.9% of the total 16S rRNA genes detected. *Geobacter* species are remarkably important metal-reducing microorganisms due their ability

amongst others of coupling Fe(III) (or metal) reduction to the complete oxidation of organic compounds (Lovley et al. 1993, Zhang et al. 2012, Orellana et al. 2013) and they are used widely for environmental applications.

Other bacterial classes detected were *Acidobacteria* and *Spirochaetes* that represented approximately 5% of the microbial community each (Figure 3.8). *Acidobacteria* closely related to the uncultured *Acidobacterial* clone *T7_12* were also identified in this sample (2.3%). These bacteria have been detected in a wetland treating 1,2-dichloroethenes (Imfeld and Richnow unpublished). The uncultured *Spirochaetaceae* bacterial clone *L6-D1* represented 2.9% of the bacterial community. This organism has been detected in sulfate-reducing bioreactors used for AMD treatment (Koschorreck et al. 2010). Unclassified microorganisms represented 6% of the sequences detected. Some representatives of this group may be closely related to the uncultured bacterial clone *GB7N87003GH4UR* (Yergeau et al. 2012) and to the uncultured bacterial clone *T4_42* (Imfeld and Richnow unpublished). The rest of the unclassified microorganisms represented less than 1% each of the total number of genes detected.

With exception of the manure additions, which contained non-indigenous microorganisms, the results of the bacterial characterisation showed changes on the microbial populations using different natural electron donors, probably due to the formation of diverse microbial niches, besides the addition of different carbon sources. It is also known that different bacteria, such as *Pseudomonas, Bacillus, Bacteroidia* and *Clostridia* detected in the Mam Tor slurries may be involved in the microbial Fe(III)-reduction of a sediment (Jones et al. 1984), therefore in our experiments it is likely that the microbial populations detected have the conditions to develop this process (Figure 3.6).

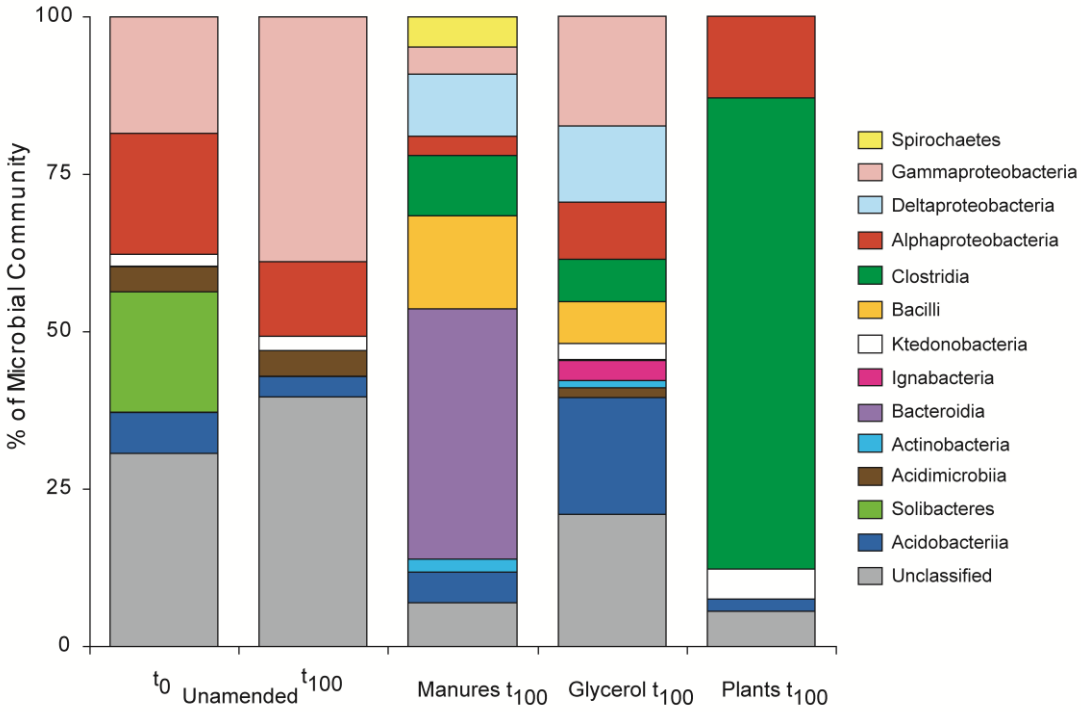

Figure 3.8. Relative abundances (%) of dominant bacterial populations stimulated with different organic sources. The bacterial diversity of the Mam Tor sediment decreased after 100 days incubation in experiments lacking of an external carbon sources and using plant additions, favouring the growth of *Gammaproteobacteria* and *Clostridia* populations, respectively. When manure and glycerol were added, the microcosms gave the highest Fe(III)-reduction rates and presented the greatest bacterial diversity.

3.3.7. Comparison of the organic analyses of plant and manure amended microcosms.

In order to monitor the use of organic matter (OM) in the microcosm experiments by the bacteria detected, the lipid analysis of the microcosm slurries after incubation was carried out as described in the method section. The *n*-alkane fractions of all the microcosm slurries were dominated by high molecular weight (HMW; $>C_{20}$) homologous series, up to the C_{31} *n*-alkane, with a clear predominance of the odd-numbered homologues, as indicated by the Carbon Preference Index values, CPI > 6 (Table 3.6).

The lipid analysis of the slurry obtained from the microcosm prepared using plant material, showed a summed concentration of HMW *n*-alkanes ranging from 1.2 to 12.5 µg/g sediment (Table 3.6). The most abundant homologues (C_{max}) were the C_{23} *n*-alkane, for moss and fern enrichments and the C_{29} *n*-alkane, for reed enrichment

(Table 3.6). The average chain length (ACL), ranged between 24.5 and 27.5. The highest degradation rate of the *n*-alkanes was recorded in these systems, on average 67% (Figure 3.9). The presence of *n*-alkanols also was observed, but no significant differences were noticed before and after incubations. This fraction was dominated by the C_{24} and C_{26} homologues; with CPI values ranging from 6.9 to 15.9 and the ACLs varying from 22.9 to 24.6 (Table 3.6). The presence of sterols was also detected, with a little decrease in moss and fern microcosms after 100 days incubation (Table 3.6), results that can be explained based on the presence and stimulation of fermentative microorganisms like *Clostridia* and *Alphabacteria* (Figure 3.8) which have the capacity of degrading plant material and were dominant in the plant-amended microcosms. However, the degradation of *n*-alkanes in these microcosms did not lead to a pH increasing, and apparently did not stimulate the microbial Fe(III) - reduction but inhibit it due the accumulation of acetate (Table 3.4; Figure 3.6).

In the slurry taken from the manure amended microcosms, the summed concentration of the *n*-alkanes, ranged from 5.3 μg/g sediment using pig manure, to 23.3 μg/g sediment using sheep manure (Table 3.6). The C_{max} was the C_{29} *n*-alkane obtained using pig manure, while for cow- and sheep manure additions the *n*-alkanes maximised at the C_{31} homologue. The average chain length, ACL, ranged from 25.1 to 29.0 in those systems. The *n*-alkane fraction decreased, on average, 14%, indicating a lower degradation, compared to the plant amended microcosms (Figure 3.9). Considerable amounts of *n*-alkanols were also quantified, specially using sheep manure (85.5 μg/g sediment) and containing homologous series from the C_{20} to C_{28} *n*-alkanols, with CPI values ranging from 2.7 to 152.3. The most abundant *n*-alkanol was the C_{26} homologue and the ACLs ranged from 26.0 to 26.7. The *n*-alkanol concentration slightly decreased after incubation. In addition, sterols were detected with no significant concentration changes after incubation (Table 3.6). Interestingly, the manure amended microcosms yielded the highest Fe(III)-reduction rate and enhanced the acidic conditions up to near neutral pH. The results indicate that the manure additions are a good option for the improvement of ARD sites.

Table 3.6. Comparison of the organic analyses of the microcosms at t_o and t_{100} days incubation.

Type	OM[a]	*n*-alkanes			*n* -alkanols			Sterols[e]
		ΣHMWC[b]	CPI[c]	ACL[d]	ΣHMWC[b]	CPI[c]	ACL[d]	
Moss t_o	17.6±0.2	7.4	8.1	24.7	4.6	15.2	23.7	4.9
Moss t_{100}	17.2±0.1	2.7	8.1	24.5	3.3	10.4	24.6	3.5
Fern t_o	18.9±0.1	4.7	7.6	25.1	3.9	15.9	24.1	9.9
Fern t_{100}	18.9±0.1	1.2	7.2	24.6	3.8	14.4	22.9	5.2
Reed t_o	19.8±0.2	12.5	9.5	26.1	4.3	8.5	24.1	4.3
Reed t_{100}	18.4±0.1	2.1	8.6	27.4	4.1	6.9	25.0	4.1
Cow t_o	19.0±0.2	10.5	22.7	28.2	8.6	2.7	26.7	46.1
Cow t_{100}	19.0±0.2	8.3	10.9	29.1	5.9	14.5	26.5	38.1
Pig t_o	19.0±0.2	5.2	12.6	27.3	19.9	38.5	26.0	64.2
Pig t_{100}	18.9±0.2	4.5	9.8	26.3	17.2	42.7	26.7	55.7
SM t_o	18.9±0.3	25.2	11.8	29.0	85.5	104.6	26.1	55.1
SM t_{100}	17.5±0.2	23.3	19.3	29.0	84.1	152.3	26.1	55.1
Gly t_o	14.3±0.1	4.6	5.3	24.9	2.8	5.9	24.5	5.1
Gly t_{100}	14.2±0.04	2.5	5.7	24.7	0.6	17.4	24.4	1.1
UM t_o	14.3±0.1	3.3	5.8	24.2	2.9	6.7	24.0	9.8
UM t_{100}	14.6±0.1	3.3	4.8	25.1	2.8	9.3	24.9	8.9

t_o=Initial conditions of experiments.
t_{100}=Final conditions of experiments, after 100 days incubation.
SM= microcosms prepared using sheep manure,
Gly= microcosms prepared with glycerol addition.
UM=unamended microcosm.
[a] OM=Total organic matter content; values in %.
[b] ΣHMWC=Summed concentration over the range C_{20}-C_{31} expressed in μg/g sediment.
[c] $CPI_{21\text{-}31}$= carbon preference index over the range C_{21}-C_{31} (van Dongen et al. 2008)
$0.5[(X_i+X_{i+2}+...+X_n)/(X_{i-1}+X_{i+1}+...+X_{n-1})]+0.5[(X_i+X_{i+2}+...+X_n)/(X_{i+1}+X_{i+3}...+X_{n+1})]$
where X is concentration.
[c] Average chain length over the range C_{20}-C_{31}, $ACL= \Sigma(iX_i + ... + nX_n)/\Sigma(X_i + ... +X_n)$,
where X is concentration.
[d] Chain length of the *n*-alkane with highest concentration.
[e] Summed concentrations of C_{27} stanol, C_{28} stanol, C_{29} stanol, C_{30} stanol, $C_{27:1}$ sterol, $C_{28:1}$ sterol, $C_{28:2}$ sterol, $C_{29:1}$ sterol and $C_{29:2}$ sterol expressed in μg/g sediment.

For comparison, data from the glycerol amended microcosms and unamended experiments were also added in Table 3.6. In the glycerol experiments the *n*-alkane fraction of the sediment was bioavailable and probably because no significant amount of acetate was detected (Table 3.4), the Fe(III) - reduction was not inhibited and gave a final concentration of 40 mM Fe(II). On the other hand, the *n*-alkane fraction of the unamended microcosms did not show any decrease and yielded the lowest reduction rate of all experiments (Table 3.6 and Table 3.4). Therefore the results obtained from the lipid analyses indicated the *n*-alkane fraction is involved in the stimulation of the microbial reduction of Fe(III), but fermentation products, for example acetate, may have a negative influence in this process. These results also showed that the *n*-alkane

fraction from plant material was more available for microbial fermentation than the *n*-alkane fraction from manure enrichments, but there was no clear evidence of a preferential degradation pattern of the n-alkanes and they all seemed to be use at the same rate (Figure 3.9).

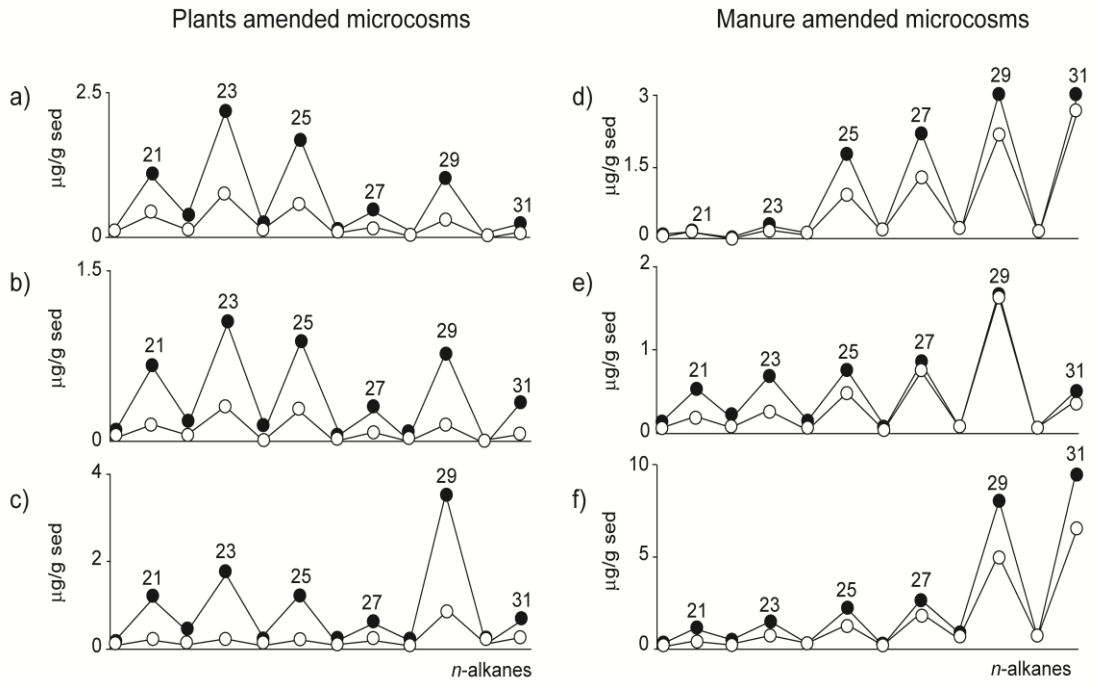

Figure 3.9. *n*-alkane distribution obtained after 100 days of incubation, by amendment type a) moss; b) fern; c) reed; d) pig manure; e) cow manure; f) sheep manure. The closed circles indicate the initial conditions of the microcosms, t_0; open circles, final conditions, t_{100}. No preferential degradation pattern was observed.

Having observed that the saturated hydrocarbons from manure additions did not substantially decrease, macromolecular analyses were performed to determine whether other carbon sources were used (Figure 3.10). In the unamended sediment at t_0 the polysaccharides represented approximately 44%, followed by lignin content of 19%, the nitrogen compounds and the phenols represented 17% and 12%, respectively, while the aromatic fraction contributed approximately with 7% However, after incubation (sediment t_{100}) the lignin contribution was apparently lower, 7% (Figure 3.10). Analysing the data from two experiments amended with plant material (Figure 3.10), a similar tendency was detected in the microcosms prepared using moss. Here, the polysaccharide fraction was dominant (64% and 71% at t_0 and t_{100}, respectively)

but the lignin content changed from 2% to 0.5% after incubation. Conversely, in microcosms amended with reeds, the relative lignin content was comparable before and after incubation (37% and 40%, respectively), and no degradation of the other macromolecular compounds was recorded (Figure 3.10). There is a controversy whether *Sphagnum* moss contains or not lignin, but our results suggested that the moss sampled at Mam Tor may contain some "lignin-like" compounds that could be easily modified, whereas the "true lignin" compounds detected in reeds were less easily modifiable.

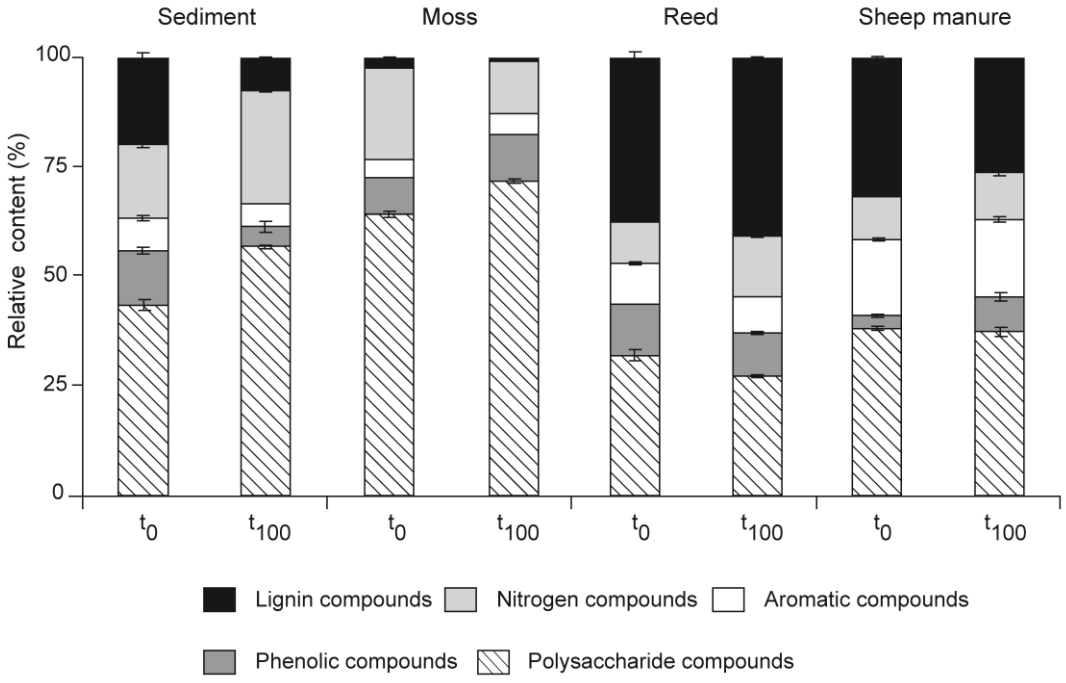

Figure 3.10. Macromolecular groups obtained from the pyrolysates of the microcosms supplemented with different carbon sources. The contribution of each group is given in relative abundance.

The stimulation of the sediment using manures increased greatly the microbial diversity (Figure 3.8) involving fermentation mechanisms that lead to the accumulation of lactate (Table 3.4). The macromolecular analysis of slurries from manure-amended microcosms indicated that the polysaccharides and lignin moieties were the most relatively abundant fractions at t_o (37% and 17%, respectively), with an aromatic content of approximately 17%; nitrogen, 10%; and phenols, 3%. After 100 days incubation, the relative content of polysaccharides, aromatic and nitrogen compounds remain unchanged (37%, 18% and 11%, respectively) but the relative

contribution of lignin decreased (25%) while the phenol contribution increased (8%), suggesting a modification in the lignin compounds (Figure 3.10). At low pH it has been suggested that the modification of lignin is inhibited (Benner et al. 1984), however, some Fe(III) reducers are capable of utilizing more complex organic molecules than fermentation products (Küsel and Dorsch 2000) which could explain the accumulation of lactate and the apparent modification of lignin compounds detected in sheep manure incubations. The presence of polysaccharide moieties in the sediment before and after incubation, may be explained on basis that, for example, labile aquatic carbon in acidic lakes become recalcitrant over time (Blodau and Peiffer 2003).

3.4. Conclusions

Samples taken at Mam Tor (UK) from the surface of an ARD pond were characterised by organic, mineralogical and microbial techniques. The mineralogical characterisation showed that the Mam Tor sediment was dominated by goethite, which was present both in small size particles and in bulk mineral form. The Mössbauer analyses demonstrated that goethite in fine particles is bioavailable and was used throughout incubation during the microbial reduction of Fe(III). The organic analyses of the start material also indicated that the sediments are not carbon limited (14% OM), and that the OM inputs detected in the sediment were from local plant origin. Within the OM contribution, the polysaccharide fraction seems not to be bioavailable, probably because the formation of complexes with iron oxides.

The results from the microcosm experiments demonstrated that the addition of different types of OM can shape the microbial population present in the sediment and, consequently, such microbial population have the potential to degrade the OM sourced. Our results also suggest that the saturated hydrocarbon (*n*-alkane) fraction from plant material is more bioavailable than those from the manure addition, but the first one does not stimulate the iron reduction, probably for the accumulation of acetate. Conversely, the *n*-alkane fraction of the manure addition, is only slightly bioavailable compared to plant material, but it stimulate greatly the microbial reduction of Fe(III) rising the pH of the experiments up to near neutral pH. Therefore the manure addition, (particularly sheep manure) can make an interesting and non-expensive electron donor in ARD/AMD treatments. In combination, our findings indicated that OM is indeed involved in the natural attenuation of ARD via Fe(III)-reduction, however further research is needed to account the specific compounds driving this process.

Acknowledgements

We gratefully acknowledge the receipt of a PhD studentship for M. E. Jiménez-Castañeda, funded by the National Council of Science and Technology of México (CONACyT). We thank to P. Wincott† for his help and advice on Mössbauer Spectrometry; C. Davies (University of Manchester) for her invaluable advice and assistance on the demineralisation protocols; C. Boothman (University of Manchester) for bacterial characterisation; P. Lythgoe and A. Bewsher (University of Manchester) for his assistance in chemical analyses.

REFERENCES

Abildgaard, L., M. B. Nielsen, K. U. Kjeldsen and K. Ingvorsen (2006). "Desulfovibrio alkalitolerans sp. nov., a novel alkalitolerant, sulphate-reducing bacterium isolated from district heating water." International Journal of Systematic and Evolutionary Microbiology **56**(5): 1019-1024.

Adams, L. K., J. M. Harrison, J. R. Lloyd, S. Langley and D. Fortin (2007). "Activity and diversity of Fe(III)-reducing bacteria in a 3000-year-old acid mine drainage site analogue." Geomicrobiology Journal **24**(3-4): 295-305.

Alazard, D., M. Joseph, F. Battaglia-Brunet, J.-L. Cayol and B. Ollivier (2010). "Desulfosporosinus acidiphilus sp. nov.: a moderately acidophilic sulfate-reducing bacterium isolated from acid mining drainage sediments." Extremophiles **14**(3): 305-312.

Allen, J. R. L. (1960). "The Mam Tor Sandstones: A "turbidite" facies of the namurian deltas of Derbyshire, England." Journal of Sedimentary Research **30**(2).

Arkwright, J. C., E. H. Rutter and R. F. Holloway (2003). "Feature. The Mam Tor landslip: still moving after all these years." Geology Today **19**(2): 59-64.

Barreto, C. C., C. A. Becerra, K. L. Froloney and K. Nusslein (unpublished). Potential role of Acidobacteria in the attenuation of acid mine drainage in a long abandoned mining site, University of Massachusetts.

Beaudoin, A. (2003). "A comparison of two methods for estimating the organic content of sediments." Journal of Paleolimnology **29**(3): 387-390.

Benner, R., A. Maccubbin and R. E. Hodson (1984). "Anaerobic biodegradation of the lignin and polysaccharide components of lignocellulose and synthetic lignin by sediment microflora." Applied and Environmental Microbiology **47**(5): 998-1004.

Berquó, T., R. Imbernon, A. Blot, D. Franco, M. Toledo and C. Partiti (2007). "Low temperature magnetism and Mössbauer spectroscopy study from natural goethite." Physics and Chemistry of Minerals **34**(5): 287-294.

Bingham, E. M., E. L. McClymont, M. Väliranta, D. Mauquoy, Z. Roberts, F. M. Chambers, R. D. Pancost and R. P. Evershed (2010). "Conservative composition of n-alkane biomarkers in Sphagnum species: Implications for palaeoclimate reconstruction in ombrotrophic peat bogs." Organic Geochemistry **41**(2): 214-220.

Bland, D. E., A. Logan, M. Menshun and S. Sternhell (1968). "The ligning of Sphagnum." Phytochemistry **7**(8): 1373-1377.

Blodau, C. and S. Peiffer (2003). "Thermodynamics and organic matter: constraints on neutralization processes in sediments of highly acidic waters." Applied Geochemistry **18**(1): 25-36.

Blumer, M. (1957). "Removal of elemental sulfur from hydrocarbon fractions." Analytical Chemistry **29**(7): 1039-1041.

Bocquet, S., R. Pollard and J. Cashion (1992). "Dynamic magnetic phenomena in fine-particle goethite." Physical Review B **46**(18): 11657.

Bond, P. L., G. K. Druschel and J. F. Banfield (2000a). "Comparison of acid mine drainage microbial communities in physically and geochemically distinct ecosystems." Applied and Environmental Microbiology **66**(11): 4962-4971.

Bond, P. L., S. P. Smriga and J. F. Banfield (2000b). "Phylogeny of Microorganisms Populating a Thick, Subaerial, Predominantly Lithotrophic Biofilm at an Extreme Acid Mine Drainage Site." Applied and Environmental Microbiology **66**(9): 3842-3849.

Bose, S., M. F. Hochella Jr, Y. A. Gorby, D. W. Kennedy, D. E. McCready, A. S. Madden and B. H. Lower (2009). "Bioreduction of hematite nanoparticles by the dissimilatory iron reducing bacterium Shewanella oneidensis MR-1." Geochimica et Cosmochimica Acta **73**(4): 962-976.

Bridge, T. A. M. and D. B. Johnson (1998). "Reduction of Soluble Iron and Reductive Dissolution of Ferric Iron-Containing Minerals by Moderately Thermophilic Iron-Oxidizing Bacteria." Applied and Environmental Microbiology **64**(6): 2181-2186.

Brož, D., J. Straková, J. Šubrt, J. Vinš, B. Sedlák and S. I. Reiman (1990). "Mössbauer spectroscopy of goethite of small particle size." Hyperfine Interactions **54**(1-4): 479-482.

Bruneel, O., N. Pascault, M. Egal, C. Bancon-Montigny, M. S. Goñi-Urriza, F. Elbaz-Poulichet, J. C. Personné and R. Duran (2008). "Archaeal diversity in a Fe–As rich acid mine drainage at Carnoulès (France)." Extremophiles **12**(4): 563-571.

Caporaso, J. G., J. Kuczynski, J. Stombaugh, K. Bittinger, F. D. Bushman, E. K. Costello, N. Fierer, A. G. Pena, J. K. Goodrich, J. I. Gordon, G. A. Huttley, S. T. Kelley, D. Knights, J. E. Koenig, R. E. Ley, C. A. Lozupone, D. McDonald, B. D. Muegge, M. Pirrung, J. Reeder, J. R. Sevinsky, P. J. Turnbaugh, W. A. Walters, J. Widmann, T. Yatsunenko, J. Zaneveld and R. Knight (2010). "QIIME allows analysis of high-throughput community sequencing data." Nat Meth **7**(5): 335-336.

Chabbi, A. (1999). "Juncus bulbosus as a Pioneer Species in Acidic Lignite Mining Lakes: Interactions, Mechanism and Survival Strategies." New Phytologist **144**(1): 133-142.

Cole, J. R., Q. Wang, E. Cardenas, J. Fish, B. Chai, R. J. Farris, A. Kulam-Syed-Mohideen, D. M. McGarrell, T. Marsh and G. M. Garrity (2009). "The Ribosomal Database Project: improved alignments and new tools for rRNA analysis." Nucleic acids research **37**(suppl 1): D141-D145.

Corkhill, C. L., P. L. Wincott, J. R. Lloyd and D. J. Vaughan (2008). "The oxidative dissolution of arsenopyrite (FeAsS) and enargite (Cu3AsS4) by Leptospirillum ferrooxidans." Geochimica et Cosmochimica Acta **72**(23): 5616-5633.

Coupland, K. and D. B. Johnson (2004). "Geochemistry and microbiology of an impounded subterranean acidic water body at Mynydd Parys, Anglesey, Wales." Geobiology **2**(2): 77-86.

Cutting, R. S., V. S. Coker, J. W. Fellowes, J. R. Lloyd and D. J. Vaughan (2009). "Mineralogical and morphological constraints on the reduction of Fe(III) minerals by Geobacter sulfurreducens." Geochimica et Cosmochimica Acta **73**(14): 4004-4022.

Dehner, C. A., L. Barton, P. A. Maurice and J. L. DuBois (2010). "Size-Dependent Bioavailability of Hematite (α-Fe2O3) Nanoparticles to a Common Aerobic Bacterium." Environmental Science & Technology **45**(3): 977-983.

del Río, J. C., P. Prinsen, J. Rencoret, L. Nieto, J. s. Jiménez-Barbero, J. Ralph, A. n. T. Martínez and A. Gutiérrez (2012). "Structural characterization of the lignin in the cortex and pith of elephant grass (Pennisetum purpureum) stems." Journal of agricultural and food chemistry **60**(14): 3619-3634.

Dézsi, I. and M. Fodor (1966). "On the Antiferromagnetism of α-FeOOH." physica status solidi (b) **15**(1): 247-254.

Dickson, L., I. D. Bull, P. J. Gates and R. P. Evershed (2009). "A simple modification of a silicic acid lipid fractionation protocol to eliminate free fatty acids from glycolipid and phospholipid fractions." Journal of microbiological methods **78**(3): 249-254.

Dixon, N. and E. Brook (2007). "Impact of predicted climate change on landslide reactivation: case study of Mam Tor, UK." Landslides **4**(2): 137-147.

Donnelly, L. (2006). The Mam Tor Landslide, Geology & Mining Legacy around Castleton, Peak District National Park, Derbyshire, UK. Engineering Geology for Tomorrow's Cities, Proceedings of the 10th Congress of The International Association for Engineering Geology and The Environment, Nottingham, UK.

Edgar, R. C. (2010). "Search and clustering orders of magnitude faster than BLAST." Bioinformatics **26**(19): 2460-2461.

Eglinton, G. and R. Hamilton (1963). "The distribution of alkanes." Chemical plant taxonomy **187**: 217.

Eglinton, G. and R. J. Hamilton (1967). "Leaf Epicuticular Waxes." Science **156**(3780): 1322-1335.

Eissa, N. A., H. A. Sallam, S. S. Gomaa, S. A. Saleh and Z. Miligy (1974). "Mössbauer study of Egyptian goethite." Journal of Physics D: Applied Physics **7**(15): 2121.

Farmer, V. C. and R. I. Morrison (1964). "Lignin in sphagnum and phragmites and in peats derived from these plants." Geochimica et Cosmochimica Acta **28**(10–11): 1537-1546.

Fenwick, G. R. (1989). "Bracken (Pteridium aquilinum)—toxic effects and toxic constituents." Journal of the Science of Food and Agriculture **46**(2): 147-173.

Ferris, F. G., K. Tazaki and W. S. Fyfe (1989). "Iron oxides in acid mine drainage environments and their association with bacteria." Chemical Geology **74**(3–4): 321-330.

Ficken, K. J., B. Li, D. L. Swain and G. Eglinton (2000). "An n-alkane proxy for the sedimentary input of submerged/floating freshwater aquatic macrophytes." Organic Geochemistry **31**(7–8): 745-749.

Ford, T., W. Sarjeant and M. Smith (1993). "Minerals of the Peak District." Bulletin of the Peak District Mines Historical Society **12**(1): 1.

Fyson, A. (2000). "Angiosperms in acidic waters at pH 3 and below." Hydrobiologia **433**(1-3): 129-135.

Gélinas, Y., J. A. Baldock and J. I. Hedges (2001). "Demineralization of marine and freshwater sediments for CP/MAS< sup> 13</sup> C NMR analysis." Organic Geochemistry **32**(5): 677-693.

Goad, L. J. and T. Akihisa (1997). Analysis of sterols, Springer Netherlands.

Golden, D. C., L. H. Bowen, S. B. Weed and J. M. Bigham (1979). "Mössbauer Studies of Synthetic and Soil-Occurring Aluminum-Substituted Goethites." Soil Sci. Soc. Am. J. **43**(4): 802-808.

Goodman, B. A. and D. G. Lewis (1981). "Mössbauer spectra of aluminious goethites (α-FeOOH)." Journal of soil science **32**(3): 351-364.

Green, S., E. Rutter and R. Holloway (2010). "The effects of groundwater level and vegetation on creep of the Mam Tor landslip." Geology Today **26**(4): 134-139.

Grimalt, J. O., M. Ferrer and E. Macpherson (1999). "The mine tailing accident in Aznalcollar." Science of The Total Environment **242**(1–3): 3-11.

Hallberg, K. B. and B. D. Johnson (2001). Biodiversity of acidophilic prokaryotes. Advances in Applied Microbiology, Academic Press. **Volume 49:** 37-84.

Hamady, M., J. J. Walker, J. K. Harris, N. J. Gold and R. Knight (2008). "Error-correcting barcoded primers for pyrosequencing hundreds of samples in multiplex." Nat Meth **5**(3): 235-237.

Heiri, O., A. F. Lotter and G. Lemcke (2001). "Loss on ignition as a method for estimating organic and carbonate content in sediments: reproducibility and comparability of results." Journal of paleolimnology **25**(1): 101-110.

Herbert, R. B. (1997). "Properties of goethite and jarosite precipitated from acidic groundwater, Dalarna, Sweden." Clays and Clay Minerals **45**(2): 261-273.

Hernandez-Eugenio, G., M.-L. Fardeau, B. K. C. Patel, H. Macarie, J.-L. Garcia and B. Ollivier (2000). "Desulfovibrio mexicanus sp. nov., a Sulfate-reducing Bacterium Isolated from an Upflow Anaerobic Sludge Blanket (UASB) Reactor Treating Cheese Wastewaters." Anaerobe **6**(5): 305-312.

Holmes, D. E., R. A. O'Neil, H. A. Vrionis, L. A. N'Guessan, I. Ortiz-Bernad, M. J. Larrahondo, L. A. Adams, J. A. Ward, J. S. Nicoll, K. P. Nevin, M. A. Chavan, J. P. Johnson, P. E. Long and D. R. Lovley (2007). "Subsurface clade of Geobacteraceae that predominates in a diversity of Fe(III)-reducing subsurface environments." ISME J **1**(8): 663-677.

Huggins, F. E., G. P. Huffman and M. C. Lin (1983). "Observations on low-temperature oxidation of minerals in bituminous coals." International Journal of Coal Geology **3**(2): 157-182.

Imfeld , G. and H. Richnow (unpublished). Germany, Hemholtz Centre for Environmental Research.

Johnson, D. B. (1995). "Acidophilic microbial communities: Candidates for bioremediation of acidic mine effluents." International Biodeterioration & Biodegradation **35**(1–3): 41-58.

Johnson, D. B. (1998). "Biodiversity and ecology of acidophilic microorganisms." FEMS Microbiology Ecology **27**(4): 307-317.

Johnson, D. B. (2012). "Geomicrobiology of extremely acidic subsurface environments." FEMS Microbiology Ecology **81**(1): 2-12.

Johnson, D. B. and T. A. M. Bridge (2002). "Reduction of ferric iron by acidophilic heterotrophic bacteria: evidence for constitutive and inducible enzyme systems in Acidiphilium spp." Journal of Applied Microbiology **92**(2): 315-321.

Johnson, D. B. and K. B. Hallberg (2003). "The microbiology of acidic mine waters." Research in Microbiology **154**(7): 466-473.

Johnson, D. B., N. Okibe and F. Roberto (2003). "Novel thermo-acidophilic bacteria isolated from geothermal sites in Yellowstone National Park: physiological and phylogenetic characteristics." Archives of Microbiology **180**(1): 60-68.

Johnson, D. B., S. Rolfe, K. B. Hallberg and E. Iversen (2001). "Isolation and phylogenetic characterization of acidophilic microorganisms indigenous to acidic drainage waters at an abandoned Norwegian copper mine." Environmental Microbiology **3**(10): 630-637.

Jones, J. G., W. Davison and S. Gardener (1984). "Iron reduction by bacteria: range of organisms involved and metals reduced." FEMS Microbiology Letters **21**(1): 133-136.

Kay, C., O. Rowe, L. Rocchetti, K. Coupland, K. Hallberg and D. Johnson (2013). "Evolution of Microbial “Streamer” Growths in an Acidic, Metal-Contaminated Stream Draining an Abandoned Underground Copper Mine." Life **3**(1): 189-210.

Kirk, T. K. and R. L. Farrell (1987). "Enzymatic "Combustion": The Microbial Degradation of Lignin." Annual Review of Microbiology **41**(1): 465-501.

Koschorreck, M., W. Geller, T. Neu, S. Kleinsteuber, T. Kunze, A. Trosiener and K. Wendt-Potthoff (2010). "Structure and function of the microbial community in an in situ reactor to treat an acidic mine pit lake." FEMS Microbiology Ecology **73**(2): 385-395.

Kuang, J.-L., L.-N. Huang, L.-X. Chen, Z.-S. Hua, S.-J. Li, M. Hu, J.-T. Li and W.-S. Shu (2013). "Contemporary environmental variation determines microbial diversity patterns in acid mine drainage." ISME J **7**(5): 1038-1050.

Küsel, K. and T. Dorsch (2000). "Effect of supplemental electron donors on the microbial reduction of Fe(III), Sulfate, and CO2 in coal mining–impacted freshwater lake sediments." Microbial Ecology **40**(3): 238-249.

Küsel, K., T. Dorsch, G. Acker and E. Stackebrandt (1999). "Microbial Reduction of Fe(III) in Acidic Sediments: Isolation of Acidiphilium cryptum JF-5 Capable of Coupling the Reduction of Fe(III) to the Oxidation of Glucose." Applied and Environmental Microbiology **65**(8): 3633-3640.

Küsel, K., T. Dorsch, G. Acker, E. Stackebrandt and H. L. Drake (2000). "Clostridium scatologenes strain SL1 isolated as an acetogenic bacterium from acidic

sediments." International Journal of Systematic and Evolutionary Microbiology **50**(2): 537-546.

Lane, D. J. (1991). "16S/23S rRNA sequencing." Nucleic acid techniques in bacterial systematics: 125-175.

Larese-Casanova, P., D. M. Cwiertny and M. M. Scherer (2010). "Nanogoethite Formation from Oxidation of Fe(II) Sorbed on Aluminum Oxide: Implications for Contaminant Reduction." Environmental Science & Technology **44**(10): 3765-3771.

Li, Y. and Q. Y. Sun (unpublished). Bacterial community structure in river sediments associated with mining. China, Anhui University.

Lin, C., Y. Wu, W. Lu, A. Chen and Y. Liu (2007). "Water chemistry and ecotoxicity of an acid mine drainage-affected stream in subtropical China during a major flood event." Journal of Hazardous Materials **142**(1–2): 199-207.

Lindsay, M. B. J., K. D. Wakeman, O. F. Rowe, B. M. Grail, C. J. Ptacek, D. W. Blowes and D. B. Johnson (2011). "Microbiology and Geochemistry of Mine Tailings Amended with Organic Carbon for Passive Treatment of Pore Water." Geomicrobiology Journal **28**(3): 229-241.

Lovley, D. R., S. J. Giovannoni, D. C. White, J. E. Champine, E. J. P. Phillips, Y. A. Gorby and S. Goodwin (1993). "Geobacter metallireducens gen. nov. sp. nov., a microorganism capable of coupling the complete oxidation of organic compounds to the reduction of iron and other metals." Archives of Microbiology **159**(4): 336-344.

Lovley, D. R. and E. J. Phillips (1986). "Organic matter mineralization with reduction of ferric iron in anaerobic sediments." Applied and environmental microbiology **51**(4): 683-689.

Lovley, D. R. and E. J. Phillips (1987). "Rapid assay for microbially reducible ferric iron in aquatic sediments." Applied and Environmental Microbiology **53**(7): 1536-1540.

Männistö, M. K., E. Kurhela, M. Tiirola and M. M. Häggblom (2013). "Acidobacteria dominate the active bacterial communities of Arctic tundra with widely divergent winter-time snow accumulation and soil temperatures." FEMS Microbiology Ecology **84**(1): 47-59.

McClymont, E. L., E. M. Bingham, C. J. Nott, F. M. Chambers, R. D. Pancost and R. P. Evershed (2011). "Pyrolysis GC–MS as a rapid screening tool for determination of peat-forming plant composition in cores from ombrotrophic peat." Organic Geochemistry **42**(11): 1420-1435.

Meier , J., F. D. Mueller, B. Kiesel, K. Wendt-Potthoff and S. Kleinsteuber (unpublished). Characterization of the sulfate-reducing community enriched during a bioremediation experiment in sediments of acidic mine pit lake. Germany, Helmholtz-Centre for Environmental Research.

Mendez-Garcia, C., V. Mesa, R. R. Sprenger, M. Richter, M. S. Diez, J. Solano, R. Bargiela, O. V. Golyshina, A. Manteca, J. L. Ramos, J. R. Gallego, I. Llorente, V. A. P. Martins dos Santos, O. N. Jensen, A. I. Pelaez, J. Sanchez and M. Ferrer (2014). "Microbial stratification in low pH oxic and suboxic macroscopic growths along an acid mine drainage." ISME J **8**(6): 1259-1274.

Mørup, S., M. Bo Madsen, J. Franck, J. Villadsen and C. J. Koch (1983). "A new interpretation of Mössbauer spectra of microcrystalline goethite:“Super-ferromagnetism” or “super-spin-glass” behaviour?" Journal of magnetism and magnetic materials **40**(1): 163-174.

Mørup, S., H. Topsøe and B. S. Clausen (1982). "Magnetic Properties of Microcrystals Studied by Mössbauer Spectroscopy." Physica Scripta **25**(6A): 713.

Murad, E. (1989). "Poorly-crystalline minerals and complex mineral assemblages." Hyperfine Interactions **47-48**(1-4): 33-53.

Murad, E. and L. H. Bowen (1987). "Magnetic ordering in Al-rich goethites; influence of crystallinity." American Mineralogist **72**(1-2): 194-200.

Murad, E. and P. Rojik (2005). "Iron mineralogy of mine-drainage precipitates as environmental indicators: review of current concepts and a case study from the Sokolov Basin, Czech Republic." Clay Minerals **40**(4): 427-440.

Murad, E. and P. Rojík (2003). "Iron-rich precipitates in a mine drainage environment: Influence of pH on mineralogy." American Mineralogist **88**(11-12): 1915-1918.

Neal, C., P. G. Whitehead, H. Jeffery and M. Neal (2005). "The water quality of the River Carnon, west Cornwall, November 1992 to March 1994: the impacts of Wheal Jane discharges." Science of The Total Environment **338**(1–2): 23-39.

Nordstrom, D. K. (2011). "Hydrogeochemical processes governing the origin, transport and fate of major and trace elements from mine wastes and mineralized rock to surface waters." Applied Geochemistry **26**(11): 1777-1791.

Nott, C. J., S. Xie, L. A. Avsejs, D. Maddy, F. M. Chambers and R. P. Evershed (2000). "n-Alkane distributions in ombrotrophic mires as indicators of vegetation change related to climatic variation." Organic Geochemistry **31**(2–3): 231-235.

Olowe, A. A., P. Refait and J. M. R. Génin (1990). "Superparamagnetic behaviour of goethite prepared in sulphated medium." Hyperfine Interactions **57**(1-4): 2037-2043.

Orellana, R., J. J. Leavitt, L. R. Comolli, R. Csencsits, N. Janot, K. A. Flanagan, A. S. Gray, C. Leang, M. Izallalen, T. Mester and D. R. Lovley (2013). "U(VI) Reduction by Diverse Outer Surface c-Type Cytochromes of Geobacter sulfurreducens." Applied and Environmental Microbiology **79**(20): 6369-6374.

Pain, D. J., A. Sánchez and A. A. Meharg (1998). "The Doñana ecological disaster: Contamination of a world heritage estuarine marsh ecosystem with acidified pyrite mine waste." Science of The Total Environment **222**(1–2): 45-54.

Pédrot, M., A. L. Boudec, M. Davranche, A. Dia and O. Henin (2011). "How does organic matter constrain the nature, size and availability of Fe nanoparticles for biological reduction?" Journal of Colloid and Interface Science **359**(1): 75-85.

Ralph, J. and R. D. Hatfield (1991). "Pyrolysis-GC-MS characterization of forage materials." Journal of Agricultural and Food Chemistry **39**(8): 1426-1437.

Ramond, J.-B., P. J. Welz, M. Le Roes-Hill, M. I. Tuffin, S. G. Burton and D. A. Cowan (2014). "Selection of Clostridium spp. in biological sand filters neutralizing synthetic acid mine drainage." FEMS Microbiology Ecology **87**(3): 678-690.

Reichenbecher, W. and B. Schink (1997). "Desulfovibrio inopinatus, sp. nov., a new sulfate-reducing bacterium that degrades hydroxyhydroquinone (1,2,4-trihydroxybenzene)." Archives of Microbiology **169**(1): 88-88.

Rimstidt, J. D. and D. J. Vaughan (2003). "Pyrite oxidation: a state-of-the-art assessment of the reaction mechanism." Geochimica et Cosmochimica Acta **67**(5): 873-880.

Rosenberg, C. E., B. N. Carpinetti and C. Apartín (2001). "Contenido de Metales Pesados en Tejidos de Sábalos (Prochilodus Lineatus) del Río Pilcomayo, Misión La Paz, Provincia de Salta." Natura Neotropicalis **2**(32): 141-145.

Rutter, E. H., J. C. Arkwright, R. F. Holloway and D. Waghorn (2003). "Strains and displacements in the Mam Tor landslip, Derbyshire, England." Journal of the Geological Society **160**(5): 735-744.

Rutter, E. H. and S. Green (2011). "Quantifying creep behaviour of clay-bearing rocks below the critical stress state for rapid failure: Mam Tor landslide, Derbyshire, England." Journal of the Geological Society **168**(2): 359-372.

Saiz-Jimenez, C. and J. W. De Leeuw (1986). "Chemical characterization of soil organic matter fractions by analytical pyrolysis-gas chromatography-mass spectrometry." Journal of Analytical and Applied Pyrolysis **9**(2): 99-119.

Sánchez-Andrea, I., A. J. M. Stams, R. Amils and J. L. Sanz (2013). "Enrichment and isolation of acidophilic sulfate-reducing bacteria from Tinto River sediments." Environmental Microbiology Reports **5**(5): 672-678.

Santofimia, E., E. González-Toril, E. López-Pamo, M. Gomariz, R. Amils and Á. Aguilera (2013). "Microbial Diversity and Its Relationship to Physicochemical Characteristics of the Water in Two Extreme Acidic Pit Lakes from the Iberian Pyrite Belt (SW Spain)." PLoS ONE **8**(6): e66746.

Sass, H., S. Ramamoorthy, C. Yarwood, H. Langner, P. Schumann, R. M. Kroppenstedt, S. Spring and R. F. Rosenzweig (2009). "Desulfovibrio idahonensis sp. nov., sulfate-reducing bacteria isolated from a metal(loid)-contaminated freshwater sediment." International Journal of Systematic and Evolutionary Microbiology **59**(9): 2208-2214.

Singer, P. C. and W. Stumm (1970). "Acidic Mine Drainage: The Rate-Determining Step." Science **167**(3921): 1121-1123.

Skempton, A. W., A. D. Leadbeater and R. J. Chandler (1989). "The Mam Tor Landslide, North Derbyshire." Philosophical Transactions of the Royal Society of London. Series A, Mathematical and Physical Sciences **329**(1607): 503-547.

Solà, C., M. a. Burgos, Á. Plazuelo, J. Toja, M. Plans and N. s. Prat (2004). "Heavy metal bioaccumulation and macroinvertebrate community changes in a Mediterranean stream affected by acid mine drainage and an accidental spill (Guadiamar River, SW Spain)." Science of The Total Environment **333**(1–3): 109-126.

Stookey, L. L. (1970). "Ferrozine- a new spectrophotometric reagent for iron." Analytical Chemistry **42**(7): 779-781.

Suresh, K., D. Prakash, N. Rastogi and R. K. Jain (2007). "Clostridium nitrophenolicum sp. nov., a novel anaerobic p-nitrophenol-degrading bacterium, isolated from a subsurface soil sample." International Journal of Systematic and Evolutionary Microbiology **57**(8): 1886-1890.

Tamura, I. and T. Mizushima (2002). "Explanation for magnetic properties of interacting iron oxide nanocrystals." Journal of Magnetism and Magnetic Materials **250**(0): 241-248.

Ueki, A., H. Akasaka, D. Suzuki and K. Ueki (2006). "Paludibacter propionicigenes gen. nov., sp. nov., a novel strictly anaerobic, Gram-negative, propionate-producing bacterium isolated from plant residue in irrigated rice-field soil in Japan." International Journal of Systematic and Evolutionary Microbiology **56**(1): 39-44.

Valente, T., J. A. Grande, M. L. de la Torre, M. Santisteban and J. C. Cerón (2013). "Mineralogy and environmental relevance of AMD-precipitates from the Tharsis mines, Iberian Pyrite Belt (SW, Spain)." Applied Geochemistry **39**(0): 11-25.

Valente, T. M. and C. Leal Gomes (2009). "Occurrence, properties and pollution potential of environmental minerals in acid mine drainage." Science of The Total Environment **407**(3): 1135-1152.

van der Kraan, A. M. and J. J. van Loef (1966). "Superparamagnetism in submicroscopic α-FeOOH particles observed by the Mössbauer effect." Physics Letters **20**(6): 614-616.

van Dongen, B. E., I. Semiletov, J. W. H. Weijers and Ö. Gustafsson (2008). "Contrasting lipid biomarker composition of terrestrial organic matter exported from across the Eurasian Arctic by the five great Russian Arctic rivers." Global Biogeochemical Cycles **22**(1): GB1011.

Vancampenhout, K., K. Wouters, B. De Vos, P. Buurman, R. Swennen and J. Deckers (2009). "Differences in chemical composition of soil organic matter in natural ecosystems from different climatic regions – A pyrolysis–GC-MS study." Soil Biology and Biochemistry **41**(3): 568-579.

Vandenberghe, R., E. De Grave, G. De Geyter and C. Landuydt (1986). "Characterization of goethite and hematite in a Tunisian soil profile by Mössbauer spectroscopy." Clays and Clay Minerals **34**(3): 275-280.

Vaughan, D. J. and J. R. Lloyd (2011). "Mineral-organic-microbe interactions: Environmental impacts from molecular to macroscopic scales." Comptes Rendus Geoscience **343**(2–3): 140-159.

Vear, A. and C. Curtis (1981). "A quantitative evaluation of pyrite weathering." Earth Surface Processes and Landforms **6**(2): 191-198.

Waltham, A. C. and N. Dixon (2000). "Movement of the Mam Tor landslide, Derbyshire, UK." Quarterly Journal of Engineering Geology and Hydrogeology **33**(2): 105-123.

Weber, K. A., L. A. Achenbach and J. D. Coates (2006). "Microorganisms pumping iron: anaerobic microbial iron oxidation and reduction." Nature Reviews Microbiology **4**(10): 752-764.

Whittleston, R. A., D. I. Stewart, R. J. G. Mortimer, Z. C. Tilt, A. P. Brown, K. Geraki and I. T. Burke (2011). "Chromate reduction in Fe(II)-containing soil affected by hyperalkaline leachate from chromite ore processing residue." Journal of Hazardous Materials **194**(0): 15-23.

Yapp, C. J. and H. Poths (1986). "Carbon in natural goethites." Geochimica et Cosmochimica Acta **50**(6): 1213-1220.

Yassir, I. and P. Buurman (2012). "Soil organic matter chemistry changes upon secondary succession in Imperata Grasslands, Indonesia: A pyrolysis–GC-MS study." Geoderma **173–174**(0): 94-103.

Yergeau, E., S. Bokhorst, S. Kang, J. Zhou, C. W. Greer, R. Aerts and G. A. Kowalchuk (2012). "Shifts in soil microorganisms in response to warming are consistent across a range of Antarctic environments." ISME J **6**(3): 692-702.

Younger, P. L., R. H. Coulton and E. C. Froggatt (2005). "The contribution of science to risk-based decision-making: lessons from the development of full-scale treatment measures for acidic mine waters at Wheal Jane, UK." Science of The Total Environment **338**(1–2): 137-154.

Zhang, T., T. S. Bain, K. P. Nevin, M. A. Barlett and D. R. Lovley (2012). "Anaerobic Benzene Oxidation by Geobacter Species." Applied and Environmental Microbiology **78**(23): 8304-8310.

Zinck, J. and W. Griffith (2013). Review of mine drainage treatment and sludge management operations. Canada, Mine Environment Neutral Drainage (MEND) Program.

CHAPTER 4

Paper 3: Determination of organic matter inputs at an acid mine drainage site, Parys Mountain, UK.

Martha E. Jiménez-Castañeda[1]; David J. Vaughan[1]; Jonathan R. Lloyd; Bart E. van Dongen[3,*].

This chapter contains the following paper which is under preparation to be submitted to the journal: to be considered.

[3] School of Earth, Atmospheric and Environmental Sciences, Williamson Research Centre for Molecular Environmental Science, University of Manchester, Manchester, UK.

* Corresponding author: Tel.: +44 161 3067460; fax: +44 161 3069361.
E-mail address: Bart.vanDongen@manchester.ac.uk

Abstract

The role of organic matter in acid drainage environments has not been fully understood. In this work sediment samples from seven acidic ponds located at Parys Mountain, UK were analysed to determine the presence of organic matter inputs. The results obtained by organic geochemical techniques (GC-MS and Py-GC-MS) indicated the presence of plant material in some ponds. In those relatively "organic-rich" ponds the conditions of pH, and Fe(II) concentration were similar to those reported form an ARD site (Mam Tor, UK). The presence of a floating biofilm and a heather litter layer demonstrated the influence of the organic matter in the pond sediment. The organic fractions transported to the sediment below the organic matter layers were mainly *n*-alkanes and a small portion of polysaccharide moieties.

Key words: Parys Mountain, organic matter, acid mine drainage, AMD.

4.1. Introduction

Mining has been part of human technology and development for very long time; however, it has also been associated to environmental hazards. The worst environmental impact that rises from active and abandoned mine working is the acid mine drainage (AMD).

AMD endangers human health, for instance, due to the acidification of fresh water streams (Smedley et al. 1996) and the contamination of agricultural lands (Lin et al. 2007). The AMD effects on the environment have been documented worldwide (Davis Jr et al. 2000, Smolders et al. 2003, Herrera et al. 2007, Tutu et al. 2008). Two well known cases in the UK are the drainage works carried out at Parys Mountain in 2003 (Coupland and Johnson 2004) which is explained later in this document, and the Wheal Jane mine accident in 1992, that released 50,000 m^3 of AMD to the Fal estuary (Banks et al. 1997).

AMD occurs in mining sites when pyrite is oxidised by air and water action, generating water streams with low pH and elevated concentrations of iron, sulfur and other dissolved metals such as Cu, As, Pb (Singer and Stumm 1970). In a similar way, when the natural oxidation of pyrite occurs, the phenomenon is known as acid rock drainage (ARD).

The oxidative dissolution of pyrite is a complex electrochemical process (Singer and Stumm 1970, Rimstidt and Vaughan 2003) that can be summarised by the overall reaction (Singer and Stumm 1970):

$$4FeS_2+15O_2+14H_2O \rightarrow 4\ Fe(OH)_3+8SO_4^{-2}+16\ H^+$$

The reaction is accelerated by the presence of acidophilic microorganisms such as *Acidithiobacillus ferrooxidans*. This microorganism is able to oxidise sulfur and reduced sulfur compounds and also possesses the capacity of reducing Fe(III) in anoxic environments (Colmer et al. 1950, Roger et al. 2012). The chemoautotrophic metabolism of *A. Ferrooxidans* is expected at AMD environments due to the scarce amount of carbon (organic matter) present (Johnson 2012).

Resent research works have shown that diverse organic matter inputs such as petroleum derived organic matter and plant material may occur at acid drainage sites. Jiménez-Castañeda et al. (in prep.-b) have suggested that mature organic matter (petroleum derived) seeping out from the source rock is not implied in the generation of ARD. However, the addition of recent organic matter in ARD sediments is involved into the attenuation of the acidic conditions (Jiménez-Castañeda et al. in prep.-a) However, it was suggested that the addition of recent organic matter sourced to ARD sediments is involved into the attenuation of the acidic conditions (Jiménez-Castañeda et al. in prep.-a). Those findings show that the processes associated to the presence of organic matter in AMD sites are still unclear. This study aims to determine the organic matter inputs present at a mine site and to compare them with those detected at an ARD environment.

4.2. Study site

Parys Mountain (Anglesey, UK), once the largest mine of copper in the world, is a volcanic-associated massive sulfide ore deposit composed of chalcopyrite, galena, sphalerite, and pyrite as the principal minerals (Johnson 2003, Batty et al. 2006). Parys Mountain was mined for approximately 3500 years at different extent, but was extensively exploited during the 18th and 19th centuries (Walton and Johnson 1992). The mine closed in 1904, but copper was continually leached, using the cementation process, until the early 1950s. When these operations ceased, the valve that controlled the water flow was left closed. In the late 1990s it was realised that a failure in this valve could cause a catastrophic flood in the town of Almwch (Younger and Potter 2012). To alleviate the charge of the mine, 274,000 m^3 of AMD (pH~2.4) were drained into the Irish Sea in 2003 (Coupland and Johnson 2004).

The diversion of the mine water was used for study the microbiology of subterranean AMD body water and to investigate how rapidly acidophilic microbial communities develop in a new drainage channel. *Acidithiobacillus ferrooxidans* was the dominant bacterium in the subterranean mine water. *Leptospirillum spp., Ferrimicrobium acidiphilum* and some methanogenic *Archaea* were also detected (Coupland and Johnson 2004). Other representative microorganisms isolated from Parys AMD were iron oxidisers such as *Acidithiobacillus ferrivorans* (Hallberg et al. 2010) and *Ferrovum myxofaciens* (Johnson et al. 2014) which are obligate chemolithotrophs and a novel genus/species, name proposed, *Acidithrix ferrooxidans* (Kay et al. 2013). Obligately heterotrophic bacteria such as *Gammaproteobacterium WJ2*, *Acidobacterium*, *Acidiphilium* and *Alicyclobacillus* sp. were also found in the mine (Kay et al. 2013) but the increase of pH with distance from the AMD source within 1 km, seems to increase the diversity of heterotrophic acidophiles (Walton and Johnson 1992). Nowadays, AMD draining from south side of Parys Mountain goes via the Dryffin Goch adit feeding the southern Afon Goch (Figure 4.1), where a natural, small wetland has developed with populations of reeds and cotton grass (Batty et al. 2006).

4.3 Sample collection

On February 2013, seven ponds were sampled at Parys Mountain, near Amlwch, UK (Figure 4.1). Surface sediment samples were collected using a stainless steel scoop and transferred into clean glass jars (acid washed and pre-furnaced), to minimise the risk of contamination. Upon return to Manchester, the samples were stored in the dark at -4°C to minimise microbial activity until freeze-drying for organic and mineralogical analyses.

Ponds A to D were located on the southern slope of Parys Mountain, with an elevation ranging from 140 m (pond A) to 115 m (pond D; Figure 4.1; Transect 1). The lowest pond sample of the transect 1 (pond D), marked the beginning of the Driffyn Goch adit. Ponds E to G were sampled along the Driffyn Goch adit (Transect 2; Figure 4.1). Sites A-D supported the eventual presence of heather (*Calluna vulgaris;* Figure 4.2a), while in sites E-G, the heather populations grew more profusely (Figure 4.2b). A floating biofilm was detected over the sediment F (Figure 4.2c) while heather litter formed a layer in pond G.

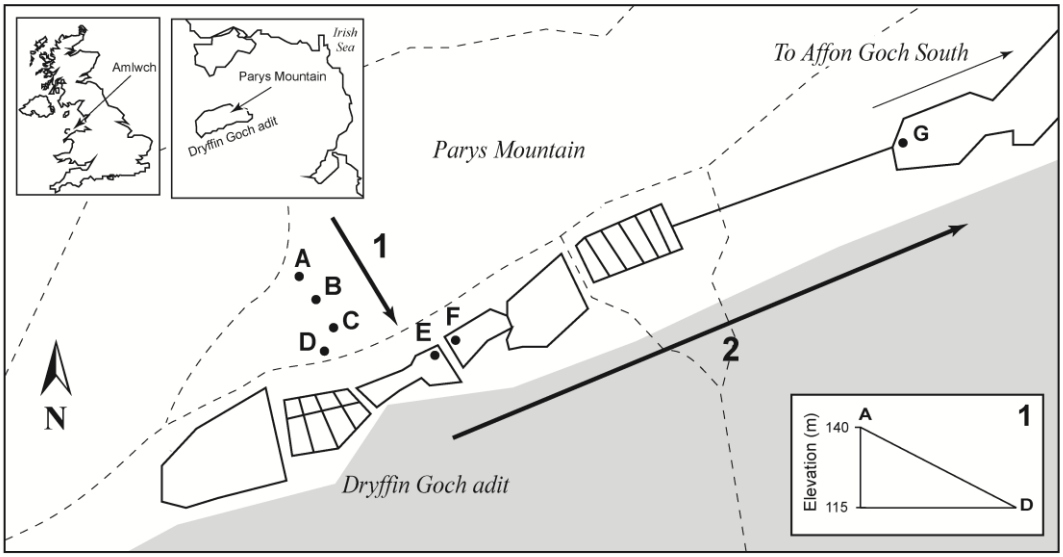

Figure 4.1. Location map of Parys Mountain, UK. Letters in bold indicate sampling ponds; numbers, transects sampled 1) North- South direction, 2) West-East direction. The box in the lower right corner shows the slope of transect 1.

4.4 Experimental

4.4.1 Geochemical parameters

Upon return to the laboratory, the pH and Eh of the pore water were measured (3x) using a Basic Denver pH/ORP meter (Denver Instrument Company) with a 3M KCl liquid-filled electrode (Ag/AgCl reference). The concentration of Volatile Organic Compounds (VOCs) was quantified on filtered (0.22 μm) subsamples if sufficient pore water was available (samples A, C, F, G), using a Bio High Pressure Liquid Chromatograph (Dionex, US) equipped with an IonPac ICE-AS1 ion-exclusion column (Dionex, US). Bioavailable Fe(II) was extracted from sediment aliquots (Lovley and Phillips 1987) and measured photometrically with ferrozine (Stookey 1970) at 562 nm on a Jenway 6715 UV/visible spectrophotometer. The remaining sediments were freeze-dried for X-Ray Fluorescence (XRF), X-Ray (powder) diffraction (XRD) and organic analyses. For the mineralogical characterisation, XRD data were collected from small sediment subsamples on a Bruker D8 Advanced Instrument with $CuK_{\alpha 1}$ radiation, over a range of $5^{o}2\theta$ to $7^{o}2\theta$, using a step size of 0.02° each 2 s. Pressed pellets, prepared from 12 g of sediment and 3 g of wax binder, were analysed for both major and trace elements on an Axios Sequential XRF Spectrometer (PANalytical, Almelo, Netherlands).

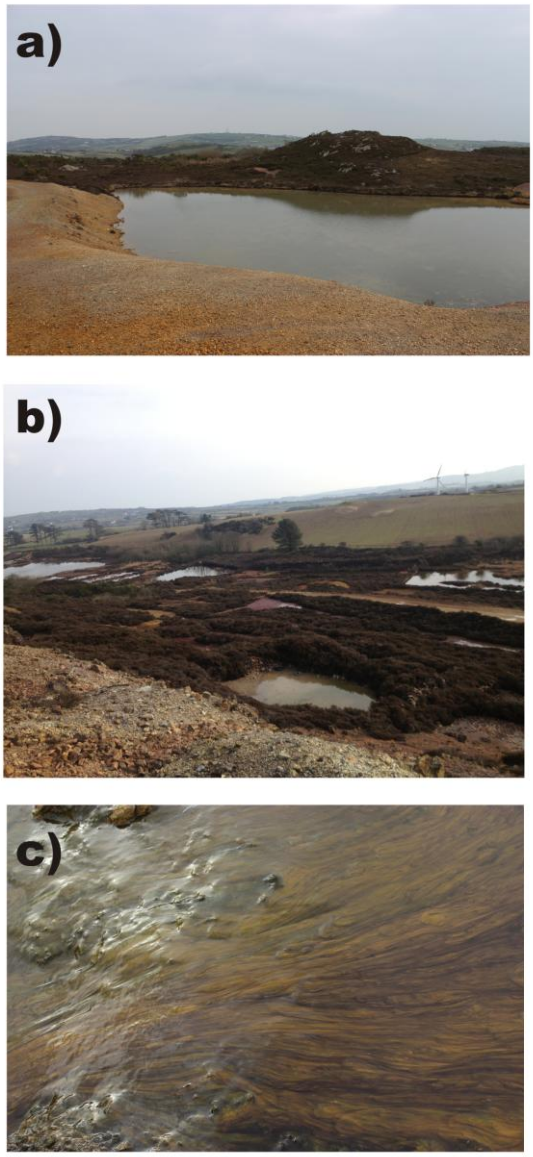

Figure 4.2. Examples of different conditions at Parys Mountain a) samplig pond in the transect 1, poorly vegetated; b) precipitation ponds (Driffyn Goch adit; Transect 2), dominated by heather; c) detail of the pond F with the floating biofilm.

4.4.2 Determination of organic matter content

The total organic matter content was determined using the sequential loss on ignition method (Heiri et al. 2001, Beaudoin 2003). Sediment subsamples (triplicates; 500 mg each), were accurately weighted into constant-weight glass vials, heated at 105°C for 12 h, cooled down into a dessicator and weighed again. Subsequently, the samples were ignited at 350°C for 16 h, allowed to cool down into a dessicator and weighed.

The organic matter content was determined calculating the difference in weight %, before and after ignition.

4.4.3 n-alkane analysis

The total lipid extracts (TLEs) were ultrasonically extracted from either 2 g of biofilm, heather litter or sediment C samples, or 7 g of other sediments, using the modified Bligh-Dyer extraction method (White et al. 1979, Frostegård et al. 1991). The samples were extracted three times using a single phase mixture of chloroform:methanol:water buffered with KH2PO4 to pH ~7.2 (1:2:0.8 v/v/v; 18 ml). The organic fractions were collected after each extraction, washed with water buffered with KH2PO4 and combined. Subsequently, they were concentrated using rotary evaporation and nitrogen blowing down and treated with active copper (Blumer 1957) to remove elemental sulfur.

Aliquots of the desulfurised TLEs were taken for further fractionation, after the addition of an internal standard of know concentration (tetracosane-d50), according to the method described in Dickson et al. (2009). To obtain the saturated hydrocarbon fraction (*n*-alkanes), the aliquots were initially eluted on a silica column using 10 ml of a solution of chloroform saturated with ammonium hydroxide. The resulting extracts were further separated via aluminium column chromatography, using 6 ml of a solution of hexane/dichloromethane (9:1, v/v). Blanks were also prepared and analysed to ensure that no contamination was introduced during the extraction and fractionation procedures.

The saturated hydrocarbon fraction were concentrated in 50 µl of hexane and analysed by Gas Chromatography Mass Spectroscopy (GC-MS) on an Agilent 7890A gas chromatography system. This system was equipped with an Agilent 7683B auto-sampler and programmable temperature vaporisation (PVT) inlet interfaced to an Agilent 5975C MSD mass spectrometer, operated in electron ionization mode (scanning a range of *m/z* 50 to 600 at 2.7 scans/s; ionisation energy, 70 eV; solvent delay, 3 min). The heated interface and PTV temperatures were set at 280°C; the mass source, at 230°C and the mass spectrometer quadrupole, at 150°C. The analytical separations of the *n*-alkanes were accomplished using a HP-5 MS capillary column (Agilent; (5%-phenyl)-methylpolysiloxane; 30 m x 0.25 mm, i.d.), programmed from 70°C to 130°C at 20°C/min, then to 320°C at 4°C/min and kept isothermally for 10 min. The samples were run using He as a carrier gas at a constant flow (1 ml/min). The *n*-alkanes were identified by comparison of their molecular mass (*m/z*) with The

National Institute of Standards and Technology (NIST) library and quantified using the peak area of the internal standard as reference.

The odd-over-even predominance of the High Molecular Weight (HMW) *n*-alkanes over the range C_{20}-C_{31}, was expressed in the carbon preference indexes (CPIs) using the following equation (van Dongen et al. 2008):

$$CPI_{i-n}=0.5[(X_i+X_{i+2}+...+X_n)/(X_{i-1}+X_{i+1}+...+X_{n-1})]+0.5[(X_i+X_{i+2}+...+X_n)/(X_{i+1}+X_{i+3}...+X_{n+1})]$$

where X is the *n*-alkane concentration in the range from *i* to *n*.

The average chain length (ACL) of the high molecular weight (HMW) *n*-alkanes was calculated using the following equation (van Dongen et al. 2008):

$$ACL= \Sigma(iX_i + ... + nX_n)/\Sigma(X_i + ... +X_n),$$

where X is the *n*-alkane concentration in the range from *i* to *n*.

4.4.4 Macromolecular analysis

For the macromolecular analyses, subsamples (250 mg) of the pond sediments were demineralised according the method described in Gélinas et al. (2001). The sediments were digested for 60 min in HCl (30 ml; 1 M) with constant agitation; subsequently, the mixtures were centrifuged for HCl removal, and digested once for 12 h in a HCl:HF solution (10% HF in 1M HCl, v/v; 20 ml) using a shaker for complete reaction. The recovered material was rinsed with distilled water (3x; 3.5 ml) and freeze-dried for Pyrolysis-GCMS (Py-GCMS) analysis. Samples from sediment C, biofilm and heather litter did not require this treatment.

Subsamples (1.2 μg; 3x) of all the sediments, including the biofilm and heather layers, were pyrolysed in a quartz tube at 600°C (10s) using a Chemical Data System (CDS) 5200 Series Pyroprobe Pyrolysis Unit, coupled to the Agilent GC-MS system as described above, using also the same GC-MS column and column program. The pyrolysis transfer line and injector temperatures were set at 350°C. The samples were injected using He as carrier gas in split mode (ratio 5:1; constant flow, 1 ml/min). The oven was programmed to hold 40°C for 3 min and then to 300°C at 4°C/min, and kept isothermally for 15 min. Individual compounds were identified by comparison of the molecular mass (*m/z*) with The National Institute of Standards and Technology (NIST) library and relevant literature (Saiz-Jiménez and De Leeuw 1986, Ralph and

Hatfield 1991, Vancampenhout et al. 2009, del Río et al. 2012, Yassir and Buurman 2012).

A variable range of compounds were identified in the samples and were grouped in different classes according their origin; polysaccharide compounds (furans, furfurals, ketones, cyclic hydrocarbons and glucopyranose compounds), aromatic compounds (benzenes), nitrogen compounds (N-containing compounds), alkenes, isoprenoid alcohols, fatty acids (C_{16},C_{18}), lignin moieties (guaicol, syringol, methoxyphenols), phenolic compounds (other than methoxyphenols) and sulfur compounds (sulfur and thiophenes). The sum of the peak areas of the compounds identified in each sample was set at 100% and the relative contribution of each compound was calculated. In the case of the polysaccharides only the five more abundant compounds were considered; for the other fractions, all the identified compounds were included.

4.5. RESULTS

4.5.1 General characterisation

The pH of the acidic ponds along the slop transect 1 (Figure 4.1) on the southern slope of Parys Mountain were comparable, with values between 2.4 (pond D) to 2.6 (pond B; Table 4.1). In contrast the pH in the ponds along transect 2 (Figure 4.1), at the Dryffin Goch adit (Figure 4.1) and the biofilm and heather litter layer, were slightly less acidic with values ranging from 2.9 (pond F) to 3.7 (pond G). The Eh of the pond waters ranged from 548 mV to 576 mV (Table 4.1), well above 500 mV in all cases indicating oxidising conditions.

The content of bioavailable Fe(II) in the pore waters of most acidic pond sediments, with the exceptions of pond C and G were comparable, ranging from 2.98 mM (pond F) to 2.35 mM (pond D; Table 4.1 and Figure 4.2). In contrast, the Fe(II) content in the pore waters of the sediments from pond C and G was substantially higher with values of 23.2 mM and 14.3 mM, respectively. These were comparable to the Fe(II) in the biofilm (22.9 mM) and the heather litter layer (15.3 mM).

The OM content of the surface sediments varied between 14.2% (pond G) and 3.1% (site A; Table 4.1; Figure 4.3), with substantial higher amounts in the sediments from pond F and G if compared to the other sediments. This high OM abundance was comparable to the OM content in the biofilm (12%). Not surprisingly the heather litter layer showed a much higher OM content (45%).

Table 4.1. Location and general characterisation of the AMD ponds at Parys Mountain

	Pond sediment[a]								
	A	B	C	D	E	F	G	Biofilm[b]	Heather[c]
Lat[d]	53°23' 2"	53°23' 1.3"	53°23' 0.6"	53°29' 59.5"	53°29' 59.9"	53°23' 0.3"	53°23' 6.4"	53°23' 0.3"	53°23' 6.4"
Long[e]	-4°20' 42.4"	-4°20' 41.6"	-4°20' 38.8"	-4°20' 40.2"	-4°20' 35.2"	-4°20' 34.4"	-4°20' 13.6"	-4°20' 34.4"	-4°20' 13.6"
OM[f] (%)	3 <1	6 <1	9 <1	6 <1	4 <1	11 <1	14 <1	12 <1	45 ±2
pH	2.5	2.6	2.5	2.4	3.1	2.9	3.7	2.9	3.7
Eh (mV)	562	568	564	576	548	553	546	553	546
Fe(II) (mM)	2.7 ±0.3	2.8 ±0.4	23.2 ±4	2.4 ±0.5	2.6 ±0.4	3.0 ±0.9	14 ±0.4	23 ±4	15 ±4

[a] As located in Figure 4.1.
[b] Layer located above pond sediment F.
[c] Litter layer collected above pond sediment G.
[d] Latitude .
[e] Longitude.
[f] variation of organic matter content <1%, measured in triplicates.

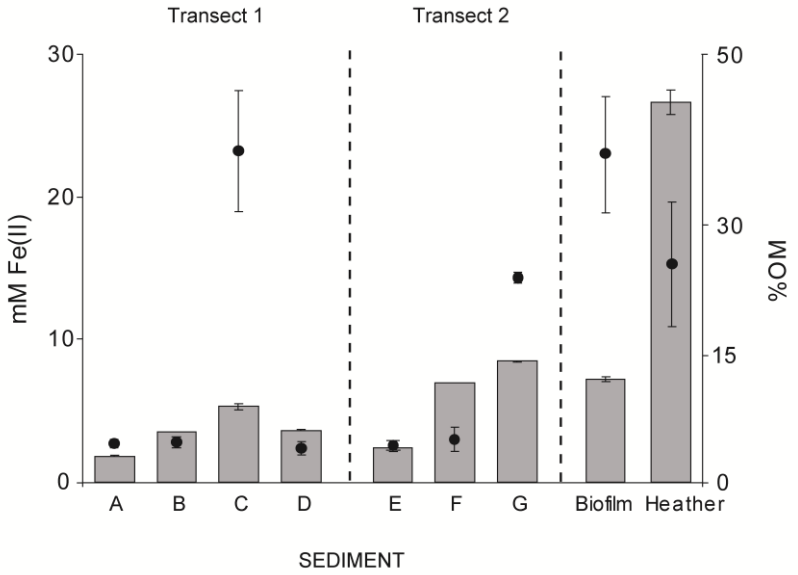

Figure 4.3. Content of Fe(II) in pore water (circles) and sedimentary organic matter (OM; bars) of acidic ponds from Parys Mt. For comparison the data of the biofilm and the heather litter layer detected at the surface sediments of pond F and G, respectively, are included.

4.5.2 Inorganic characterisation of the sediments

The mineralogical composition of the pond sediments sampled at Parys Mountain, was determined by XRF and XRD analyses. According to the XRF data, the sediment from pond A, B and D were dominated by iron oxide compounds and contained significant concentrations of copper, arsenic, and lead (Table 4.2). Sediments from ponds C and E were dominated by silica, with high content of tin, lead and copper while sediments F and G were almost totally defined by the presence of iron oxides, Sediment F also contained quantities of other minerals, specially lead, copper and tin, compared to site G (Table 4.2).

Table 4.2. Elemental composition sediments from Parys Mt. ponds

	A	B	C	D	E	F	G
Major oxides %[a]							
SiO_2	37.0	24.0	45.9	21.0	51.0	7.0	2.0
TiO_2	0.3	0.4	0.2	0.3	0.4	<0.001*	<0.001*
Al_2O_3	9.0	9.0	11.2	8.0	10.0	2.0	0.5
Fe_2O_3	42.0	46.0	33.8	51.0	30.0	80.0	91.0
MgO	<0.01*	0.4	0.5	0.3	1.0	0.1	0.1
CaO	0.4	<0.005*	<0.005*	<0.005*	0.3	<0.005*	<0.005*
Na_2O	0.01*	0.2	0.3	0.3	0.4	0.2	0.1
K_2O	0.5	3.0	3.2	3.0	2.0	1.0	0.8
P_2O_5	3.0	<0.01*	<0.01*	<0.01*	0.3	<0.01*	<0.01*
SO_3	0.1	13.0	3.6	12.0	4.0	8.0	6.0
Total	*100.2*	*96.1*	*98.7*	*95.9*	*99.4*	*98.3*	*100.5*
Other elements (ppm)							
Cu	2590	5360	649	8060	1984	2216	333
Zn	1850	4360	272	4380	787	663	974
As	1180	2390	271	2320	326	352	847
Pb	7260	29500	1432	33240	2722	5351	746
Ba	288.8	449	254	527	460	117	66
Sn	60	127	2515	584	2167	276	559

[a] error <0.1%

* values below detection limit (expressed in %)

The results from the XRD analyses indicate a similar composition from samples A to E, including quartz, muscovite, hematite albite and jarosite. Goethite was also detected in site C and both goethite and clinochlore in sites F and G with no phyllosilicate contribution in the two former. In accordance with the XRF data, the iron oxides in samples A, B and D were represented by jarosite while in samples C, E, F and G, the iron oxides were a mixture of jarosite and goethite.

4.5.3 Organic characterisation of the sediments

The saturated hydrocarbon fraction of the sediments analysed (C, F and G) were dominated by a high molecular weight (HMW; $>C_{20}$) homologous series *n*-alkanes, ranging from C_{20} to C_{32}, with a clear predominance of the odd-numbered homologues, as indicated by the Carbon Preference Index values CPI_{21-31} which ranged from 2.2 (sediment F) to 5.9 (sediment C; Table 4.3 and Figure 4.4). The summed concentration of HMW *n*-alkanes (ΣC_{20-32}) in sediment C was 6.8 $\mu g/g_{sed}$, considerably higher if compared to the other two sediments (1.3– 2.0 $\mu g/g_{sed}$). The C_{31} *n*-alkane was the most abundant homologue (Cmax) in sediments C and F, while the C_{29} *n*-alkane was the most abundant homologue in sediment G (Table 4.3 and Figure 4.4) and the average chain length (ACL_{20-32}) ranged from 26.4 (sediment G) to 27.5 (sediment F; Table 4.3).

Substantial amounts of *n*-alkanes were also present in the biofilm, ΣC_{20-32} = 2.7 $\mu g/g_{sed}$, and the heater litter layer, ΣC_{20-32}=4.0 $\mu g/g_{sed}$. In addition, for the biofilm, the CPI_{21-31} was 1.5, the most abundant *n*-alkane was the C_{31} homologue and the ACL_{20-32} was 28.6. In the case of the heather litter, the CPI was 3.4, the most abundant *n*-alkane was the C_{27} homologue and the ACL_{20-32} was 26.9 (Table 4.3 and Figure 4.4).

Products of organic matter fermentation were also detected in the aqueous phase of the ponds A, C, F and G (Table 4.3). Acetate and formate were the most abundant ions, with concentrations up to 21.3 mg/l and 0.84 mg/l, respectively (pond C). Propionate was also abundantly present in pond C (0.65 mg/l) and in trace amounts in pond F, but was below detection limit in the other ponds (Table 4.2).The sulfate concentration in the ponds varied between 264 mM/l (pond A) and 1720 mM/l (pond F; Table 4.3). Interestingly, no *n*-alkanes could be detected in the sediment A (Table 4.3).

Table 4.3. Characterisation of the saturated hydrocarbon fraction and volatile organic compounds detected in Parys Mountain ponds.

Pond sediment	A	C	F	G	Biofilm[a]	Heather[b]
n-alkanes	nd[c]					
ΣC_{20-32}[d] (µg/g sediment)		6.8	1.3	2.0	2.7	4.0
C_{max}[e]		31	31	29	31	27
CPI_{21-31}[f]		5.9	2.2	3.0	1.8	3.6
ACL_{20-32}[g]		28.6	27.5	26.4	28.6	26.9
*Volatile organic compounds**						
Sulfate (mM/l)	264	684	1720	415	<0.01	<0.01
Lactate (mg/l)	0.05	0.12	0.10	0.03	<0.01	<0.01
Acetate (mg/l)	0.41	21.3	0.52	0.25	<0.01	<0.01
Propionate (mg/l)	<0.01	0.65	0.01	<0.01	<0.01	<0.01
Formate (mg/l)	0.19	0.85	0.44	0.09	<0.01	<0.01

[a] Layer located above pond sediment F.
[b] Litter layer collected above pond sediment G.
[c] nd= no detected.
[d] Summed concentration over the C_{20}-C_{32} range.
[e] C_{max} = chain length of the *n*-alkane with the highest concentration.
[f] CPI_{21-31}= carbon preference index over the range C_{21}-C_{31}.
[g] ACL_{20-32} = Average chain length over the range C_{20}-C_{32}.
* values below the typical routine detection limits (0.01 – 0.1 mg/l) reported as <0.01

The relative macromolecular composition of the samples (Figure 4.5) as determined by Py-GC-MS, indicated that the pond sediments can be divided in two groups. The first group consisted of the sediments from ponds A, B, D, E and F, where aromatic compounds (90 to 30, % of total), mainly benzene, dominated the macromolecular distribution. Substantial amounts of alkenes were detected in sediments from pond A and pond B, 45% and 14% of total, respectively (mainly C_{16} and 2-4-di-methyl-2-decene) and sulfur compounds in pond sediments B, D, E and F, 30% to 10% of total (mainly SO_2). Pond sediment A also contained a substantial fatty acid contribution, 24% (mainly C_{16}) while pond sediment B contained minor amounts of nitrogen containing compounds, 3% (2-Butenenitrile) and pond sediment F, a substantial amount of polysaccharide derived moieties, 14% (mainly 3-methylfuran and furfural).

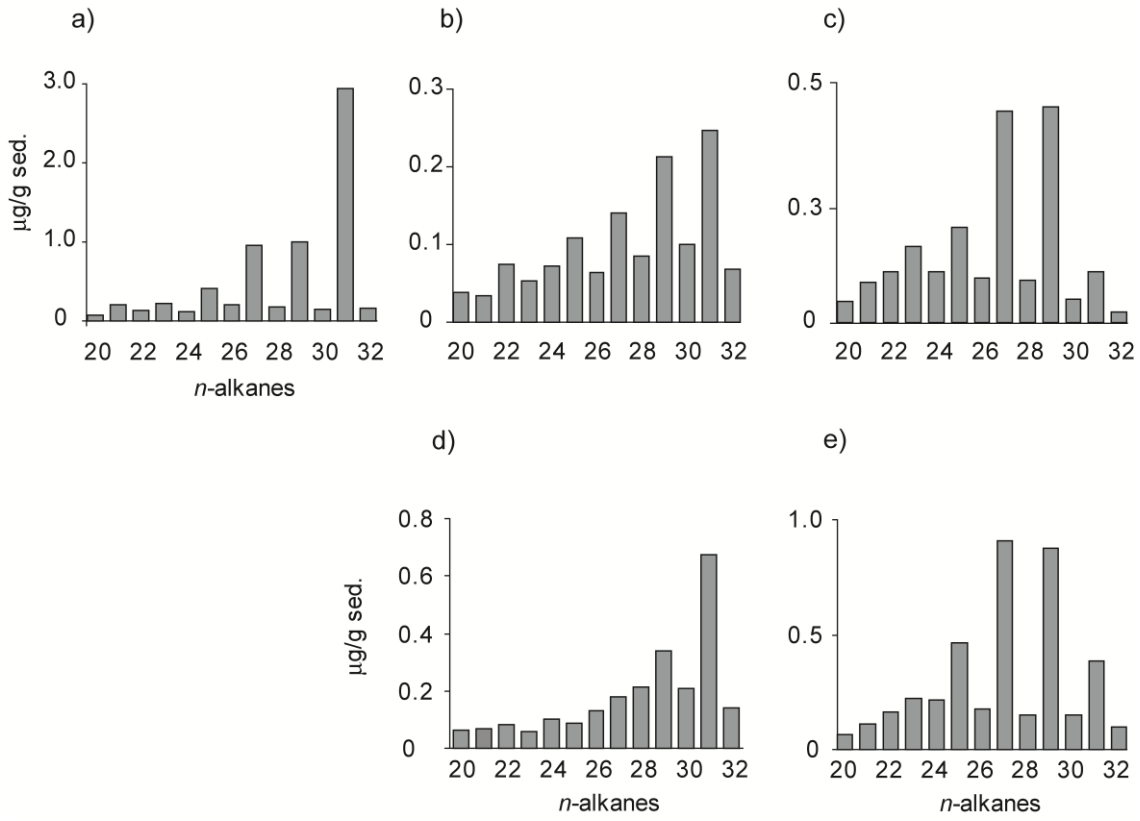

Figure 4.4. Distribution pattern showing the *n*-alkane content of the surface sediments of a) pond C; b) pond F; c) pond G; d) biofilm layer detected at pond F; e) heather litter layer at pond G.

The second group of sediments included pond sediments C and G, which were dominated by a polysaccharide derived contribution, 42% and 66%, respectively, (Figure 4.5). Considerable amounts of fatty acids (29%) were also present in pond sediment C with minor amounts of aromatics (10%), isoprenoidal alcohols (8%), alkenes (7%), nitrogen containing (2.5%) and lignin derived (1%) moieties. Pond sediment G presented a substantial contribution of sulfur containing compounds (32%) and minor amounts of aromatic moieties (2.5%).

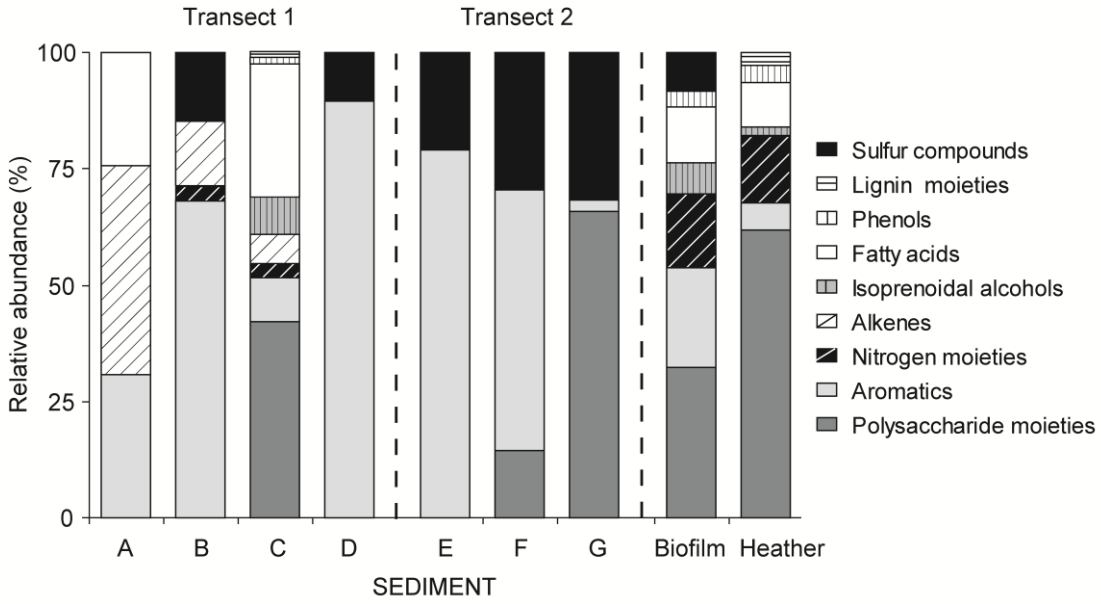

Figure 4.5. Relative macromolecular composition as determined by Py-GCMS from the sediments sampled at Parys Mountain. For comparison the data of the biofilm and the heather litter layer detected at the surface sediments of pond F and G, respectively, are included.

For comparison, the biofilm and the heather litter layer were also analysed; both samples were dominated by polysaccharides, 32% and 62%, respectively (Figure 4.5). The biofilm also contained elevated amounts of aromatic moieties (22%), nitrogen compounds (15%) and fatty acids (12%) with minor contributions of sulfur, phenol and lignin moieties (Figure 4.5). The litter layer had a notable contribution of nitrogen containing compounds (14%) and fatty acids (12%), the rest of the compounds (Figure 4.5) were less abundant.

4.6. Discussion

The inorganic characterisation of the pond sediments was typical of AMD environments, with iron phases such as goethite and jarosite and an important silica contribution (Ferris et al. 1989, Murad and Rojík 2003, Valente et al. 2013). The pH of the ponds was as well within the values expected for an AMD site (Banks et al. 1997).

Younger and Potter (2012) reported a pH of approximately 2.2 for the site. This value is similar to those observed in the ponds of transect1, (Table 4.1). However, there was a slight pH increase in the ponds of transect 2. This change could be explained due to a dilution factor (Boult et al. 1994) rather than to the presence of local vegetation. The

acidic conditions of these ponds (F and G) were similar to those reported by (Jiménez-Castañeda et al. in prep.-a) for an ARD site (pH ~3.5) where local vegetation has already developed.

OM data on other AMD sites is limited but the concentrations of the transect 1, for instance, were comparable to those recently determined for a pond at the Mam Tor landslide close to the point where ARD is generated (Jiménez-Castañeda et al. in prep.-b) while the values of the transect 2 are closer to an ARD environmnet with local OM input (Jiménez-Castañeda et al. in prep.-a). In that work was also suggested that plant-derived OM in an ARD systems limits the microbial Fe(III)-reduction rate in presence of acetate, which was also detected in Parys Mountain ponds (Table 4.3). The presence of short chain acids (VOCs) in different ponds, also indicate that the OM present is being degraded in a fermentative metabolism. The detection of acetate, is in line with other results reported for the stimulation of ARD sediments using plant material (Jiménez-Castañeda et al. in prep.-a).

Within transect 1 the sedimentary OM of pond C is substantially higher if compared to the other pond sediments in the same transect. The macromolecular OM composition of the other sediments was dominated by moieties most likely originating from the original source rocks, including aromatic and sulfur containing moieties. In addition, macromolecular analyses indicate that the organic contributors in this sediment are different as well, more likely from plant origin primarily dominated by polysaccharide and fatty acids moieties (Ralph and Hatfield 1991, Vancampenhout et al. 2009). This is supported by the presence of substantial amounts of HMW *n*-alkanes with a high CPI values (Eglinton and Hamilton 1963) observed in this sediment. However, the distribution pattern was substantially different if compared to that of the heather (Figure 4.4 and 4.5). For instance, the C_{31} *n*-alkane was the dominant HMW homologous series in sediment C while the C_{27} *n*-alkane was the most abundant component in the distribution pattern in the heather. This result indicates that, although abundantly present around Parys Mountain, heather was not the dominant plant input in pond C, suggesting that a part of the OM present is originating from an unknown source.

Ponds F and G presented a direct OM input, and the sediments was expected to have a diverse OM composition. However the organic characterisation of these sites indicated that the biofilm and the plant material influenced the sediment composition with *n*-alkanes but interestingly, the Pyro-GC-MS analyses showed that the OM composition of the sediments F and G was different from the layers above (biofilm, heather litter)

indicating that the OM has not been transported to the sediment, and therefore is non-available for anaerobic microorganisms.

4.7. Conclusions

The present study was undertaken to determine the natural organic matter inputs occurring at an AMD site. The results from the organic analyses indicated that fresh (plant origin) OM inputs are present *in situ*, but also suggest that apart from the influence of heather (*Calluna vulgaris*), there is another unidentified carbon source occurring at Parys Mountain.

Analysis of the sediments below the organic layers detected (F and G) indicated that the surface OM is not available for the use of the microbial community present in the pond sediment below. However, the detection of fermentation products suggested microbial activity within the biofilm and on the heather litter layer, probably related to the creation of microenvironments.

The comparison of Parys Mountain data with previous studies carried out at an ARD site, indicated that the presence OM is possible and occurs in diverse forms at acid drainage environments, but its influence is rather ambiguous. Further research is needed for understanding the controlling factors and the processes involved with the degradation of organic matter at AMD sites.

Acknowledgements

We gratefully acknowledge the receipt of a PhD studentship for M. E. Jiménez-Castañeda, funded by the National Council of Science and Technology of México (CONACyT) and a complementary scholarship for Postgraduate Studies Abroad funded by the Secretariat of Public Education of Mexico (SEP). We thank to C. Davies (University of Manchester) for her assistance in chemical analyses.

REFERENCES

Banks, D., P. L. Younger, R.-T. Arnesen, E. R. Iversen and S. B. Banks (1997). "Mine-water chemistry: the good, the bad and the ugly." Environmental Geology **32**(3): 157-174.

Batty, L., A. M. Baker and B. Wheeler (2006). "The effect of vegetation on porewater composition in a natural wetland receiving acid mine drainage." Wetlands **26**(1): 40-48.

Beaudoin, A. (2003). "A comparison of two methods for estimating the organic content of sediments." Journal of Paleolimnology **29**(3): 387-390.

Blumer, M. (1957). "Removal of elemental sulfur from hydrocarbon fractions." Analytical Chemistry **29**(7): 1039-1041.

Boult, S., D. N. Collins, K. N. White and C. D. Curtis (1994). "Metal transport in a stream polluted by acid mine drainage—The Afon Goch, Anglesey, UK." Environmental Pollution **84**(3): 279-284.

Colmer, A. R., K. L. Temple and M. E. Hinkle (1950). "An iron-oxidizing bacterium from the acid drainage of some bituminous coal mines." Journal of Bacteriology **59**(3): 317.

Coupland, K. and D. B. Johnson (2004). "Geochemistry and microbiology of an impounded subterranean acidic water body at Mynydd Parys, Anglesey, Wales." Geobiology **2**(2): 77-86.

Davis Jr, R. A., A. T. Welty, J. Borrego, J. A. Morales, J. G. Pendon and J. G. Ryan (2000). "Rio Tinto estuary (Spain): 5000 years of pollution." Environmental Geology **39**(10): 1107-1116.

del Río, J. C., P. Prinsen, J. Rencoret, L. Nieto, J. s. Jiménez-Barbero, J. Ralph, A. n. T. Martínez and A. Gutiérrez (2012). "Structural characterization of the lignin in the cortex and pith of elephant grass (Pennisetum purpureum) stems." Journal of agricultural and food chemistry **60**(14): 3619-3634.

Dickson, L., I. D. Bull, P. J. Gates and R. P. Evershed (2009). "A simple modification of a silicic acid lipid fractionation protocol to eliminate free fatty acids from glycolipid and phospholipid fractions." Journal of Microbiological Methods **78**(3): 249-254.

Eglinton, G. and R. Hamilton (1963). "The distribution of alkanes." Chemical plant taxonomy **187**: 217.

Ferris, F. G., K. Tazaki and W. S. Fyfe (1989). "Iron oxides in acid mine drainage environments and their association with bacteria." Chemical Geology **74**(3–4): 321-330.

Frostegård, Å., A. Tunlid and E. Bååth (1991). "Microbial biomass measured as total lipid phosphate in soils of different organic content." Journal of Microbiological Methods **14**(3): 151-163.

Gélinas, Y., J. A. Baldock and J. I. Hedges (2001). "Demineralization of marine and freshwater sediments for CP/MAS 13C NMR analysis." Organic Geochemistry **32**(5): 677-693.

Hallberg, K., E. González-Toril and D. B. Johnson (2010). "Acidithiobacillus ferrivorans, sp. nov.; facultatively anaerobic, psychrotolerant iron-, and sulfur-oxidizing acidophiles isolated from metal mine-impacted environments." Extremophiles **14**(1): 9-19.

Heiri, O., A. F. Lotter and G. Lemcke (2001). "Loss on ignition as a method for estimating organic and carbonate content in sediments: reproducibility and comparability of results." Journal of paleolimnology **25**(1): 101-110.

Herrera, S. P., H. Uchiyama, T. Igarashi, K. Asakura, Y. Ochi, F. Ishizuka and S. Kawada (2007). "Acid mine drainage treatment through a two-step neutralization ferrite-formation process in northern Japan: Physical and chemical characterization of the sludge." Minerals Engineering **20**(14): 1309-1314.

Jiménez-Castañeda, M. E., J. R. Lloyd, V. D. J and B. E. van Dongen (in prep.-a). "Importance of organic matter in the microbial Fe(III) reduction at an acid rock drainage environment."

Jiménez-Castañeda, M. E., J. R. Lloyd, V. D. J and B. E. van Dongen (in prep.-b). "The potential metabolism of petroleum-derived hydrocarbons in acid rock drainage systems."

Johnson, D. B. (2003). "Chemical and microbiological characteristics of mineral spoils and drainage waters at abandoned coal and metal mines." Water, Air and Soil Pollution: Focus **3**(1): 47-66.

Johnson, D. B. (2012). "Geomicrobiology of extremely acidic subsurface environments." FEMS Microbiology Ecology **81**(1): 2-12.

Johnson, D. B., K. B. Hallberg and S. Hedrich (2014). "Uncovering a Microbial Enigma: Isolation and Characterization of the Streamer-Generating, Iron-Oxidizing, Acidophilic Bacterium "Ferrovum myxofaciens"." Applied and Environmental Microbiology **80**(2): 672-680.

Kay, C. M., O. F. Rowe, L. Rocchetti, K. Coupland, K. B. Hallberg and D. B. Johnson (2013). "Evolution of Microbial "Streamer" Growths in an Acidic, Metal-Contaminated Stream Draining an Abandoned Underground Copper Mine." Life : Open Access Journal **3**(1): 189-210.

Lin, C., Y. Wu, W. Lu, A. Chen and Y. Liu (2007). "Water chemistry and ecotoxicity of an acid mine drainage-affected stream in subtropical China during a major flood event." Journal of Hazardous Materials **142**(1–2): 199-207.

Lovley, D. R. and E. J. Phillips (1987). "Rapid assay for microbially reducible ferric iron in aquatic sediments." Applied and Environmental Microbiology **53**(7): 1536-1540.

Murad, E. and P. Rojík (2003). "Iron-rich precipitates in a mine drainage environment: Influence of pH on mineralogy." American Mineralogist **88**(11-12): 1915-1918.

Ralph, J. and R. D. Hatfield (1991). "Pyrolysis-GC-MS characterization of forage materials." Journal of Agricultural and Food Chemistry **39**(8): 1426-1437.

Roger, M., C. Castelle, M. Guiral, P. Infossi, E. Lojou, M. T. Giudici-Orticoni and M. Ilbert (2012). "Mineral respiration under extreme acidic conditions: from a supramolecular organization to a molecular adaptation in Acidithiobacillus ferrooxidans." Biochemical Society Transactions **40**(part 6): 1324-1329.

Saiz-Jiménez, C. and J. W. De Leeuw (1986). "Chemical characterization of soil organic matter fractions by analytical pyrolysis-gas chromatography-mass spectrometry." Journal of Analytical and Applied Pyrolysis **9**(2): 99-119.

Singer, P. C. and W. Stumm (1970). "Acidic Mine Drainage: The Rate-Determining Step." Science **167**(3921): 1121-1123.

Smedley, P. L., W. M. Edmunds and K. B. Pelig-Ba (1996). "Mobility of arsenic in groundwater in the Obuasi gold-mining area of Ghana: some implications for human health." Geological Society, London, Special Publications **113**(1): 163-181.

Smolders, A. J. P., R. A. C. Lock, G. Van der Velde, R. I. Medina Hoyos and J. G. M. Roelofs (2003). "Effects of mining activities on heavy metal concentrations in water, sediment, and macroinvertebrates in different reaches of the Pilcomayo River, South America." Archives of Environmental Contamination and Toxicology **44**(3): 0314-0323.

Stookey, L. L. (1970). "Ferrozine- a new spectrophotometric reagent for iron." Analytical Chemistry **42**(7): 779-781.

Tutu, H., T. S. McCarthy and E. Cukrowska (2008). "The chemical characteristics of acid mine drainage with particular reference to sources, distribution and remediation: The Witwatersrand Basin, South Africa as a case study." Applied Geochemistry **23**(12): 3666-3684.

Valente, T., J. A. Grande, M. L. de la Torre, M. Santisteban and J. C. Cerón (2013). "Mineralogy and environmental relevance of AMD-precipitates from the Tharsis mines, Iberian Pyrite Belt (SW, Spain)." Applied Geochemistry **39**(0): 11-25.

van Dongen, B. E., H. A. L. Rowland, A. G. Gault, D. A. Polya, C. Bryant and R. D. Pancost (2008). "Hopane, sterane and n-alkane distributions in shallow sediments hosting high arsenic groundwaters in Cambodia." Applied Geochemistry **23**(11): 3047-3058.

Vancampenhout, K., K. Wouters, B. De Vos, P. Buurman, R. Swennen and J. Deckers (2009). "Differences in chemical composition of soil organic matter in natural ecosystems from different climatic regions – A pyrolysis–GC/MS study." Soil Biology and Biochemistry **41**(3): 568-579.

Walton, K. C. and D. B. Johnson (1992). "Microbiological and chemical characteristics of an acidic stream draining a disused copper mine." Environmental Pollution **76**(2): 169-175.

White, D. C., W. M. Davis, J. S. Nickels, J. D. King and R. J. Bobbie (1979). "Determination of the sedimentary microbial biomass by extractible lipid phosphate." Oecologia **40**(1): 51-62.

Yassir, I. and P. Buurman (2012). "Soil organic matter chemistry changes upon secondary succession in Imperata Grasslands, Indonesia: A pyrolysis–GC-MS study." Geoderma **173–174**(0): 94-103.

Younger, P. and H. Potter (2012). "Parys in springtime: hazard management and steps towards remediation of the uk's most polluted acidic mine discharge."

CHAPTER 5

Conclusions and Future work

5.1 Conclusions

The objectives of this study were to a) combine mineralogical, molecular and geochemical techniques to characterise Acid Rock Drainage (ARD) and Acid Mine Drainage (AMD) environments, b) identify and characterise the natural sources of organic matter (OM) occurring both at ARD or AMD sites and c) determine whether the OM source(s) identified is(are) involved in the generation/amelioration of ARD.

Based on the objectives described above, this study has attempted to extend the knowledge of the organic processes occurring at AMD/ARD environments. This work showed that:

i. Natural organic matter (OM) sources occur in acid drainage environments. Multiple forms of OM were identified, including mature, petroleum-derived hydrocarbons originating from the original source rocks (Chapter 2) and plant derived material (Chapter 3 and 4).

ii. Although acidophilic bacteria that have the capability to degrade a range of organic products including mature, petroleum-derived hydrocarbons have been detected in ARD systems, this metabolism is apparently not involved in the acid generation. The combined analyses (Chapter 2) suggesting that carbon dioxide is likely to be the main carbon source for acid-generating microorganisms (Shively et al. 1998, Baker and Banfield 2003), indicating that it is predominantly a chemoautotrophic process

iii. In fine particles, goethite can make a bioavailable mineral substrate to support the growth of Fe(III)-reducing bacteria (Chapter 3). Interestingly this mineral phase is also present in the zone of ARD-generation (Chapter 2). These results indicate that the particle size (Swoboda-Colberg and

Drever 1993) may determine the bioavailability of goethite in this sort of systems.

iv. The stimulation of ARD sediments using plant derived OM, abundantly present in and around ARD/AMD pond systems (Chapter 3 and 4), does not result in the neutralization of ARD/AMD. This suggests that OM of plant origin is not used by Fe(III)-reducing bacteria. Some fermentation products such as acetate, detected in microcosm experiments and *in situ*, could limit the microbial Fe(III)-reduction (Chapter 3 and 4). These results are comparable to the thermodynamic calculations of Blodau and Peiffer (2003) which indicate that the hydrolysis/fermentation of organic matter is a limiting factor for sulfate and Fe(III)-reduction in acidic lakes (Chapter 3).

v. In contrast, the stimulation of ARD sediments using manure (particularly sheep manure) raises the pH of the system up to near neutral conditions to values above those obtained using glycerol in this work and in other previous study (Adams et al. 2007). However, it remains unclear which OM fraction from the manure is involved in the neutralization of ARD. On the other hand, manure can make an interesting and non-expensive electron donor in ARD/AMD treatments.

Overall, this work shows that OM may occcur in multiple forms at acid drainage environments. However, during ARD/AMD generation the presence of OM apparently has no direct influence on the process. This suggests that the ARD/AMD generation is a completely inorganic process microbially catalysed.

Interestingly, when OM is present or added to ARD/AMD sites, it could affect the natural attenuation produced by Fe(III)-reduction. Either it could prevent the amelioration, potentially due to the fermentation of organic matter, or it could enhance the amelioration, as shown in the case of the manure experiments. However, the specific organic components and the mechanisms involved in these processes remain unclear.

5.2. Future work

From the above it is clear that more research is needed and this should concentrate on:

1. The determination of the specific organic compounds present in manure, that are involved/responsible of enhancing the microbial reduction of Fe(III) under acidic conditions and thus promotes the natural attenuation of ARD/AMD.

2. To study the microbial metabolism involved in the use of manure additions that promotes the amelioration of ARD/AMD.

3. To investigate the relationship between the use of manure amendments with the bioavailability and distal fate of trace elements typically present in ARD/AMD environments and the organic-metallic complexes that could be produced.

4. To upscale the experiment for testing the attenuation processes of AMD *in situ*.

5. To expand the existing experiments, considering other factors such as different AMD sampling sites worldwide and the use of sterilised manure additions to prevent the presence of pathogens in the environment.

REFERENCES

Adams, L. K., J. M. Harrison, J. R. Lloyd, S. Langley and D. Fortin (2007). "Activity and diversity of Fe(III)-reducing bacteria in a 3000-year-old acid mine drainage site analogue." Geomicrobiology Journal **24**(3-4): 295-305.

Baker, B. J. and J. F. Banfield (2003). "Microbial communities in acid mine drainage." FEMS Microbiology Ecology **44**(2): 139-152.

Blodau, C. and S. Peiffer (2003). "Thermodynamics and organic matter: constraints on neutralization processes in sediments of highly acidic waters." Applied Geochemistry **18**(1): 25-36.

Shively, J. M., G. van Keulen and W. G. Meijer (1998). "Something from almost nothing: carbon dioxide fixation in chemoautotrophs." Annual Review of Microbiology **52**(1): 191-230.

Swoboda-Colberg, N. G. and J. I. Drever (1993). "Mineral dissolution rates in plot-scale field and laboratory experiments." Chemical Geology **105**(1–3): 51-69.

Appendix A. Sample preparation methods

1. Soxhlet extraction

Grid the sample using a mortar and pestle and transfer a subsample into a 7 ml glass vial for bulk analysis.

Solution

Methanol (MeOH)/Dichloromethane (DCM) 1:2 V/V (eg. 150 mL/300 mL). Use aprox. 350 mL.

Cleaning of thimbles and glass wool

1. *Switch on the cooler almost 30 min before start the extraction to let temperature drop to zero.*
2. *Set up the extraction equipment, thimble, glass wool and enough solution for the process.*
3. *Plug in the heating mantles, and leave the cleaning process 24 hours.*
4. *Stop the extraction*
5. *Unplug the heat mantles.*
6. *Leave the soxhlet cool down about 30 min.*
7. *Switch off the cooler.*
8. *Disconnect the carefully the equipment and take off the extractor and the round bottom flask.*
9. *Drain the solvent from the extractor into the flask and from the flask to the solvent container (labelled CLEANING SOLUTION FOR SOXHLET).*
10. *Take out the thimble, avoiding any contact with it, use tweezers rinsed with DCM.*
11. *Wrap loosely the thimble with aluminium foil and store it in the cupboard to dry until the next day.*

Use of thimbles

1. After dryness, remove the thimbles from the cupboard.
2. Unwrap the thimble and take the glass wool aside.
3. Put the thimble in a beaker and tare.
4. Put an appropriate amount of sample, weight again and write the weight.
5. Put the glass wool inside the thimble using the tweezers covering the sample.
6. Place the thimble into the extractor.
7. Start the solid-liquid extraction (24hours).

After the extraction

1. Unplug the heat mantles.
2. Leave the soxhlet cool down about 30 min.
3. Weight a vial with cap (using an analytical balance).

4. Switch off the cooler.
5. Disconnect the carefully the equipment and take off the extractor and the round bottom flask.
6. Drain the solvent from the extractor into the flask.
7. Place the flask in the roto-vap to evaporate the solvent (almost complete dryness).
8. Transfer the extract from the flask to the pre-weighted vial.
9. Rinse the flask few times using DCM to remove completely the sample and transfer to the vial.
10. Expose the vial to a smooth flow of Nitrogen to complete dryness.
11. Reweight the vial* (using an analytical balance).
12. The sample can be stored in the freezer.

2. Ultrasonic extraction (TLE)

Freeze drying

1. Transfer the sample to an appropriate glass recipient, cover with foil and freeze it (-20°C) overnight.
2. Next day put the recipient in the freeze-dryer for 24 hours. Remember make a few holes on the foil to allow water evaporation.
3. Before further analysis ensure that the sample is completely dried.

Ultrasonic extraction

1. Grid the sample using a mortar and pestle.
2. Transfer a subsample into a 7 ml glass vial for bulk analysis.
3. Some plants like grass are difficult to grain, if necessary use the agar-mil or scissors.

Solutions
DCM, DCM:MeOH (1:1), MeOH

1. Weight a centrifuge tube.
2. Transfer a known amount of sample (5 g) into the centrifuge tube.
3. Weight the tube again to record the accurate weight of your sample.
4. Add 10 ml of DCM and mix well (if necessary use a spatula).
5. Sonicate for 5 minutes.
6. Centrifuge tubes at 2300 rpm for 15 minutes.
7. Transfer the supernatant into a 100 ml pear-shape bottom flask.

Repeat the procedure (3-7) two more times with 10 ml of DCM
Repeat the procedure (3-7) two times with 10 ml of DCM:MeOH (1:1)
Repeat the procedure (3-7) three times with 10 ml of MeOH

8. Transfer the sediments into an appropriate recipient and store it at -20C for further analysis.
9. Get the samples near dryness using the roto-vap.

10. Rinse the flask with DCM to dissolve the precipitate and transfer into a reweight vial.

2. Chloroform /ammonium hydroxide extraction (for simple lipids and free fatty acids)

Preparation of aliquot

1. From the TLE vial add 4 ml of DCM.
2. Take a subsample of TLE (0.5 ml).
3. Add 10 µl of tetracosane 540 µg/ml to the aliquot.
4. Add 10 µl of 2-hexadecanol 540 µg/ml to the aliquot.

Preparation of blank

1. Rinse a vial with DCM.
2. Add 10 µl of tetracosane 540 µg/ml.
3. Add 10 µl of 2-hexadecanol 540 µg/ml.

Silica gel column fractionation

1. Make a column using a large pipette, silica from the oven and glass wool.
2. Attach the silica column to a clamp.

Do not allow the column run dry once the extraction has started.

1. Rinse the column twice with $CHCl_{3(satNH_3OH)}$ (2x, 4 ml).
2. Place a 25 ml pear-shaped flask below the column.
3. Pipette out sample solution from vial by suspending with $CHCl_{3\ (satNH_3OH)}$ solution and allow run through column (3x).
4. Label "SL" and close the flask with its stopper.
5. Place a new 25 ml pear-shaped flask below the column.
6. Pipette out sample solution from vial by suspending with chloroform: acetic acid solution (100:1) allow run through column (3x).
7. Label "FFA" and close the flask with its stopper.
8. Place a new 25 ml pear-shaped flask below the column.
9. Pipette out sample solution from vial by suspending with DCM/MeOH solution (1:1).
10. Allow run through column (3x).
11. Label "LR" and close the flask with its stopper.
12. Repeat the procedure for each sample and for the blank.
13. Evaporate by using the roto-vap until near dry.
14. Transfer the extracts into vials washing the flasks with DCM (3x).
15. Dry under N_2.
16. The samples now can be stored for further analysis.

SL: Simple lipids
FFA: Free fatty acids
LR: Lipid residue

Preparation of chloroform saturated with hydroxide ammonium (Dickson et al. 2009):

1. Shake together $CHCl_3$ and $NH_3OH_{(sol\ 35\%)}$ (ratio 5:1 eg. 100 ml $CHCl_3$ and 20 ml NH_3OH).
2. Separate the Chloroform layer (lower).
3. Put enough anhydrous sodium sulphate in a beaker or Erlenmeyer flask, let sediment and decant through a column of anhydrous sodium sulphate ($Na_2SO_410H_2O$) cleaned with chloroform.
4. Collect into an appropriate recipient and label.

Separation of the polar and apolar fractions via aluminium column chromatography (simple lipid fraction, SL)

a) Hexane/Dichloromethane (9:1, v/v) .- apolar
b) Dichloromethane/ MeOH (1:1, v/v).- polar

1. Prepare a column of aluminum using pre-extracted and activated aluminum oxide (Al_2O_3) from the oven.
2. Use a furnaced short pipette for the column and plug with pre-extracted glass wool.
3. Fill the column with approx. 4 cm de aluminum oxide.
4. Wash the aluminum column (once)with a mixture of Hexane/DCM (9:1, V/V).
5. Rinse the simple fraction vial and elute:
   a) Apolar fraction.- 4 column volumes of hexane/DCM (9:1) and collect in a vial previously labeled.
   b) Polar fraction.- 3 column volumes of DCM/MeOH (1:1) and collect in a vial previously labeled.
6. Dry under N_2.

Silylation (polar fraction)
Just before GC-MS

1. Pre-heat the block heater until 70°C.
2. Add 25 µL of bis(trimethylsilyl)trifluoroacetamide, BSTFA, a silylation reagent that converts the alcohol into R-O-Si$(R)_3$ and heat for 1 hour at 70C.
3. Blow down with N_2.
4. Add 1 ml de hexane.
5. Transfer into a vial with insert for analysis on the GC and GC-MS.

Remember rinse the syringe using DCM for every sample/blank

Apolar fraction

1. Add 1 ml of hexane.
2. Take an aliquot of 0.5 ml for analysis on the GC and GC-MS.

Methylation (FFA fraction)

1. Turn on the block heater until reach a temperature of 70°C.
2. Add 10 µL of tetracosane (standard) to the acid fraction vial and dry under a N_2 smooth flow.
3. Add 100 µL of BF/MeOH and heat 1 hour at 70°C using the heater.
4. Let it cool down.
5. Add 1 ml of bi-distilled water.
6. Wash the aqueous layer with approx. 1 ml of DCM three times in order to extract organic compounds (bottom layer).
7. Combine all organic extracts in a vial and reduce under a flow of N_2 less than 1 ml.
8. Prepare a column of anhydrous Na_2SO_4 (remember that this compound takes humidity from the environment, so I recommend to prepare the column few minutes before running the extraction).
9. Elute the organic extracts using approx. 2 ml of DCM to take out the water (DON'T LET THE COLUMN RUN DRY DURING ELUTION).
10. Dry under a flow of N_2.
11. Pre-heat the block heater until 70°C
12. Add 25 µL of bis(trimethylsilyl)trifluoroacetamide, BSTFA, a silylation reagent that converts the alcohol into R-O-Si(R)$_3$ and heat for 1 hour at 70°C.
13. Blow down with N_2.
14. Add 1 ml de hexane.
15. Transfer into a vial with insert for analysis on the GC and GC-MS.

3. Solutions for Bligh –Dyer extraction

Bi-distilled water

Bi-distilled water is distilled water washed using DCM in a separation funnel to eliminate any organic interference. (Use the aquatic phase, top layer).

300mL, 0.05M buffered water using KH2PO4

RMM KH2PO4 = 135.35
M = mass/RMM, 0.05 moles = mass/135.35
Mass KH2PO4 in 1 litre = 6.7677g/L
Need 300mL of buffered solution
6.804g/1000mL x 300mL = 2.0303g per 300mL of bi-distilled water.

1. Add 2.0303g of KH2PO4 to 300mL bi-distilled water while mixing with a magnetic stirrer.
2. Adjust pH and NaOH pellets to 7.2 (approx 3 pellets needed).
3. Place solution into a 500mL separating funnel.
4. Wash solution with 50mL DCM (3x). Ensure opening of funnel during shaking to release build up of gases. DCM has a greater mass than water

and they are both immiscible so the DCM will sink to the bottom and the buffered water will lie as a layer on top (to get bi-distilled water).
5. Therefore the DCM can be drained out of the separating funnel and the buffered water will remain in the funnel ready to use.

Monophasic Bligh – Dyer solvent
The Bligh – Dyer solvent mixture is made up of the following solutions:

1. Buffered water: chloroform: methanol in the following ratios; 4 : 5 : 10 (prepared above; 100mL : 125mL : 250mL).

4. Activate Cu for desulfurisation

Preparation of activate copper (Blumer 1957).

1. Place copper in a vial and rinse with distilled water. Add a couple of drops of concentrate HCl and shake until activated. Place in ultrasonic bath for 5 minutes
2. Use pH paper to test the solution
3. Pipette out the liquid and with another pipette add distilled water to the vial. Rinse the edges of the vial with the water. Pipette out the liquid and rinse 4 more times with distilled water. Test the pH –until neutral solution.
4. Rinse the vial with Methanol/DCM
5. Rinse with DCM
6. Scoop small amount of the now activated copper into sample. Place in Sonic Bath from a few minutes. If the Cu has turned black it has reacted with the elemental sulfur to produce copper sulfide, add more copper until it finishes reacting with the sulfur

5. Demineralisation of OM (Gélinas et al. 2001)

1. Weigh 0.25 gr of freeze dried sample into centrifuge tubes.
2. Add 30 ml of 1N HCl.
3. Agitate for 1 hour at room temperature (using a magnetic stirrer).
4. Centrifuge for 15 min.
5. Take the supernatant into another centrifuge tube and discard.
6. Wash 3 times the product with 6. 6 ml of DI water every time.
7. Add 20 ml of 10% (v/v) HF -1N HCl mixture.
8. Agitate for 12 h at room temperature (overnight, 12h).
9. Centrifuge for 15 min and remove carefully the supernatant (HF-HCl mixture).
10. Wash the residue 3 times with 3.3 ml of DI water and remove the supernatant every time (cent. 15 min).
11. Freeze-dried the precipitate.

REFERENCES

Blumer, M. (1957). "Removal of Elemental Sulfur from Hydrocarbon Fractions." Analytical Chemistry **29**(7): 1039-1041.

Dickson, L., I. D. Bull, P. J. Gates and R. P. Evershed (2009). "A simple modification of a silicic acid lipid fractionation protocol to eliminate free fatty acids from glycolipid and phospholipid fractions." Journal of Microbiological Methods **78**(3): 249-254.

Gélinas, Y., J. A. Baldock and J. I. Hedges (2001). "Demineralization of marine and freshwater sediments for CP/MAS 13C NMR analysis." Organic Geochemistry **32**(5): 677-693.

Appendix B. Conference contributions

Analysis of sediments from an old AMD site analogue

Martha E. Jiménez-Castaneda, Jonathan R. Lloyd, David J. Vaughan and Bart van Dongen.

22nd Meeting of the British Organic Geochemical Society

Swansea University July 6-7, 2011

Effect of natural carbon sources on the microbial attenuation of AMD

Martha E. Jiménez-Castañeda, Carolina V. Scarincci, Bart E. van Dongen, David J. Vaughan and Jonathan R. Lloyd

Geomicrobiology and its significance for biosphere processes.

Manchester Interdisciplinary Biocentre at the University of Manchester UK, April 19-20, 2012.

Effect of natural carbon sources on the microbial attenuation of AMD

Martha E. Jiménez-Castañeda, Carolina V. Scarincci, Bart E. van Dongen, David J. Vaughan and Jonathan R. Lloyd.

10th Symposium of Mexican Students in the UK

Imperial College London UK, May 10-12, 2012.

Influence of natural organic matter sources on the Fe(III) reduction of an ARD site

Martha E. Jiménez-Castañeda, Carolina V. Scarincci, Jonathan R. Lloyd, David J. Vaughan and Bart E. van Dongen.

23nd Meeting of the British Organic Geochemical Society

Leeds University UK, July 4-5, 2012.

Attenuation of Acid Rock Drainage promoted by natural electron donors.

Jiménez-Castaneda, M. E., Vaughan, D., Lloyd, J., and van Dongen, B. E.

Short course of the International Society for Environmental Biogeochemistry

Microbe-mineral interactions: Molecular to Global Scale Processes

Riviera Maya, México, November 4-8, 2012.

Promotion of Microbial Fe(III) reduction by using natural electron donors at an ARD site

Martha Jimenez-Castaneda, Jonathan Lloyd, David Vaughan, Bart van Dongen.

Iron Biogeochemistry -From Molecular Processes to Global Cycles

Ascona, Switzerland, March 3-8, 2013